



Lebenswissenschaftliche Fakultät
Institut für Biologie

Bachelorarbeit

Zum Erwerb des akademischen Grades Bachelor of Science

Physiologically based pharmacokinetic/pharmacodynamic modeling of the direct renin inhibitor aliskiren: Exploring the impact of hepatorenal impairment and drug-drug interactions

Physiologisch basierte pharmakokinetische/pharmakodynamische Modellierung des direkten Reninhemmers Aliskiren: Untersuchung der Auswirkungen von hepatorenalen Beeinträchtigungen und Arzneimittelwechselwirkungen

vorgelegt von

Yusuf Ali Kulanoglu

Matrikelnummer: 625014

E-Mail: yusuf.ali.kulanoglu@student.hu-berlin.de

Geburtsdatum und -ort: 04.10.2003 in Wilhelmshaven

Arbeitsgruppe: Systems Medicine of the liver

Berlin, den 05.01.2025

Erstprüfer: Dr. Matthias König

Zweitprüfer: Prof. Dr. Hanspeter Herzl

Contents

Abstract	3
1 Introduction	5
1.1 Hypertension	5
1.2 Renin-Angiotensin-Aldosterone System (RAAS)	6
1.3 Blood pressure medications	8
1.4 Aliskiren	9
1.5 Aliskiren pharmacokinetics	10
1.6 Hepatic and renal functional impairment	12
1.7 Drug-drug interactions	13
1.7.1 P-glycoprotein (P-gp)	14
1.7.2 CYP3A4	14
1.8 Physiologically based pharmacokinetic (PBPK) model	15
1.9 Question, scope and hypotheses	16
2 Methods	17
2.1 Literature research	17
2.2 Data curation	17
2.3 Model	17
2.4 Parameter Adjustments for Drug-Drug Interactions	18
2.5 Parameter fitting	18
2.6 Pharmacokinetic parameters	18
2.7 Effect of drug-drug interactions (DDI)	20
3 Results	23
3.1 Aliskiren data	23
3.2 Computational model	26
3.2.1 Model overview	26
3.2.2 Intestine model	27
3.2.3 Kidney model	29
3.2.4 Liver model	30
3.2.5 Renin inhibition	32
3.2.6 Whole-body model	33
3.2.7 Model of hepatic and renal impairment	35
3.3 Parameter fitting	35
3.4 Model performance	36
3.4.1 Single dose	39
3.4.2 Multiple dose	42
3.5 Model application	44
3.5.1 Hepatic functional impairment	44
3.5.2 Renal functional impairment	47

3.5.3	Drug-drug interactions (enzyme activities)	50
3.6	Summary	59
4	Discussion	60
4.1	Data	60
4.2	Model performance	60
4.3	Impairments	61
4.4	Drug-drug interactions	62
5	Outlook	63
6	Acknowledgment	65
Supplements		66
References		84

Abstract

English

Aliskiren is an antihypertensive drug classified as a direct renin inhibitor and stands out as the first renin inhibitor approved for oral administration in clinical practice. Its mechanism of action involves the direct inhibition of renin, an enzyme that plays a critical role in the Renin-Angiotensin-Aldosterone System (RAAS), which regulates blood pressure and fluid balance in the body. By inhibiting renin, aliskiren reduces the conversion of angiotensinogen to angiotensin I, thereby decreasing the subsequent production of angiotensin II and aldosterone, both of which are key contributors to vasoconstriction and sodium retention. This cascade ultimately results in effective blood pressure reduction.

Hypertension is often accompanied by other pathophysiological conditions, such as obesity, diabetes, and hepatic, renal, or cardiac dysfunction. As a result, patients frequently require multiple medications to manage these comorbidities. This raises important questions regarding the use of aliskiren in such populations, particularly how these functional impairments and potential drug-drug interactions might influence the pharmacokinetics and pharmacodynamics of the drug.

In this thesis, an extensive dataset of aliskiren pharmacokinetics and pharmacodynamics was compiled and used to develop a physiologically based pharmacokinetic/pharmacodynamic (PBPK/PD) model. This model was applied to address three primary research questions: I. How does hepatorenal impairment influence the pharmacokinetics of aliskiren?; II. What effects do co-administered medications have on the pharmacokinetics of aliskiren?; III. What are the consequences of these pharmacokinetic changes for the pharmacodynamics of aliskiren, particularly its ability to modulate the renin-angiotensin-aldosterone system (RAAS)?

The PBPK/PD model enables the prediction of aliskiren's concentration-time profiles following oral and intravenous administration and provides detailed insights into the factors that affect its pharmacological efficacy. By exploring these influences, the study offers a foundation for developing optimized therapeutic strategies tailored to individual patients.

Key findings of this research include a deeper understanding of how hepatorenal impairments and drug-drug interactions alter aliskiren's pharmacokinetics and pharmacodynamics. Additionally, the model elucidates the impact of these changes on the drug's modulation of the RAAS, providing crucial information for the development of personalized treatment regimens aimed at maximizing therapeutic outcomes. These results contribute to the broader goal of achieving precise and effective hypertension management in patients with complex clinical profiles.

German

Aliskiren ist ein blutdrucksenkender Wirkstoff, der als direkter Reninhemmer eingestuft wird und als erster Reninhemmer in der klinischen Praxis für die orale Verabreichung zugelassen ist. Sein Wirkmechanismus besteht in der direkten Hemmung von Renin, einem Enzym, das eine entscheidende Rolle im Renin-Angiotensin-Aldosteron-System (RAAS) spielt, das den Blutdruck und den Flüssigkeitshaushalt im Körper reguliert. Durch die Hemmung von Renin reduziert Aliskiren die Umwandlung von Angiotensinogen in Angiotensin I, wodurch die anschließende Produktion von Angiotensin II und Aldosteron verringert wird, die beide wesentlich zur Gefäßverengung und Natriumretention beitragen. Diese Kaskade führt letztlich zu einer wirksamen Senkung des Blutdrucks.

Bluthochdruck geht häufig mit anderen pathophysiologischen Zuständen einher, wie Fettleibigkeit, Diabetes und Leber-, Nieren- oder Herzfunktionsstörungen. Infolgedessen benötigen die Patienten häufig mehrere Medikamente, um diese Begleiterkrankungen zu behandeln. Dies wirft wichtige Fragen hinsichtlich der Anwendung von Aliskiren in solchen Bevölkerungsgruppen auf, insbesondere wie diese funktionellen Beeinträchtigungen und mögliche Wechselwirkungen zwischen Medikamenten die Pharmakokinetik und Pharmakodynamik des Medikaments beeinflussen könnten. Im Rahmen dieser Arbeit wurde ein umfangreicher Datensatz zur Pharmakokinetik und zur Pharmakodynamik von Aliskiren zusammengestellt und zur Entwicklung eines physiologisch basierten pharmakokinetischen/pharmakodynamischen (PBPK/PD) Modells verwendet. Dieses Modell wurde angewandt, um drei primäre Forschungsfragen zu beantworten: I. Wie beeinflusst eine hepatorenale Beeinträchtigung die Pharmakokinetik von Aliskiren?; II. Welche Auswirkungen haben gleichzeitig verabreichte Medikamente auf die Pharmakokinetik von Aliskiren?; III. Welche Folgen haben diese pharmakokinetischen Veränderungen für die Pharmakodynamik von Aliskiren, insbesondere für seine Fähigkeit, das Renin-Angiotensin-Aldosteron-System (RAAS) zu modulieren?

Das PBPK/PD-Modell ermöglicht die Vorhersage der Konzentrations-Zeit-Profile von Aliskiren nach oraler und intravenöser Verabreichung und liefert detaillierte Einblicke in die Faktoren, die seine pharmakologische Wirksamkeit beeinflussen. Durch die Erforschung dieser Einflüsse bietet die Studie eine Grundlage für die Entwicklung optimierter therapeutischer Strategien, die auf den einzelnen Patienten zugeschnitten sind.

Zu den wichtigsten Ergebnissen dieser Forschung gehört ein tieferes Verständnis dafür, wie hepatorenale Beeinträchtigungen und Wechselwirkungen zwischen Medikamenten die Pharmakokinetik und Pharmakodynamik von Aliskiren verändern. Darüber hinaus klärt das Modell, wie sich diese Veränderungen auf die Modulation des RAAS durch das Medikament auswirken, was entscheidende Informationen für die Entwicklung personalisierter Behandlungsschemata zur Maximierung der therapeutischen Ergebnisse liefert. Diese Ergebnisse tragen zu dem weiter gefassten Ziel bei, eine präzise und wirksame Behandlung des Bluthochdrucks bei Patienten mit komplexen klinischen Profilen zu erreichen.

1 Introduction

1.1 Hypertension

Hypertension, commonly referred to as high blood pressure, is a condition characterized by persistently elevated pressure in the blood vessels. Arterial hypertension is a significant global health issue and a major risk factor for the development of heart failure, stroke, cardiovascular, and renal diseases [3, 8, 59]. Research indicates that high blood pressure contributes to approximately 54% of strokes, 47% of ischemic heart diseases, 75% of hypertensive diseases, and 25% of other cardiovascular conditions worldwide [38, 84, 48]. It is a widespread condition, affecting an estimated 1.28 billion individuals globally [81].

Although hypertension is often asymptomatic, some individuals may experience symptoms such as headaches, nausea, or blurred vision [81]. Prolonged high blood pressure can lead to severe complications, including heart, kidney, and liver failure, significantly increasing mortality risk [80]. This underscores the importance of timely diagnosis and effective management. Without treatment, hypertension poses a critical health threat due to its high prevalence and potentially severe consequences.

Management of hypertension typically involves adherence to prescribed medications, combined with lifestyle modifications. Risk factors for developing hypertension include advanced age, genetic predisposition, obesity, excessive alcohol consumption, and a sedentary lifestyle [80]. Blood pressure levels are assessed using systolic and diastolic measurements, which form the basis for categorization according to the American Heart Association (Table 1) [4, 80]. These categories range from low and normal blood pressure to elevated, hypertension stages 1 and 2, and hypertensive crisis.

Table 1: **Blood Pressure Levels**

Category	Systolic [mmHg]	Diastolic [mmHg]
Low	< 90	and < 60
Normal	< 120	and < 80
Elevated	120 - 129	and < 80
Hypertension Stage 1	130 - 139	or 80 - 89
Hypertension Stage 2	≥ 140	or ≥ 90
Hypertensive Crisis	> 180	or > 120

Classifications of blood pressure levels according to the American Heart Association [4, 80].

1.2 Renin-Angiotensin-Aldosterone System (RAAS)

The Renin-Angiotensin-Aldosterone System (RAAS) (shown in Figure 1) is a vital regulatory pathway that maintains blood pressure and fluid balance in the body [58]. This system begins with angiotensinogen, a protein produced by the liver, which is converted into Angiotensin I by renin, an enzyme secreted by the kidneys [24, 54, 75]. Renin release is triggered by conditions such as low blood pressure, reduced sodium levels, or activation of the sympathetic nervous system. Angiotensin I is then converted into the more active Angiotensin II by the Angiotensin-Converting Enzyme (ACE), primarily located in the lungs [75].

Angiotensin II plays a central role in regulating physiological responses. It binds on specific receptors, particularly the AT1 receptor, to stimulate a variety of processes. These include the vasoconstriction, which increases vascular resistance and raises blood pressure [7, 24, 54]. It also enhances the sympathetic nervous system's activity, resulting in a higher heart rate and increased cardiac output. In the kidneys, Angiotensin II promotes sodium reabsorption and fluid retention, further contributing to blood volume and pressure regulation. It stimulates the adrenal glands to release aldosterone, a hormone that amplifies sodium retention and potassium excretion, resulting in greater fluid retention. Additionally, Angiotensin II affects the heart and blood vessels by promoting hypertrophy (thickening of the heart muscle) and fibrosis (stiffening of tissues), both of which can have long-term consequences on cardiovascular health. It is also known to activate inflammatory and oxidative pathways, leading to endothelial dysfunction and potential organ damage over time [24, 58, 75].

Aldosterone, produced in the adrenal cortex, plays a crucial role in this system by acting on the kidneys' distal tubules and collecting ducts. It increases sodium and water reabsorption while promoting the excretion of potassium, which helps to increase blood volume and pressure [54]. Beyond its renal effects, aldosterone also contributes to tissue remodeling and fibrosis, exacerbating conditions like hypertension and heart failure.

Dysfunction of the RAAS can have significant health implications. Overactivation of the system is a major factor in hypertension, as persistent vasoconstriction, fluid retention, and cardiac remodeling contribute to chronically high blood pressure. Prolonged RAAS activity is also linked to heart failure, chronic kidney disease, and vascular damage, including endothelial dysfunction and arterial stiffness.

Understanding the RAAS has been critical in the development of effective treatments for these conditions. Medications such as ACE inhibitors, angiotensin receptor blockers (ARBs), and aldosterone antagonists target specific components of this pathway, offering valuable tools for managing hypertension and reducing the risk of cardiovascular and renal complications.

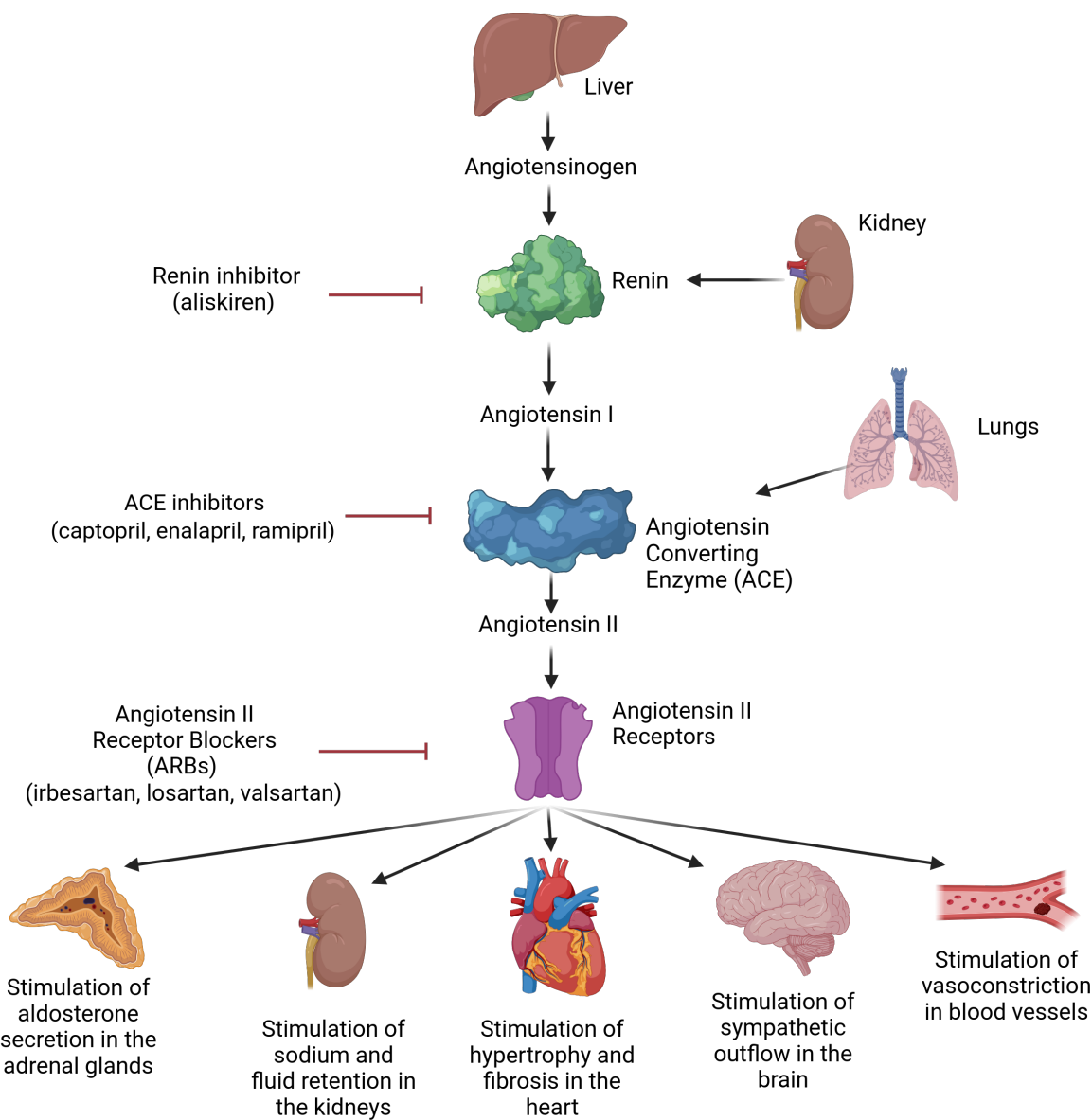


Figure 1: Renin-Angiotensin-Aldosterone System (RAAS). Angiotensinogen, produced by the liver, is converted to Angiotensin I by renin, which is secreted by the kidneys. Angiotensin I is further converted to Angiotensin II by the Angiotensin-Converting Enzyme (ACE) in the lungs. Angiotensin II acts on its receptors to stimulate various physiological responses, including vasoconstriction of blood vessels, stimulation of sympathetic outflow in the brain, fluid retention and sodium reabsorption in the kidneys, aldosterone secretion in the adrenal glands, and hypertrophy and fibrosis in the heart. Medications such as renin inhibitors (e.g., aliskiren), ACE inhibitors (e.g., captopril, enalapril, ramipril), and Angiotensin II receptor blockers (ARBs; e.g., irbesartan, losartan, valsartan) target specific points in this pathway to effectively manage hypertension and related conditions.

1.3 Blood pressure medications

Hypertension, commonly known as high blood pressure, is managed through various medications that target specific pathways involved in blood pressure regulation. These medications reduce blood pressure and prevent complications such as cardiovascular disease, kidney damage, and stroke.

Renin-Angiotensin-Aldosterone System (RAAS) Modulators:

Medications targeting the RAAS are key in managing hypertension:

- **Renin Inhibitors [9] (e.g., aliskiren):** These drugs directly inhibit the activity of renin, an enzyme that converts angiotensinogen to angiotensin I. By blocking this initial step, the production of angiotensin II, a potent vasoconstrictor, is reduced. This leads to vasodilation and lower blood pressure.
- **Angiotensin-Converting Enzyme (ACE) Inhibitors [66, 68] (e.g., captopril, enalapril, ramipril):** ACE inhibitors prevent the conversion of angiotensin I to angiotensin II by blocking the angiotensin-converting enzyme. Since angiotensin II promotes vasoconstriction and fluid retention, reducing its levels leads to vasodilation, reduced blood volume, and decreased blood pressure.
- **Angiotensin II Receptor Blockers (ARBs) [66, 68] (e.g., irbesartan, losartan, valsartan):** ARBs block angiotensin II from binding to its receptors (AT1 receptors), thereby inhibiting its effects on vasoconstriction and aldosterone secretion. This results in blood vessel relaxation, reduced sodium retention, and lower blood pressure[12, 23].

Other Common Classes of Antihypertensive Medications:

In addition to RAAS modulators, other commonly used classes of antihypertensive drugs include:

- **Thiazide-Type Diuretics [18, 66, 68] (e.g., hydrochlorothiazide [HCTZ]):** Thiazide diuretics act at the distal tubule of the nephron to block Na^+ reabsorption, thus reducing water retention, intravascular volume and total body sodium [12, 77]. Thiazide diuretics are often used as first-line therapy for hypertension due to their effectiveness and cost efficiency [17].
- **β -Adrenergic Receptor Antagonists (Beta-Blockers) [16, 18] (e.g., atenolol, metoprolol):** Beta-Blockers work by blocking the β -adrenergic receptors. This reduces heart rate, contractility, and cardiac output, thereby lowering blood pressure [23].
- **Calcium Channel Blockers (CCBs) [18, 69] (e.g., amlodipine, nifedipine):** A calcium channel blocker inhibits the transmembrane influx of calcium ions into vascular smooth muscle and cardiac muscle [12]. This promotes vasodilation, reduces vascular resistance, and effectively lowers blood pressure [17].

These medications can be used individually or in combination, depending on the severity of hypertension, patient-specific characteristics, and any coexisting medical conditions. Table 2, which has been adapted from [14, 15, 25, 41, 43, 58, 75, 76], provides an overview of the effects of the different modulators on the renin-angiotensin-aldosterone system (RAAS).

Table 2: **Medication effects on the RAAS pathway.** The table illustrates the effects of medications on Plasma Renin Concentration (PRC), Plasma Renin Activity (PRA), Angiotensin I (Ang I), Angiotensin II (Ang II), and Aldosterone, all of which play crucial roles in the Renin-Angiotensin-Aldosterone System (RAAS). Increases and decreases in effects are indicated by \uparrow and \downarrow , respectively.

Medication	PRC	PRA	Angiotensin I	Angiotensin II	Aldosterone
Renin Inhibitor	\uparrow	\downarrow	\downarrow	\downarrow	\downarrow
ACE Inhibitor	\uparrow	\uparrow	\uparrow	\downarrow	\downarrow
ARB	\uparrow	\uparrow	\uparrow	\uparrow	\downarrow
Thiazide Diuretics	\uparrow	\uparrow	\uparrow	\uparrow	\uparrow
Beta-Blockers	\downarrow	\downarrow	\downarrow	\downarrow	\downarrow

1.4 Aliskiren

Aliskiren is an antihypertensive medication belonging to a novel class of drugs known as direct renin inhibitors (DRIs). Approved by the Food and Drug Administration (FDA) [2] in the United States and the European Medicines Agency (EMA) [1], aliskiren is indicated for the treatment of hypertension. By directly inhibiting renin, a key enzyme in the renin-angiotensin-aldosterone system (RAAS), aliskiren plays a crucial role in regulating blood pressure and fluid balance. Administered once daily, it can be used either as monotherapy or in combination with other antihypertensive agents, offering flexibility in managing hypertension [9].

Despite its potential, the application of aliskiren faces significant challenges, particularly in patients with hepatorenal impairments or those undergoing simultaneous use of multiple medications. These conditions can alter its pharmacokinetics and pharmacodynamics, leading to variability in therapeutic outcomes. Understanding these interactions is important for optimizing its use in complex scenarios. This study aims to address these gaps by employing physiologically based pharmacokinetic/pharmacodynamic modeling to investigate the effects of hepatorenal dysfunction and drug-drug interactions on aliskiren’s behavior, contributing to more effective, personalized hypertension treatments.

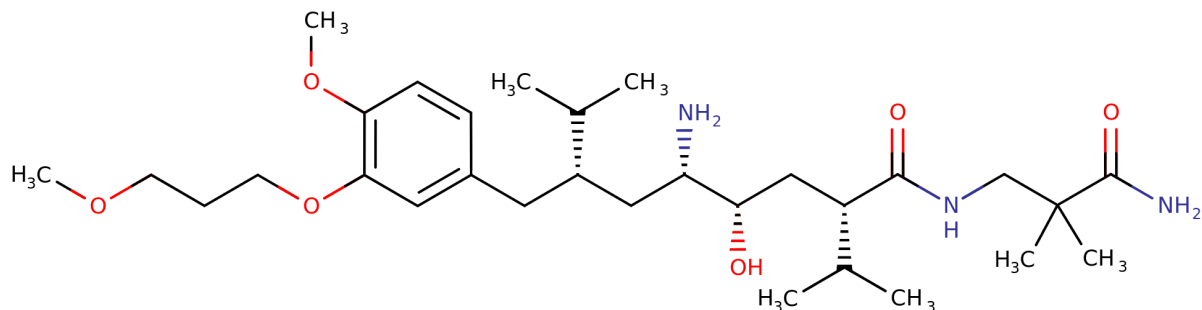


Figure 2: **Structure of aliskiren.** Image from <https://go.drugbank.com/drugs/DB09026> [42]

1.5 Aliskiren pharmacokinetics

The main processes affecting aliskiren pharmacokinetics are absorption, distribution, metabolism and excretion (or ADME for short).

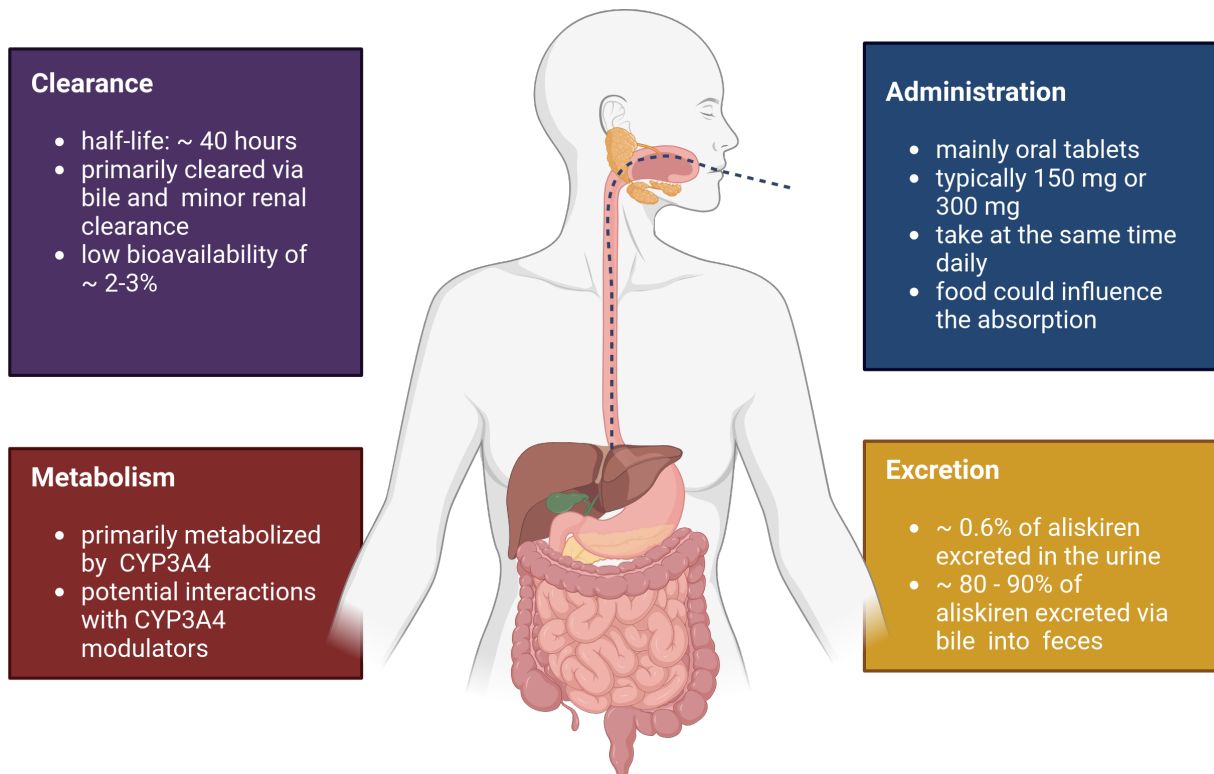


Figure 3: **Summary of aliskiren pharmacokinetics.** This figure illustrates the pharmacokinetic properties of aliskiren. The drug exhibits an oral bioavailability of approximately 2-3% and an elimination half-life of 40 hours. It is administered mainly as oral tablets (typically 150 mg or 300 mg) and is metabolized by CYP3A4, primarily in the liver and intestine. Aliskiren is predominantly excreted via the biliary/fecal route (80-90%), with less than 1% eliminated through urinary excretion. The chart summarizes the drug's clearance, metabolism, administration, and excretion pathways contributing to its pharmacokinetic profile.

Absorption

Aliskiren exhibits poor absorption following oral administration, with a bioavailability of approximately 2-3% [31, 45, 49, 57, 65]. This low bioavailability is largely attributed to its interaction with P-glycoprotein (P-gp), a transporter protein in the intestinal epithelium that pumps aliskiren back into the gut, reducing its systemic availability [20, 70, 69]. Additionally, poor solubility and extensive first-pass metabolism in the liver further limit absorption.

Aliskiren is primarily administered as oral tablets in typical doses of 150 mg or 300 mg. Some studies (e.g. *Fisher et al.* and *Hu et al.*) have investigated alternative dosages ranging from 75 mg to 600 mg, while others, such as *Nussberger et al.*, have explored doses up to 640 mg to analyze pharmacokinetics [27, 22, 40]. Peak plasma concentrations (c_{max}) are achieved within 1 to 3 hours, while steady-state concentrations are reached after 7-8 days of consistent dosing [42, 20, 70].

Food influences absorption significantly. High-fat meals reduce bioavailability by lowering the area under the curve (*AUC*) by 71% and the maximal concentration (c_{max}) by 85%, whereas light meals minimize this effect. To optimize absorption, it is recommended to take aliskiren at the same time daily, preferably with light, low-fat meals [20]. Variability in absorption may also occur due to differences in P-gp activity, gastrointestinal motility, and hepatic metabolism.

Distribution

According to *Waldmeier et al.*, 81% of total plasma radioactivity (aliskiren labeled with ^{14}C) following aliskiren administration is attributed to unchanged drug, indicating minimal metabolism [78]. Aliskiren binds moderately to plasma proteins, with approximately 47-51% of the drug bound in human plasma [70]. The volume of distribution (V_d) at steady state is estimated at approximately 135 liters after a single 20-mg intravenous dose, suggesting substantial extravascular distribution [6, 70]. This distribution aligns with its action on the renin-angiotensin system, as it penetrates vascular tissues and kidney sites to exert its antihypertensive effects.

Metabolism

Aliskiren undergoes minimal metabolism, with only 1.4% of the administered radioactive dose accounted for by oxidized metabolites in the excreta [31, 78, 70]. The two primary metabolites identified are an O-demethylated alcohol derivative and a carboxylic acid derivative, while minor oxidized and hydrolyzed metabolites may also be present in plasma [42, 78, 70].

The metabolism of aliskiren is likely mediated by the Cytochrome P450 enzyme CYP3A4, which plays a key role in its biotransformation [42, 62, 63, 78, 70]. This limited metabolism contributes to the drug's pharmacokinetic predictability and reduces the formation of potentially active or toxic metabolites. However, interactions with CYP3A4 inhibitors (e.g., ketoconazole, grapefruit juice) or inducers (e.g., rifampicin) could alter aliskiren's metabolism, potentially affecting its efficacy or safety (see Table 4 for details).

Most of the drug is excreted unchanged, primarily via bile, which reflects its minimal reliance on metabolic transformation for elimination.

Excretion

Aliskiren is excreted primarily via the biliary/fecal route, accounting for approximately 91% of the total dose, with the bulk of the drug (77.5%) recovered as unchanged aliskiren [65, 73, 78, 85]. Oxidized metabolites in the excreta represent approximately 1.4% of the orally administered radioactive dose.

Renal excretion is minimal, contributing only 0.6% of the radioactive dose, of which 0.4% (approximately 70% of the recovered radioactivity in urine) is unchanged aliskiren [30, 31, 45, 60, 70, 78, 85].

According to *Waldmeier et al.*, aliskiren's excretion is almost entirely via the biliary/fecal route. Total excretion (mass balance) over the 168-hour collection period was $91.5 \pm 4.5\%$ of the dose, with moderate interindividual variability (range: 85–95%) [78]. Unchanged aliskiren accounted for 0.4% of the dose in urine (approximately 70% of urinary radioactivity) and 77.5% of the dose in feces, corresponding to approximately 85% of the recovered radioactivity [78].

1.6 Hepatic and renal functional impairment

Hepatic impairment

Hepatic impairment significantly impacts the pharmacokinetics of many drugs, particularly those metabolized or excreted via the liver. The liver plays a central role in drug metabolism through enzymatic pathways such as those mediated by cytochrome P450 (CYP) enzymes, including CYP3A4. In patients with hepatic impairment, reduced liver function can lead to alterations in drug metabolism, potentially resulting in increased systemic exposure, reduced clearance, and prolonged half-life. Hepatic impairment may also affect biliary excretion, a critical pathway for drugs such as aliskiren undergoing enterohepatic circulation (EHC), leading to changes in drug elimination and secondary absorption.

Vaidyanathan *et al.*'s study used the Child-Turcotte-Pugh (CTP) scoring system to classify the hepatic impairment [47, 68].

The CTP system categorizes patients into stages of cirrhosis based on clinical and biochemical markers, such as serum bilirubin, albumin, prothrombin time, ascites, and encephalopathy [53]. Figure 4 provides an overview of the different stages of hepatic impairment based on the CTP classification.

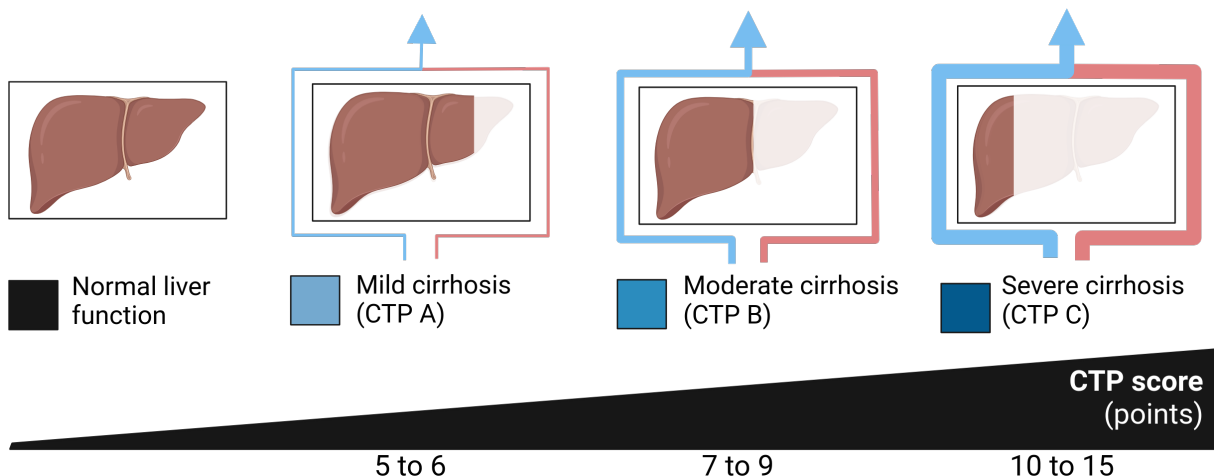


Figure 4: **Stages of cirrhosis.** This figure illustrates the stages of liver cirrhosis categorized by the Child-Turcotte-Pugh (CTP) scoring system. The stages include normal liver function (CTP score: < 5), mild cirrhosis (CTP A, 5 – 6), moderate cirrhosis (CTP B, 7 – 9), and severe cirrhosis (CTP C, 10 – 15). The colors in the boxes indicate the corresponding stages and are used in simulations to represent different levels of hepatic function. This classification provides a clear visual framework for understanding the progression of cirrhosis and its impact on liver performance in modeling and simulation studies.

Renal impairment

Renal impairment primarily affects the elimination of drugs and their metabolites that are cleared through the kidneys. In patients with impaired renal function, decreased Glomerular Filtration Rate (GFR), tubular secretion, and reabsorption can result in drug accumulation and prolonged half-life. Although aliskiren is primarily eliminated through the hepatobiliary route, renal impairment may still influence its pharmacokinetics, particularly for the minor fraction

excreted unchanged in the urine [70, 78]. Additionally, renal dysfunction can alter plasma protein levels, such as albumin, potentially affecting drug distribution.

Evaluating renal function is essential to ensure safe and effective drug therapy in individuals with renal impairment. This is typically achieved using markers like creatinine or estimated GFR. Adjustments in drug dosage are often required based on the extent of renal impairment to avoid toxicity or therapeutic failure.

Vaidyanathan *et al.*'s study employed the classification of renal impairment based on creatinine clearance values [68]. These values are used to estimate the GFR, which determines the stage of renal impairment [47, 55].

The stages of renal impairment range from normal kidney function to severe renal impairment, reflecting progressive declines in GFR. Figure 5 provides an overview of the stages of renal impairment based on GFR values.

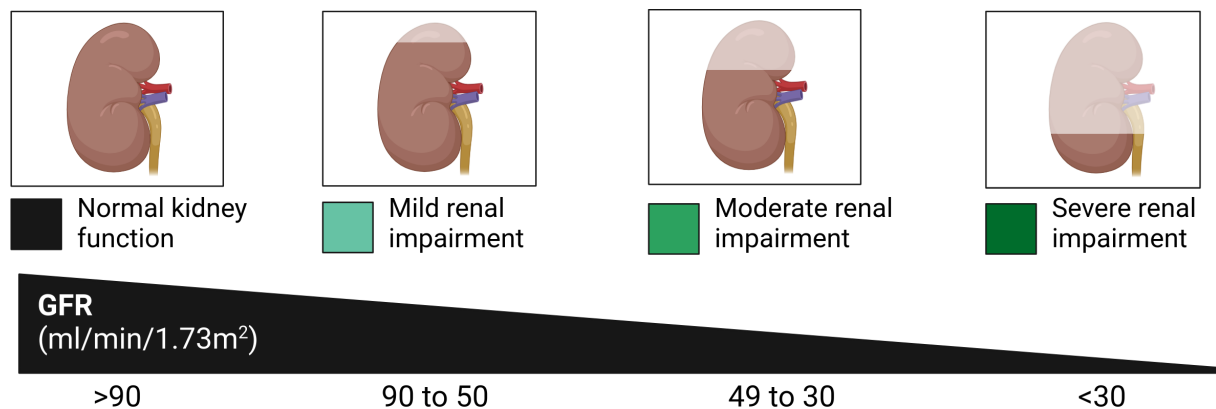


Figure 5: Stages of renal impairment. This figure classifies renal impairment based on Glomerular Filtration Rate (GFR) values, expressed in $\frac{ml}{min \cdot 1.73m^2}$. The stages range from normal kidney function ($GFR > 90$) to severe renal impairment ($GFR < 30$). Mild ($90 - 50$) and moderate ($49 - 30$) renal impairment stages are also shown. The colors in the boxes represent the corresponding stages and are used in simulations to differentiate between levels of renal function. This classification provides a visual reference for the impact of varying degrees of kidney function on pharmacokinetic simulations.

1.7 Drug-drug interactions

Drug-drug interactions (DDIs) are crucial for understanding how coadministered drugs affect the pharmacokinetics and pharmacodynamics of aliskiren. DDIs are evaluated through coadministration studies that measure changes in absorption, metabolism, and elimination. These studies also help isolate aliskiren's pharmacokinetic properties in the absence of interacting substances. Coadministered drugs may enhance (induce) or reduce (inhibit) the therapeutic effect of aliskiren [70]. For instance, drugs that modulate CYP3A4, a key enzyme in aliskiren metabolism, can significantly alter its area under the concentration-time curve (AUC) (see Table 4 for details). Changes in AUC provide insights into interaction mechanisms and support the development of personalized, safe, and effective treatment plans.

1.7.1 P-glycoprotein (P-gp)

P-glycoprotein 1 (P-gp), also known as permeability glycoprotein, multidrug resistance protein 1 (MDR1), ATP-binding cassette sub-family B member 1 (ABCB1), or cluster of differentiation 243 (CD243), is a crucial membrane protein responsible for pumping various foreign substances out of cells. As an ATP-dependent efflux transporter with broad substrate specificity, P-gp is widely distributed across tissues. It is expressed in the intestinal epithelium, where it pumps xenobiotics (e.g. toxins or drugs) back into the intestinal lumen; in liver cells, where it transports substances into bile ducts; in the proximal tubule cells of the kidney, where it contributes to urinary filtrate formation; and in the capillary endothelial cells of the blood-brain and blood-testis barriers, where it returns substances to the capillaries [13, 20, 39, 69, 83].

The oral direct renin inhibitor aliskiren is a known substrate of P-glycoprotein [62, 69, 78]. This efflux transporter plays a critical role in regulating the absorption and elimination of aliskiren [69]. P-glycoprotein activity can be modulated by coadministered drugs, which may act as inducers or inhibitors, thereby influencing the pharmacokinetics of aliskiren. Table 3 provides a list of common P-gp inhibitors and inducers.

Table 3: Effect of different drugs on the P-glycoprotein (P-gp)

P-glycoprotein inhibitors	P-glycoprotein inducers
cyclosporine [19, 60, 50]	rifampicin [19, 21]
itraconazole [21, 60, 50]	
ketoconazole [19, 69, 50]	
lovastatin [69]	
verapamil [19, 21]	

1.7.2 CYP3A4

Cytochrome P450 3A4 (CYP3A4) is a key enzyme in the body, primarily located in the liver and intestine, and is encoded by the CYP3A4 gene. This enzyme is responsible for oxidizing small foreign organic molecules (xenobiotics), such as toxins and drugs, to facilitate their elimination from the body [82].

CYP3A4 plays a critical role in the metabolism of aliskiren [20, 70, 78], primarily in the liver but also in the intestine. The activity of this enzyme can be influenced by certain drugs, which may function as either inducers or inhibitors. These interactions can significantly affect the metabolic rate of aliskiren, thereby altering its pharmacokinetics and, consequently, its efficacy and safety. Table 4 provides examples of drugs that modulate CYP3A4 activity and their potential impact on aliskiren metabolism.

Table 4: Effect of different drugs on CYP3A4

CYP3A4 inhibitors	CYP3A4 inducers
azamulin [19]	rifampicin [19, 21]
cimetidine [19, 21, 69]	bosentan [21]
cyclosporine [19, 60, 50]	elagolix [21]
grapefruit juice [21]	
itraconazole [19, 60, 50]	
ketoconazole [19, 69, 50]	
verapamil [19, 21, 51]	

1.8 Physiologically based pharmacokinetic (PBPK) model

Physiologically based pharmacokinetic (PBPK) models are advanced tools that use mathematical frameworks to describe and simulate drug pharmacokinetics through coupled ordinary differential equations (ODEs) [36]. These models integrate physiological, pharmacokinetic, and biochemical parameters to accurately represent drug behavior within various compartments of the body and its transport via the systemic circulation.

By incorporating detailed descriptions of physiological compartments and their interconnections, PBPK models enable precise predictions of drug absorption, distribution, metabolism, and elimination. This approach forms the foundation for generating predictive simulations, which are valuable for understanding complex pharmacokinetic processes.

PBPK models serve as a powerful in silico tool to address medical questions, test hypotheses, and predict drug pharmacokinetics under various conditions. Their predictive capabilities make them a indispensable resource in drug development and personalized medicine.

1.9 Question, scope and hypotheses

Within this project, a combined PBPK/PD model of aliskiren and its effect on renin was developed to investigate the impact of hepatic and renal functional impairment, as well as drug-drug interactions between aliskiren and other substances.

The model development focuses on addressing the following key questions:

- I. How does hepatorenal impairment influence the pharmacokinetics of aliskiren?
- II. What effects do co-administered medications have on the pharmacokinetics of aliskiren?
- III. What are the consequences of these pharmacokinetic changes for the pharmacodynamics of aliskiren, particularly its ability to modulate the renin-angiotensin-aldosterone system (RAAS)?

The primary objective of the study is to understand how hepatorenal impairment and drug-drug interactions affect the pharmacokinetics and pharmacodynamics of aliskiren. The central hypothesis is that renal impairment may have minimal effects on aliskiren pharmacokinetics, whereas hepatic impairment may lead to more pronounced changes. Furthermore, drug-drug interactions are hypothesized to influence aliskiren pharmacokinetics differently depending on the mechanisms and classifications of the interacting drugs.

By systematically investigating these aspects, this thesis aims to enhance the clinical understanding of aliskiren, with the ultimate goal of improving hypertension management in patients with complex clinical needs

2 Methods

2.1 Literature research

For an overview of the available pharmacokinetic literature for aliskiren, an initial search via PKPDAI for 'aliskiren' was performed, a web service providing pharmacokinetic articles (<https://www.pkpdai.com/publications>) [44]. The search results were extended via a Pubmed search with the search terms `aliskiren AND pharmacokinetics` (<https://pubmed.ncbi.nlm.nih.gov/>) [46]. The resulting publications were screened and filtered based on the following criteria: the clinical trials had to contain pharmacokinetic parameters or time course data for aliskiren. Data had to be for human subjects (i.e. other species were excluded such as rat or mouse). Main focus was on data in healthy subjects but data for renal impairment and hepatic impairment was included. Concerning the intervention, it was ensured that aliskiren was administered at least once alone or as a co-medication with another substance. Also of high interest were studies that published information about the pharmacodynamics of aliskiren. The literature corpus was extended by additional literature available in the primary references.

To address the effects of co-administered drugs on aliskiren's pharmacokinetics, specific studies were prioritized that provided interaction data with known CYP3A4 inhibitors (e.g. ketoconazole) or inducers (e.g., rifampicin), as well as P-glycoprotein and OATP modulators (e.g. verapamil) (see Tables 3 and 4 to get more information about the different modulators). Pharmacokinetic parameters such as AUC and c_{max} under single and multiple dosing schemes were extracted to inform model adjustments.

2.2 Data curation

Data on study design, pharmacokinetic, and pharmacodynamic parameters were systematically extracted from the relevant studies and organized into tables using LibreOffice, adhering to established data curation workflows. The study design included detailed information on the subjects, grouping, and interventions.

Subject data encompassed anthropometric information (e.g., height, BMI), ethnicity, health status, lifestyle factors (e.g., non-smoking status), and concurrent medications, such as oral contraceptives. Intervention details specified the substance administered, dosage, route of administration (oral in all cases), and treatment course duration.

Numerical data presented in charts and tables were manually extracted using the "PlotDigitizer" tool and digitized into spreadsheets for analysis. A standardized JSON file was then created to encode the study's metadata in a uniform format. The curated data underwent a review process by a second curator to ensure accuracy and consistency before being uploaded to the publicly accessible database PK-DB (<https://pk-db.com>) [26].

2.3 Model

The PBPK and tissue models were developed in the Systems Biology Markup Language (SBML) [29, 32]. Software such as sbmlutils [34] and cy3sbml [35] were used for the programmatic manipulation and visualisation of the models. The models are ordinary differential equation

(ODE) models solved numerically using sbmlsim [33] based on the high performance SBML simulator libroadrunner [56, 79]. The model is made available in SBML under a CC-BY 4.0 licence from <https://github.com/matthiaskoenig/aliskiren-model> with model equations available from the repository. The version of the model used in this thesis is 0.5.1 [37].

2.4 Parameter Adjustments for Drug-Drug Interactions

Parameter adjustments were implemented to account for the pharmacokinetic effects of co-administered drugs on aliskiren. For inhibitors of CYP3A4 (e.g. ketoconazole), the enzyme activity was reduced based on the calculated increase in aliskiren’s *AUC* from clinical studies. Inducers such as rifampicin were modeled by increasing the enzyme activity parameter, with fold-change values derived from published data (see Section 2.7 for more information).

Similarly, P-glycoprotein activity was adjusted to reflect its role in intestinal efflux, with efflux rates reduced or increased iteratively to optimize the fit with observed concentration-time profiles.

2.5 Parameter fitting

Parameter fitting is an optimization method which allows to adapt parameters $\vec{p} = (p_1, \dots, p_n)$ in a given model so that the distance between model predictions and experimental data is minimized. Model parameters were adjusted by minimizing the residuals r between model prediction $f(x_{i,k})$ and experimental data $y_{i,k}$ using an objective cost function F . SciPy’s least square method was used as cost function F which depends on the parameters \vec{p} and adheres to a L2-norm which corresponds to the sum of weighted residuals, as described by the following equation:

$$F(\vec{p}) = \frac{1}{2} \cdot \sum_{i,k} (w_k \cdot w_{i,k} \cdot r_{i,k})^2$$

Where:

- w_k describes the weighting factor of time course k ,
- $w_{i,k}$ describes the weighting of the respective data point i over time k based on the error of the data point, and
- $r_{i,k} = (y_{i,k} - f(x_{i,k}))$ represents the residue of time i over time k .

These parameters were further evaluated under drug-drug interaction conditions, allowing for the quantification of changes in aliskiren’s pharmacokinetics due to altered enzyme activity or efflux transporter modulation.

2.6 Pharmacokinetic parameters

The following pharmacokinetic parameters were calculated and used for evaluation of the predicted pharmacokinetics:

Maximum concentration, c_{max} [μM]:

The maximum concentration c_{max} is the peak plasma or serum concentration by aliskiren. It is calculated by finding the maximal concentration value in the time course.

Elimination rate, k_{el} [$\frac{1}{h}$]:

The elimination rate k_{el} describes the rate at which a drug is eliminated from the blood. Assuming that the elimination is exponential, the elimination rate k_{el} can be calculated from the log-transformed data using linear regression:

$$C_{ali}(t) = C_{ali}(0) \cdot e^{-k_{el} \cdot t}$$

$$\log(C_{ali}(t)) = \log(C_{ali}(0)) - k_{el} \cdot t$$

Where:

- $C_{ali}(t)$ is the aliskiren concentration at time t ,
- $C_{ali}(0)$ is the initial aliskiren concentration at $t = 0$, and
- t represents the time.

Area under the curve, AUC [$\frac{ng \cdot h}{ml}$]:

AUC describes the area under the concentration time curve and is proportional to the bioavailable amount of the drug of the administered dose. There are two types of AUC : AUC_{end} which describes the area under the curve up to a certain time, and the AUC_{∞} which describes the AUC extrapolated to infinity (assuming mono-exponential decrease). AUC_{end} is calculated using the trapezoidal rule:

$$AUC_{0 \rightarrow t_{end}} = AUC_{end} = \frac{1}{2} \sum_{i=1}^{n-1} ((t_{i+1} - t_i)(C_i - C_{i+1}))$$

The AUC from a certain time point t_{last} to ∞ can be calculated as follows:

$$AUC_{t_{last} \rightarrow \infty} = \frac{C_{last}}{k_{el}}$$

The total AUC can be determined by:

$$AUC_{tot} = AUC_{\infty} = AUC_{0 \rightarrow t_{end}} + AUC_{t_{last} \rightarrow \infty}$$

Half-life, $t_{\frac{1}{2}}$ [h]:

The half-life $t_{\frac{1}{2}}$ is defined by the time required for plasma or serum concentration of aliskiren to be reduced by 50%. This parameter can be calculated from the elimination rate via equation:

$$t_{half} = \frac{\ln(2)}{k_{el}}$$

Volume of distribution, V_d [l]:

The volume of distribution V_d is a virtual compartment which describes the tendency of a drug to either circulate in plasma or to disperse to other tissue compartments. This parameter can be calculated with the given dose $dose_{ali}$ and the plasma concentration of aliskiren C_{ali} via equation:

$$V_d = \frac{dose_{ali}}{C_{ali}}$$

Clearance, Cl [$\frac{l}{h}$]:

Clearance describes the ability of the body to excrete a drug. This parameter is calculated by multiplying the rate of elimination k_{el} with the volume of distribution V_d , as described by following equation:

$$Cl = k_{el} \cdot V_d$$

Renal clearance, Cl_{Renal} [$\frac{l}{h}$]:

Renal clearance describes the process in which a drug is excreted by the kidneys. This parameter can be calculated by dividing the amount of aliskiren recovered in the urine (A_{urine}) over a certain period of time Δt by the AUC over the same period of time as described in equation:

$$Cl_{Renal} = \frac{A_{urine,\Delta t}}{AUC_{\Delta t}}$$

Hepatic clearance, $Cl_{Hepatic}$ [$\frac{l}{h}$]:

Hepatic clearance describes the process in which a drug is eliminated by the liver. This parameter can be calculated by subtracting the renal clearance from the total clearance via the following equation:

$$Cl_{Hepatic} = Cl_{total} - Cl_{Renal}$$

2.7 Effect of drug-drug interactions (DDI)

The pharmacokinetics of aliskiren vary depending on the drugs administered at the same time. Depending on their effect on the enzymes relevant for pharmacokinetics, the drugs can increase or decrease the absorption or also the metabolism of aliskiren. There are various drug classes such as ACE inhibitors, ARBs, P-gp inhibitors/inducers, CYP3A4 inhibitors/inducers or OATP inhibitors/inducers. Depending on the effect and the enzyme targeted, the pharmacokinetics and thus the influence of aliskiren can be influenced.

To determine the effect of an additionally administered drug, the ratios between the mean values of AUC and c_{max} for aliskiren administered alone and aliskiren with concomitantly administered drugs were calculated. These values were taken from the tables of the respective studies.

Table 5: **Types of effects based on the calculated ratios**

Ratio	Effect
ratio ≥ 5.0	strong induction ($\uparrow\uparrow\uparrow$)
$5.0 > \text{ratio} \geq 2.0$	moderate induction ($\uparrow\uparrow$)
$2.0 > \text{ratio} \geq 1.25$	weak induction (\uparrow)
$1.25 > \text{ratio} \geq 0.8$	no effect (\emptyset)
$0.8 > \text{ratio} \geq 0.5$	weak inhibition (\downarrow)
$0.5 > \text{ratio} \geq 0.2$	moderate inhibition ($\downarrow\downarrow$)
$0.2 > \text{ratio}$	strong inhibition ($\downarrow\downarrow\downarrow$)

Depending on the ratio between the mean values, a rough statement can be made about the effect. If the *ratio* is > 1 , it means that there was an increase in the certain mean value and a *ratio* < 1 indicates a corresponding reduction in the mean values after the coadministration with the drug. The following equation was used for the calculation of the ratios for the *AUC* and c_{max} ratios where the control represents the values for aliskiren administered alone and the drug for aliskiren in combination with other drugs:

$$\text{ratio} = \frac{\mu_{\text{drug}}}{\mu_{\text{control}}}$$

The standard deviation of the ratios (σ_{ratio}) can be approximated by using the ratio, the means (μ) for the control, and drug the SDs (σ) of the means:

$$\sigma_{\text{ratio}} \approx \text{ratio} \cdot \sqrt{\left(\frac{\sigma_{\text{control}}}{\mu_{\text{control}}}\right)^2 + \left(\frac{\sigma_{\text{drug}}}{\mu_{\text{drug}}}\right)^2}$$

The calculated ratios and the conditions listed in Table 5 can be used to determine the type and the strength of the effect on the *AUC* [28]. The symbols in parentheses were used to represent the varying effects of the drugs.

The two-sided t-test was used to compare the two means and determine the significance levels from the t-test results.

The value for the test statistic t was calculated using the following equation with the means μ_1 for aliskiren alone and μ_2 for aliskiren in combination with other drugs, the standard deviations σ_1 for aliskiren alone and σ_2 for aliskiren in combination with other drugs and the sample sizes n_1 for aliskiren alone and n_2 for aliskiren in combination with other drugs:

$$t = \frac{\mu_1 - \mu_2}{\sigma_{\text{pooled}} \times \sqrt{\frac{1}{n_1} + \frac{1}{n_2}}}$$

With the following definition for the pooled standard deviation σ_{pooled} :

$$\sigma_{\text{pooled}} = \sqrt{\frac{(n_1 - 1) \cdot \sigma_1^2 + (n_2 - 1) \cdot \sigma_2^2}{n_1 + n_2 - 2}}$$

The degrees of freedom df can be calculated from the sample sizes n_1 and n_2 using the following equation:

$$df = n_1 + n_2 - 2$$

The p-values, which provide insights into the relationship between the two groups, are determined using the t-statistic t and the degrees of freedom df . Once calculated, the p-values can be used to assess the significance level α :

- $p \leq 0.001$ (***)
- $p \leq 0.01$ (**)
- $p \leq 0.05$ (*)

The significance level α , represented by stars (*), is a critical threshold in hypothesis testing that determines the probability of rejecting the null hypothesis H_0 when it is actually true. It represents the risk of making a Type I error, which occurs when a true null hypothesis is incorrectly rejected. Commonly, the significance level is set at $\alpha = 0.05$, meaning there is a 5% risk of concluding an effect is significant when it might have occurred by chance.

The null hypothesis H_0 is the assumption of no effect, no difference, or no relationship. It is tested against the alternative hypothesis, which proposes the presence of an effect or difference. During hypothesis testing, a p -value is calculated to quantify the evidence against H_0 . If the p -value is smaller than α , the null hypothesis is rejected, and the result is considered statistically significant. Otherwise, H_0 is accepted. Two types of errors can occur in hypothesis testing:

- **Type I Error:** Rejecting H_0 when it is true (false positive).
- **Type II Error:** Accepting H_0 when it is false (false negative).

The choice of the significance level α balances the trade-off between these errors. Lowering the significance level reduces the risk of Type I errors but increases the risk of Type II errors.

After determining the effect of each drug on the pharmacokinetics of aliskiren, we can anticipate their effects on the enzymes (like P-gp, CYP3A4 and OATP2B1) which are playing important roles in the absorption and metabolism of aliskiren.

3 Results

This thesis presents the development of a physiologically-based model of aliskiren, which was used to investigate the influence of hepatorenal impairment and drug-drug interactions on its pharmacokinetics and pharmacodynamics. This chapter outlines the results of this work, including the curated data from clinical studies on aliskiren (Section 3.1), the creation of individual tissue-specific models that together comprise the whole-body model of aliskiren (Section 3.2), the methodology for model fitting (Section 3.3), and the performance of the model in predicting the pharmacokinetics and pharmacodynamics of aliskiren through simulation experiments (Section 3.4). Finally, the model was applied to explore the effects of hepatorenal impairment and drug-drug interactions on aliskiren’s pharmacokinetics and pharmacodynamics (Section 3.5).

3.1 Aliskiren data

The first step in building the model involved the curation of data from clinical studies. Articles were selected based on a systematic literature search, focusing on publications that included time course data and pharmacokinetic parameters for aliskiren. This search identified 51 studies from PKPDAI [44] and 124 studies from PubMed [46], with an additional 26 studies added manually.

A filtering process was used to ensure the data was relevant and high-quality. Duplicates and studies without full-text PDFs were removed first. The remaining studies had to meet specific criteria: they had to involve human participants, include time course and in vivo pharmacokinetic data, and address both healthy individuals and patients with hepatorenal dysfunction. Studies that were reviews, lacked pharmacokinetic data, or had very noisy data were excluded. In the end, one study was removed due to noisy data. See Figure 6 for more details.

This selection process resulted in 25 clinical studies being curated for the development and evaluation of the PK-DB model [5, 7, 11, 10, 22, 27, 40, 51, 50, 52, 60, 62, 64, 61, 63, 66, 71, 74, 73, 68, 69, 67, 72, 78, 86]. These studies provided the foundation for the modeling work and offered detailed insights into aliskiren’s pharmacokinetics under different conditions.

The curated dataset included diverse information, such as dosing protocols, routes of administration, participant health status, co-administered drugs, and brief descriptions of the studies. Each study was assigned a unique identifier in the PK-DB database (PK-DB ID) and linked to its corresponding PubMed ID (PMID), ensuring straightforward access to the data. To promote transparency and reproducibility, all curated datasets were made publicly available as open data. Table 6 summarizes the curated studies, highlighting key details such as dosing protocols, participant health conditions, and co-administered drugs. These curated data formed the foundation of the aliskiren model, enabling comprehensive analysis and simulation of its pharmacokinetics and pharmacodynamics under various clinical scenarios.

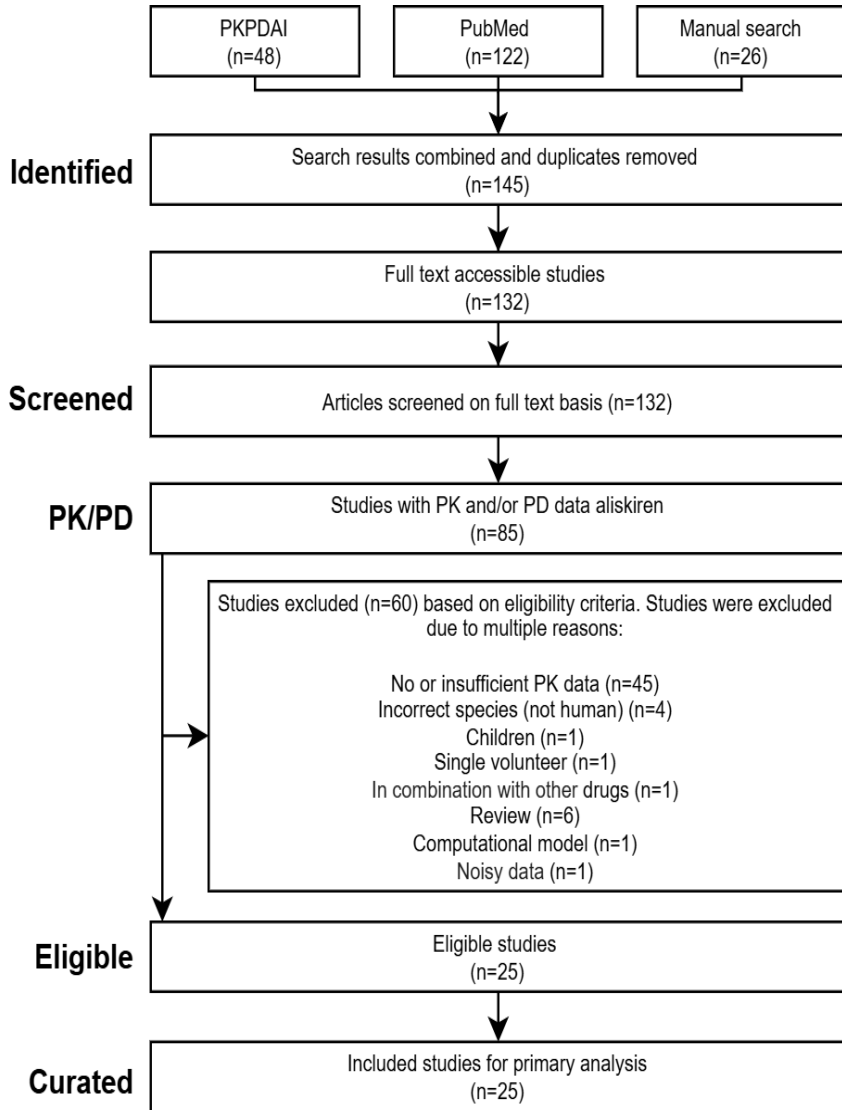


Figure 6: PRISMA flow diagram. This diagram outlines the data selection process for the pharmacokinetics (PK) and pharmacodynamics (PD) dataset of aliskiren. A total of 145 studies were identified from PubMed (n=122), PKPDAI (n=48), and manual searches (n=26), with duplicates removed. After screening 132 full-text articles, 85 studies with PK/PD data were assessed for eligibility. Of these, 60 were excluded due to reasons such as insufficient PK data (n=45), non-human studies (n=4), or other criteria (e.g., reviews, noisy data). Ultimately, 25 eligible studies were curated for the primary analysis (see Table 6).

Table 6: Overview of data used for the modelling. This table summarizes the studies included in the modeling of aliskiren pharmacokinetics and pharmacodynamics. It provides key details such as the dosing protocol (single dose, multiple doses, or both), the administered dose (in mg), the health status of participants (e.g., healthy, hepatic impairment, renal impairment, or type 2 diabetes), and any co-administered drugs (DDI). The included studies represent diverse conditions to ensure a comprehensive dataset, covering both healthy individuals and specific subpopulations. Each study is identified by its PMID, PK-DB ID, and relevant dosing and participant characteristics.

Study	PMID	PK-DB ID	dosing	dose [mg]	healthy	DDI
Ayalasomaya2008a [5]	18234150	PKDB00917	multiple	300	✓	allopurinol celecoxib cimetidine
Balcarek2014 [7]	24470465	PKDB00933	multiple	300	✓	
Burckhardt2014 [11]	24788577	PKDB00854	single	300	✓	
Burckhardt2014a [10]	24739274	PKDB00934	single	300	✓	
Fisher2008 [22]	18559696	PKDB00859	single	75, 150, 300, 600	✓	
Hu2010 [27]	20192280	PKDB00855	both	75, 150, 300, 600	✓	
Nussberger2002 [40]	11799102	PKDB00860	multiple	40, 80, 160, 640	✓	
Rebello2011 [51]	20413453	PKDB00861	single	300	✓	verapamil
Rebello2011a [50]	21406600	PKDB00862	single	75	✓	cyclosporine
Rebello2012 [52]	22124880	PKDB00863	single	300	✓	
Tapaninen2010 [60]	20664534	PKDB00918	single	150	✓	grapefruit juice
Tapaninen2010a [62]	20496145	PKDB00937	single	150	✓	
Tapaninen2010b [64]	20179914	PKDB00864	single	150	✓	rifampicin
Tapaninen2011 [61]	20400651	PKDB00865	single	150	✓	itraconazole
Tapaninen2011a [63]	21204914	PKDB00866	single	150	✓	apple juice
						orange juice
						HCTZ
Vaidyanathan2006 [66]	17073832	PKDB00681	multiple	300	✓	valsartan
						ramipril
						amlodipine
Vaidyanathan2006a [71]	17118124	PKDB00867	both	300	✓	
					✓	
Vaidyanathan2007 [74]	17244770	PKDB00868	single	300	(hepatic impairment)	
Vaidyanathan2007a [73]	17389554	PKDB00869	single	300	✓	
Vaidyanathan2007b [68]	17655373	PKDB00870	both	300	✓	irbesartan
					(renal impairment)	digoxin
Vaidyanathan2008a [69]	18784280	PKDB00935	multiple	300	✓	atorvastatin
						ketoconazole
Vaidyanathan2008b [67]	19035874	PKDB00936	multiple	300	✓	furosemide
						ISMN
Vaidyanathan2008c [72]	18786303	PKDB00871	multiple	300	✓	metformin
						pioglitazone
Waldmeier2007 [78]	17510248	PKDB00872	single	300	✓	fenofibrate
Zhao2006 [86]	17048976	PKDB00873	single	300	✓	(type 2 diabetes)

3.2 Computational model

3.2.1 Model overview

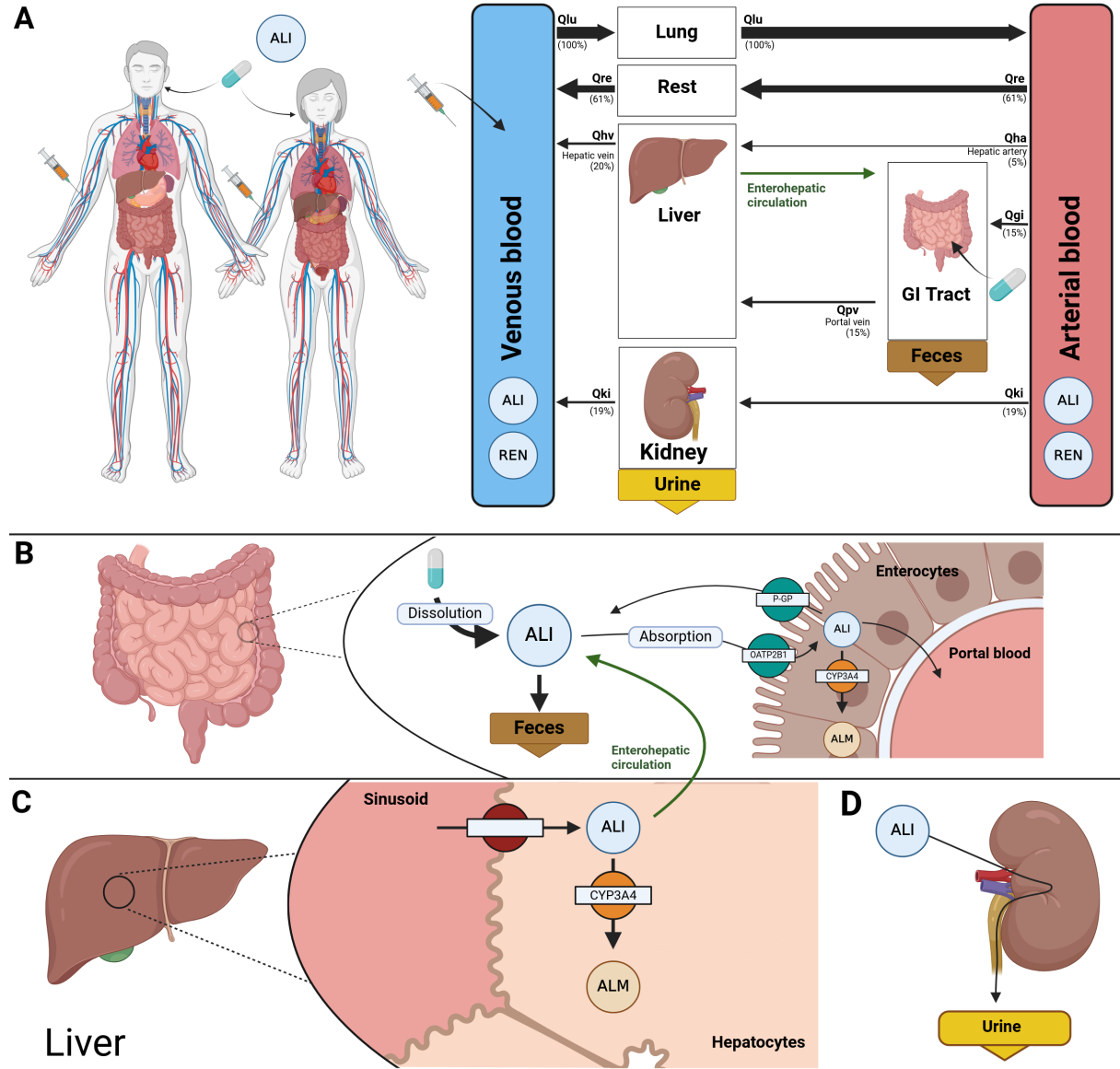


Figure 7: PBPK model of aliskiren (ALI).A**)** A whole-body PBPK model representing blood flow through the circulatory system, connecting key organs. Only the most relevant organs were explicitly modeled, while remaining organs were grouped into a "rest" compartment. Aliskiren is administered orally. **B)** The intestinal model includes the processes of dissolution, absorption, and excretion into feces. Aliskiren is absorbed into the blood through enterocytes but can be reduced by efflux transporters like P-gp in these cells, which pump it back into the intestine. Some aliskiren is also metabolized within the enterocytes by the enzyme CYP3A4. Enteropathic circulation further influences the availability of aliskiren. **C)** In the liver, aliskiren can be metabolized by CYP3A4 or eliminated into bile, contributing to enteropathic circulation. **D)** Urinary excretion of aliskiren is modeled through kidney elimination.

3.2.2 Intestine model

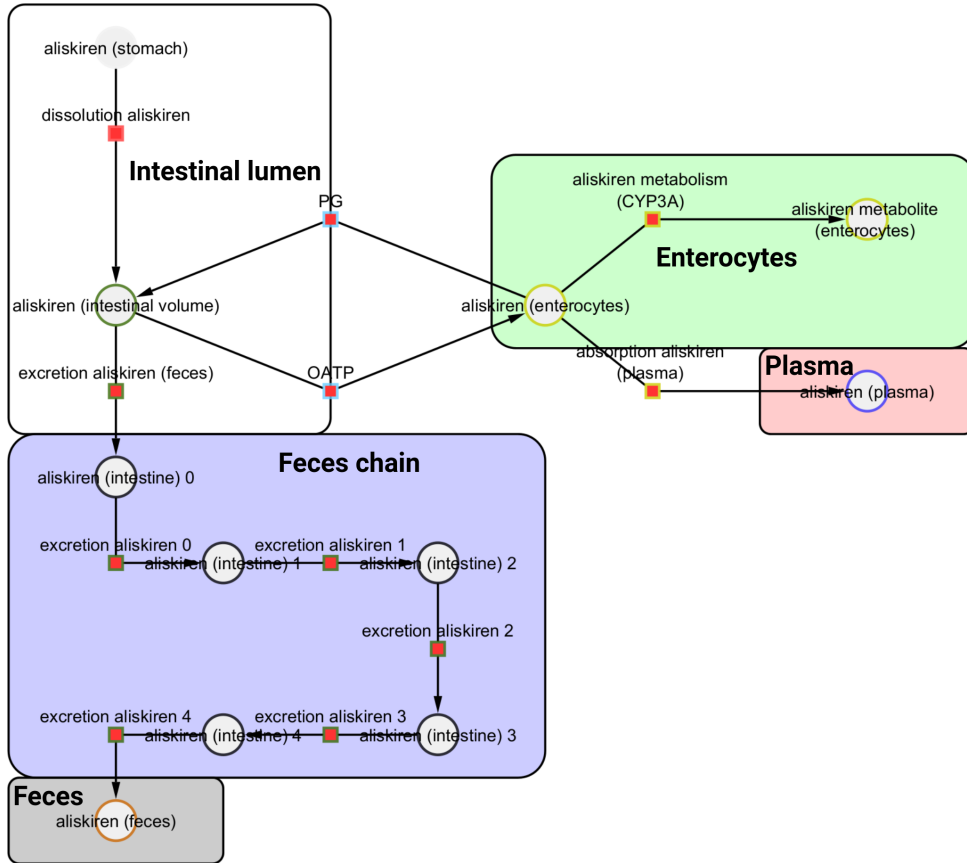


Figure 8: **Intestine model.** Aliskiren is transported from the intestinal lumen into the enterocytes by OATP2B1. Simultaneously, a reverse transport of aliskiren from the enterocytes back into the intestinal lumen via P-glycoprotein takes place. From the enterocytes aliskiren can enter the systemic circulation (plasma) or undergoes a metabolism via CYP3A4. Unabsorbed aliskiren is excreted via the feces.

Dissolution of aliskiren:

Dissolution is the process where a drug dissolves in a solvent, making it ready for absorption and therapeutic action. In this process, aliskiren moves from the stomach to the intestinal lumen, where it dissolves. The equation for the dissolution of aliskiren ($dissolution_{ali}$, [$\frac{mmole}{min}$]) calculates the amount of aliskiren dissolving per minute, expressed in millimoles, based on the dose administered ($PODOSE_{ali}$, [mg]), the molecular weight of aliskiren (Mr_{ali} , [$\frac{g}{mmole}$]) and the rate of dissolution ($Ka_{dis,ali}$, [$\frac{1}{hr}$]). To express the rate of dissolution in terms of minutes, the unit is converted by dividing the rate constant by the factor $60 \frac{min}{hr}$. This ensures consistency in the calculation, reflecting the dissolution process in millimoles per minute.

$$dissolution_{ali} = \frac{Ka_{dis,ali}}{60 \frac{min}{hr}} \cdot \frac{PODOSE_{ali}}{Mr_{ali}}$$

Aliskiren import into the lumen:

The import of aliskiren describes the process where aliskiren is transported from the intestinal lumen into the enterocytes via organic anion-transporting polypeptides (OATP). In this process,

aliskiren moves from the lumen, where it is dissolved, into the enterocytes for further absorption. The rate of aliskiren import ($ALIIM$, [$\frac{mmole}{min}$]) is determined by the product of the activity of OATP (f_{oatp} , dimensionless), the rate constant for aliskiren import ($ALIIM_k$, [$\frac{1}{min}$]), the gut volume (V_{gu} , [l]), and the concentration of aliskiren in the intestinal lumen (ali_{lumen} , [$\frac{mmole}{l}$]). Following equation is used to define the import:

$$ALIIM = f_{oatp} \cdot ALIIM_k \cdot V_{gu} \cdot ali_{lumen}$$

Aliskiren efflux transport:

Efflux transport refers to the process by which a drug is actively pumped from the enterocytes back into the intestinal lumen. The rate of the aliskiren efflux transport ($ALIPG$, [$\frac{mmole}{min}$]) is determined by the product of the activity of the P-glycoprotein (f_{pg} , dimensionless), the rate constant for aliskiren export by P-glycoprotein ($ALIPG_k$, [$\frac{1}{min}$]), the volume of the intestinal lining (enterocytes) (V_{entero} , [l]), and the concentration of aliskiren in the enterocytes (ali_{entero} , [$\frac{mmole}{l}$]).

$$ALIPG = f_{pg} \cdot ALIPG_k \cdot V_{entero} \cdot ali_{entero}$$

Metabolism via CYP3A4 in enterocytes:

A small amount of aliskiren can be metabolized by the CYP3A4 enzyme in the enterocytes. The rate of the aliskiren metabolism via CYP3A4 ($ALIMET$, [$\frac{mmole}{min}$]) is determined by the product of the activity of CYP3A4 (f_{cyp3a4} , dimensionless), the rate constant for aliskiren metabolism ($ALIMET_k$, [$\frac{1}{min}$]), the volume of the enterocytes (V_{entero} , [l]), and the concentration of aliskiren in the enterocytes (ali_{entero} , [$\frac{mmole}{l}$]).

$$ALIMET = f_{cyp3a4} \cdot ALIMET_k \cdot V_{entero} \cdot ali_{entero}$$

Fecal excretion of aliskiren:

Aliskiren is mainly excreted in the feces (unabsorbed fraction). The rate of the aliskiren excretion in the feces ($ALIEXC$, [$\frac{mmole}{min}$]) is determined by the product of the rate constant for aliskiren fecal excretion ($ALIEXC_k$, [$\frac{1}{min}$]), the gut volume (V_{gu} , [l]), and the concentration of aliskiren in the lumen (ali_{lumen} , [$\frac{mmole}{l}$]). Following equation can be used to define $ALIEXC$:

$$ALIEXC = ALIEXC_k \cdot V_{gu} \cdot ali_{lumen} \quad (1)$$

Absorption of aliskiren in the plasma:

Absorption describes the process of the aliskiren transport in the enterocytes to the plasma (blood). The rate of the aliskiren absorption ($ALIABS$, [$\frac{mmole}{min}$]) is determined by the product of the rate constant for aliskiren absorption ($ALIABS_k$, [$\frac{1}{min}$]), the volume of the enterocytes (V_{entero} , [l]), and the concentration of aliskiren in the enterocytes (ali_{entero} , [$\frac{mmole}{l}$]). The equation to describe the process can be written as:

$$ALIABS = ALIABS_k \cdot V_{entero} \cdot ali_{entero}$$

3.2.3 Kidney model

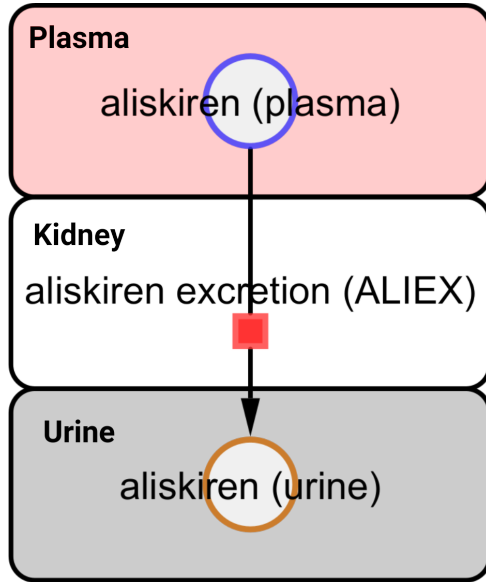


Figure 9: **Kidney model.** Renal excretion pathway of aliskiren via the kidney into the urine.

Urinary excretion of aliskiren:

Aliskiren is also excreted in small amounts through the urine. The rate of the aliskiren excretion in the urine ($ALIEX$, [$\frac{mmole}{min}$]) is determined by the product of the parameter for the renal function ($f_{renal\ function}$, dimensionless), the rate constant for aliskiren urinary excretion ($ALIEX_k$, [$\frac{1}{min}$]), the kidney volume (Vki , [l]), and the concentration of aliskiren in the plasma (ali_{ext} , [$\frac{mmole}{l}$]). The equation describing the urinary excretion rate is:

$$ALIEX = f_{renal\ function} \cdot ALIEX_k \cdot Vki \cdot ali_{ext}$$

3.2.4 Liver model

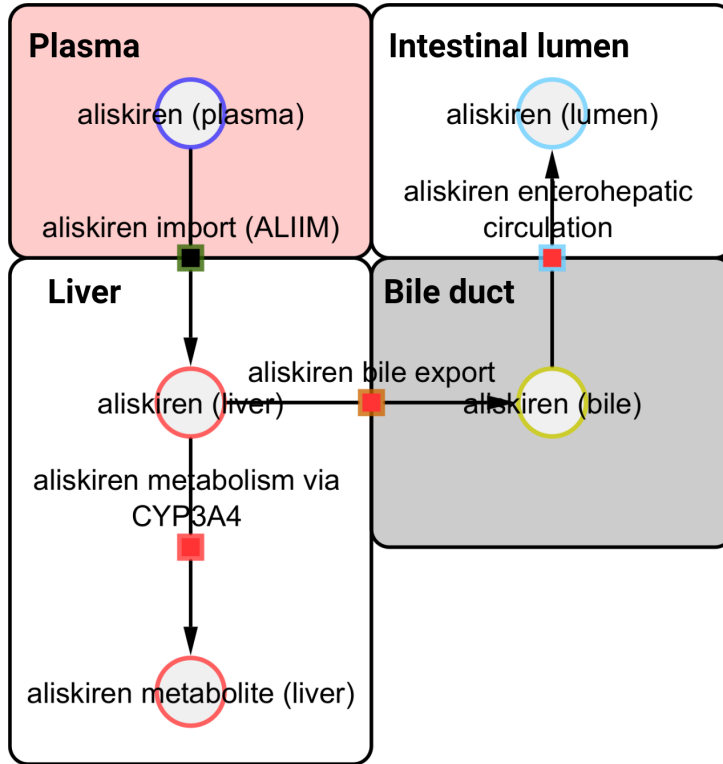


Figure 10: Liver model. Aliskiren is excreted into the bile and can reach the intestinal lumen via the enterohepatic circulation (EHC). The metabolism of aliskiren via CYP3A4 can also take place in the hepatocytes.

Aliskiren import into the liver:

Aliskiren import into the liver describes the process by which the drug is transported from the plasma into liver cells, known as hepatocytes. The rate of this import, denoted as ($ALIIM$, $\frac{\text{mmole}}{\text{min}}$), depends on several key factors: the maximal transport capacity of liver transporters ($ALIIM_{Vmax}$, $\frac{\text{mmole}}{\text{min}\cdot\text{l}}$), which represents the highest rate at which transporters can move aliskiren into the liver; the Michaelis constant ($ALIIM_{Km,ali}$, $\frac{1}{\text{min}}$), which indicates the plasma concentration of aliskiren at which the transport rate is half-maximal; the liver volume (Vli , l), and the concentration of aliskiren in the plasma (ali_{ext} , $\frac{\text{mmole}}{\text{l}}$), and in the liver (ali , mmole). This equation below is based on the Michaelis-Menten kinetic and the saturation. The equation for this process is given by:

$$ALIIM = \frac{ALIIM_{Vmax}}{ALIIM_{Km,ali}} \cdot Vli \cdot \frac{ali_{ext} - ali}{1 + \frac{ali_{ext}}{ALIIM_{Km,ali}} + \frac{ali}{ALIIM_{Km,ali}}}$$

This equation reflects a reversible Michaelis-Menten process, where the direction of transport depends on the concentration gradient between the plasma and the liver ($ali_{ext} - ali$). If the plasma concentration of aliskiren (ali_{ext}) is higher, the drug flows into the liver. Conversely, if the liver concentration (ali) is higher, aliskiren may flowback into the plasma. The denominator, $1 + \frac{ali_{ext}}{ALIIM_{Km,ali}} + \frac{ali}{ALIIM_{Km,ali}}$, accounts for the saturation of transporters, which limits the rate of transport at higher substrate concentrations.

Metabolism via CYP3A4 in the liver:

The metabolism of aliskiren in the liver is primarily catalyzed by the enzyme CYP3A4. The rate of this metabolism (ALM , [$\frac{mmole}{min}$]) depends on the activity of CYP3A4 (f_{cyp3a4} , dimensionless), the maximal velocity of the aliskiren metabolism (ALM_{Vmax} , [$\frac{mmole}{min \cdot l}$]), the Michaelis constant for aliskiren import ($ALIIM_{Km,ali}$, [$\frac{1}{min}$]), the liver volume (Vli , [l]), and the concentration of aliskiren in the liver (ali , [$\frac{mmole}{l}$]). Following equation is used to describe the metabolism rate:

$$ALM = f_{cyp3a4} \cdot ALM_{Vmax} \cdot Vli \cdot \frac{ali}{(ali + ALM_{Km,ali})}$$

This equation describes an irreversible Michaelis-Menten process (MMK, Irreversible), as the reaction progresses in a single direction from aliskiren to its metabolized products. At low concentrations of aliskiren in the liver (ali), the metabolism rate increases proportionally with the concentration. However, as the concentration rises and CYP3A4 becomes saturated, the rate of metabolism approaches a maximum value ($f_{cyp3a4} \cdot ALM_{Vmax} \cdot Vli$).

Bile export of aliskiren:

Aliskiren is excreted into bile by the liver through specialized transport proteins. After being released into the bile, it travels to the intestine, where the majority is eliminated in the feces, while a small portion may be reabsorbed into the bloodstream. This recycling process, known as enterohepatic circulation, can slightly prolong aliskiren's presence in the body. Proper liver function and bile flow are crucial for this elimination pathway, as they help clear aliskiren from the system. The rate of the aliskiren bile export ($ALIEX$, [$\frac{mmole}{min}$]) is determined by the product of the rate constant of the aliskiren bile export ($ALIEX_k$, [$\frac{1}{min}$]), the liver volume (Vli , [l]), and the concentration of aliskiren in the liver (ali , [$\frac{mmole}{l}$]). The equation is as follows:

$$ALIEX = ALIEX_k \cdot Vli \cdot ali$$

Enterohepatic circulation (EHC):

Enterohepatic circulation (EHC) refers to the recycling process in which a compound, such as aliskiren, moves between the liver, bile, intestines, and bloodstream. During this process, aliskiren excreted into bile can be reabsorbed into the bloodstream after reaching the intestine, contributing to its prolonged systemic presence. The rate of the enterohepatic circulation ($ALIEHC$, [$\frac{mmole}{min}$]) is directly linked to the rate of bile export ($ALIEX$, [$\frac{mmole}{min}$]), as it represents the same flow of aliskiren entering the intestines. Therefore, $ALIEHC$ is defined as:

$$ALIEHC = ALIEX$$

3.2.5 Renin inhibition

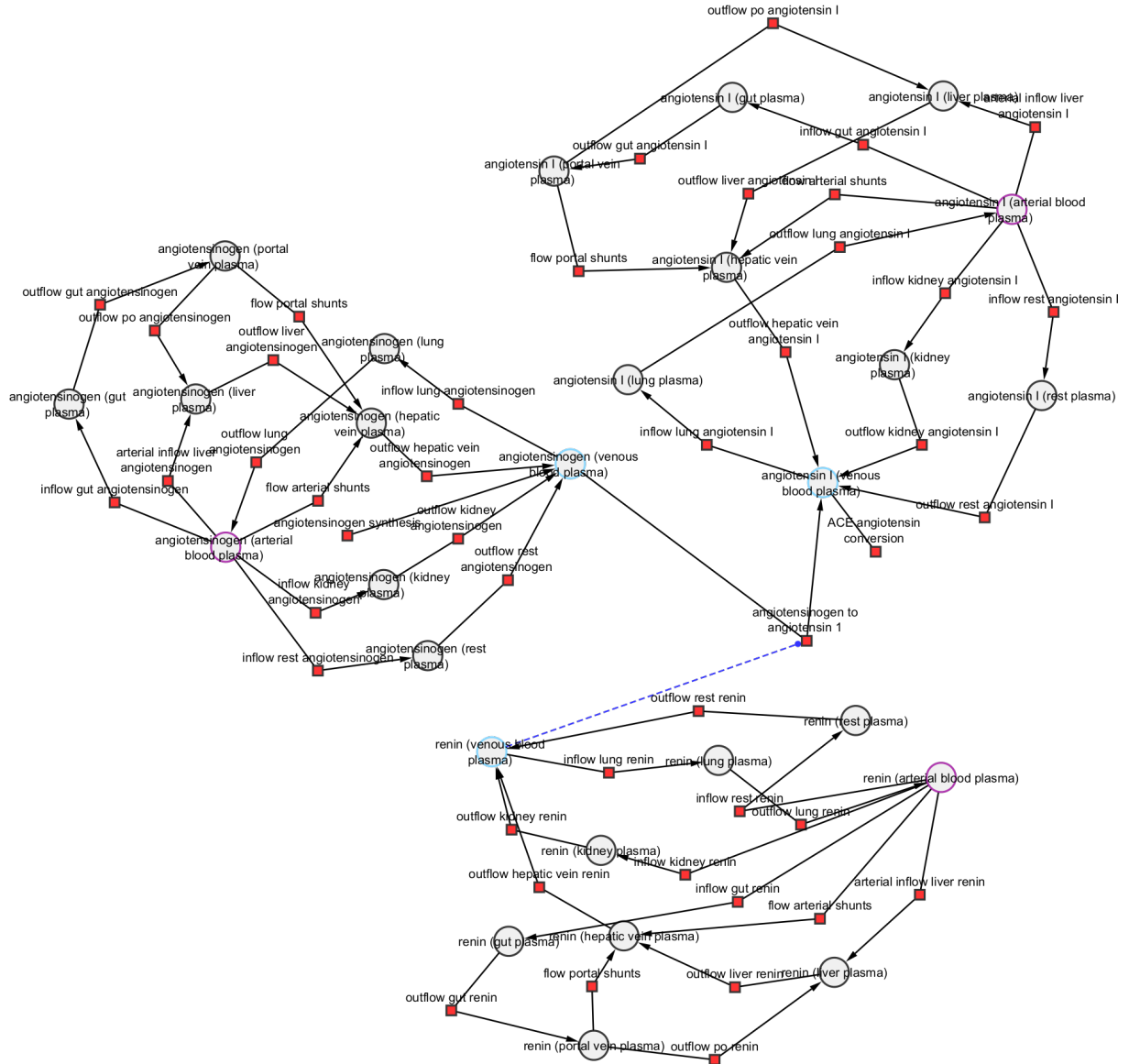


Figure 11: **Overview of the RAAS model.** This figure illustrates the renin-angiotensin-aldosterone system (RAAS) model, detailing the flow and regulation of key components such as angiotensinogen, angiotensin I, and renin. The model depicts the conversion of angiotensinogen to angiotensin I by renin and subsequent downstream processes critical for vasoconstriction and aldosterone release.

Arrows indicate the directional flow of substances through compartments such as the liver, lungs, kidneys, and blood plasma. Red squares highlight key regulatory points in the system, providing a clear visualization of the interconnected pathways within the RAAS. This diagram emphasizes the physiological processes involved in blood pressure regulation and fluid balance. For a visualization of the RAAS, refer to Figure 1.

3.2.6 Whole-body model

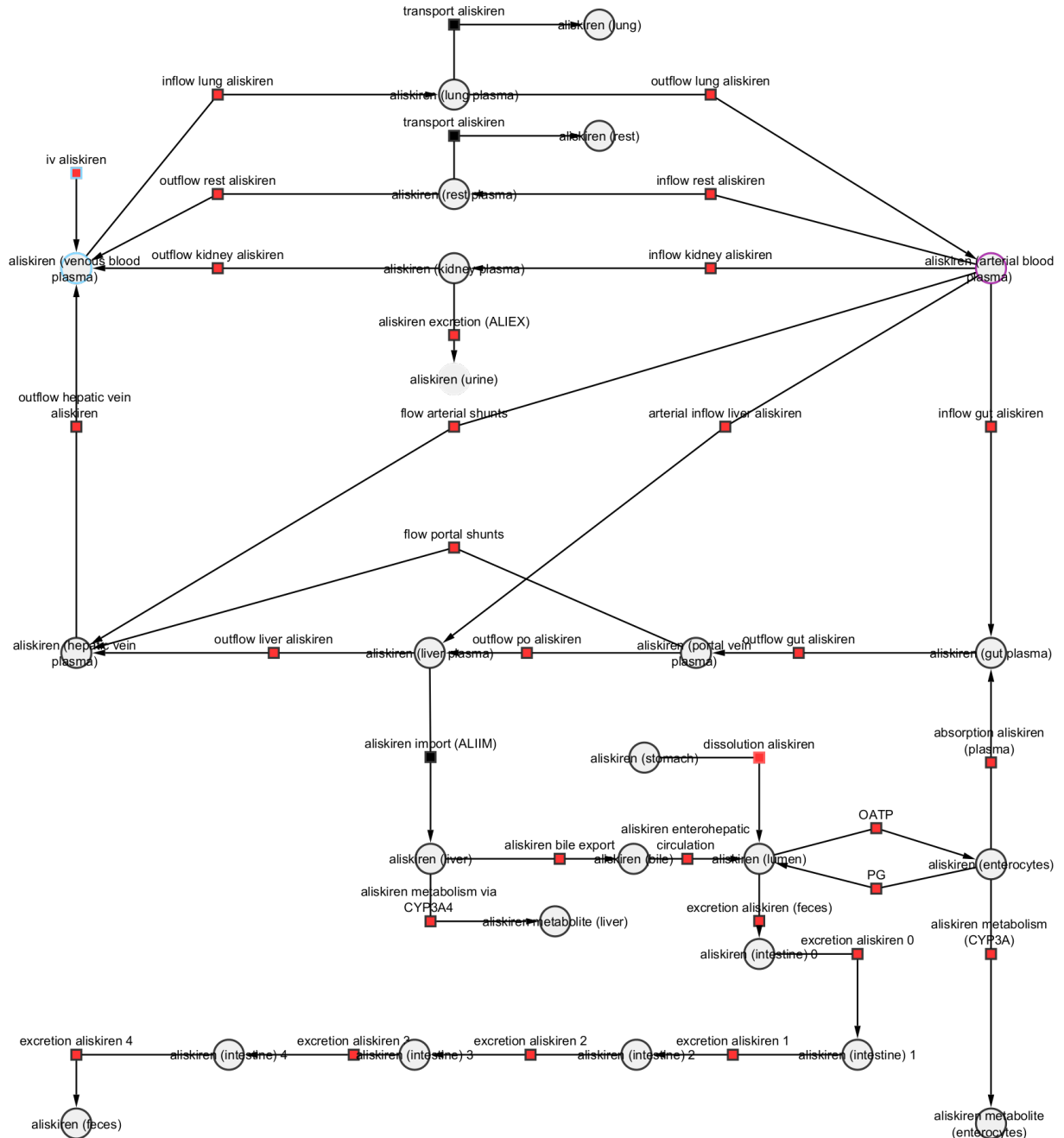


Figure 12: Overview of the whole-body model. This figure illustrates the whole-body model of aliskiren, integrating key tissue compartments such as the gut, liver, kidney, and lung. It demonstrates the processes of absorption, distribution, metabolism, and excretion. Aliskiren is absorbed in the gut, where it undergoes dissolution and interacts with transporters like P-glycoprotein. It is then distributed through arterial and venous circulation to various tissues, including the liver and kidney. Metabolism primarily occurs in the liver via the CYP3A4 enzyme, producing metabolites. Excretion pathways include renal elimination through urine and biliary/fecal excretion. Arrows represent the flow of aliskiren through the system, while red squares indicate key control points in the pharmacokinetic process. For a more detailed visualization of aliskiren's distribution throughout the body, refer to Figure 7.

Table 7: **Overview of the main parameters for the PBPK model.** This table provides a detailed overview of the main parameters applied in the model, including their descriptions, values, and units. These parameters represent key physiological and pharmacokinetic aspects, such as body characteristics, organ-specific blood flow, transporter activities, and drug-specific processes like absorption, metabolism, and excretion. Prefixes GU, LI, and KI denote parameters specific to the intestinal, liver, and kidney models, respectively.

Parameter	Description	Value	Unit
<i>BW</i>	Body weight	75.0	<i>kg</i>
<i>HEIGHT</i>	Body height	170.0	<i>cm</i>
<i>COBW</i>	Cardiac output per bodyweight	1.548	<i>ml</i> <i>s·kg</i>
<i>COHRI</i>	Increase of cardiac output per heartbeat	150.0	<i>ml</i>
<i>HCT</i>	Hematocrit	0.51	—
<i>HR</i>	Heart rate	70.0	<i>1</i> <i>min</i>
<i>HRrest</i>	Heart rate while resting	70.0	<i>1</i> <i>min</i>
<i>KI_frenalfunction</i>	Parameter for renal function	1.0	—
<i>fcirrhosis</i>	Scaling factor of the severity of cirrhosis	0.0 [0, 0.95]	—
<i>LI_fcyp3a4</i>	Scaling factor of cyp3a4 activity (liver)	1.0	—
<i>GU_fcyp3a4</i>	Scaling factor of CYP3A4 activity (intestine)	1.0	—
<i>GU_foatp</i>	Scaling factor of OATP transporter activity	1.0	—
<i>GU_fg_p</i>	Scaling factor of P-gp transporter activity	1.0	—
<i>flumen</i>	Fraction lumen of intestine	0.9	—
<i>FQgu</i>	Gut fractional tissue blood flow	0.18	—
<i>FQh</i>	Hepatic (venous side) fractional tissue blood flow	0.215	—
<i>FQki</i>	Kidney fractional tissue blood flow	0.19	—
<i>FQlu</i>	Lung fractional tissue blood flow	1.0	—
<i>FVar</i>	Arterial fractional tissue volume	0.0257	<i>l</i> <i>kg</i>
<i>FVgu</i>	Gut fractional tissue volume	0.0171	<i>l</i> <i>kg</i>
<i>FVhv</i>	Hepatic venous fractional tissue volume	0.001	<i>l</i> <i>kg</i>
<i>FVki</i>	Kidney fractional tissue volume	0.0044	<i>l</i> <i>kg</i>
<i>FVli</i>	Liver fractional tissue volume	0.021	<i>l</i> <i>kg</i>
<i>FVlu</i>	Lung fractional tissue volume	0.0076	<i>l</i> <i>kg</i>
<i>FVpo</i>	Portal fractional tissue volume	0.001	<i>l</i> <i>kg</i>
<i>FVve</i>	Venous fractional tissue volume	0.0514	<i>l</i> <i>kg</i>
<i>Fblood</i>	Blood fraction of organ volume	0.02	—
<i>Mr_{ali}</i>	Molecular weight of aliskiren	551.7583	<i>g</i> <i>mole</i>
<i>GU_ALIABS_k</i>	Rate of aliskiren absorption	0.1	<i>1</i> <i>min</i>
<i>GU_ALIMET_k</i>	Rate of aliskiren metabolism	0.1	<i>1</i> <i>min</i>
<i>GU_F_{ali,abs}</i>	Fraction of absorbed aliskiren	0.05	—
<i>GU_F_{ali,met}</i>	Fraction of metabolized aliskiren in the enterocytes	0.5	—
<i>GU_Ventero</i>	Volume of the enterocytes	0.12825	<i>l</i>
<i>GU_Vstomach</i>	Volume of the stomach	1.0	<i>l</i>
<i>GU_Kadis,ali</i>	Dissolution aliskiren	2.0	<i>1</i> <i>hr</i>
<i>KI_ALIEX_k</i>	Rate of urinary excretion of aliskiren	1.0	<i>1</i> <i>min</i>
<i>LI_ALIEX_k</i>	Rate of aliskiren export in bile	0.0001	<i>1</i> <i>min</i>
<i>LI_ALIIM_{Km,ali}</i>	Km of aliskiren import	0.1	<i>mmole</i> <i>l</i>
<i>LI_ALIIM_{Vmax}</i>	Vmax of aliskiren import	100.0	<i>mmole</i> <i>min·l</i>
<i>LI_ALM_{Km,ali}</i>	Km of aliskiren metabolism	0.1	<i>mmole</i> <i>l</i>
<i>LI_ALM_{Vmax}</i>	Vmax of aliskiren metabolism	1.0	<i>mmole</i> <i>min·l</i>
<i>LI_Vbi</i>	Volume of the bile	1.0	<i>l</i>
<i>ti_{ali}</i>	Injection time for aliskiren	10.0	<i>s</i>

3.2.7 Model of hepatic and renal impairment

Hepatic impairment (cirrhosis)

Cirrhosis was integrated into the model by introducing a parameter for cirrhosis ($f_{cirrhosis}$). This parameter was used to modify the liver model and assess the different effects depending on the stages of cirrhosis. To classify these stages, *Vaidyanathan et al.*'s study employed the CTP score, with scores of 5 to 6 representing mild hepatic impairment, 7 to 9 indicating moderate hepatic impairment, and 10 to 15 corresponding to severe hepatic impairment [68].

By modifying this parameter, the model can replicate various degrees of hepatic function, enabling the observation of substantial differences in the pharmacokinetics of aliskiren between healthy individuals and those with cirrhosis. The values assigned to the parameter $f_{cirrhosis}$ in all hepatic scans were 0.00 for the control group, 0.39 for mild cirrhosis (CTP A), 0.69 for moderate cirrhosis (CTP B), and 0.81 for severe cirrhosis (CTP C). The different stages of cirrhosis were visualized with the colors shown in Figure 4 .

Renal impairment

Renal impairment was simulated using the parameter $KI_{-f_{renalfunction}}$ to adjust the kidney's ability to excrete aliskiren in the urine. The parameter values for mild, moderate, and severe renal impairment were determined by dividing the creatinine clearance ($CLCR$) of individuals with renal impairment by the creatinine clearance of healthy subjects [47].

The study by *Vaidyanathan et al.* classified renal impairment based on creatinine clearance, with mild impairment corresponding to a clearance of 50–80 mL/minute, moderate impairment defined as 30–49 mL/minute, and severe impairment as less than 30 mL/minute. Healthy subjects were identified as having a creatinine clearance of at least 80 mL/minute [68].

To ensure simplicity and consistency, the parameter values for $KI_{-f_{renalfunction}}$ were set at 1.00 for the control group, 0.69 for mild renal impairment, 0.32 for moderate renal impairment, and 0.19 for severe renal impairment. These values align with those commonly used in other PBPK models. The different stages of renal impairment were visualized with the colors shown in Figure 5 .

3.3 Parameter fitting

Plasma, serum, and urine aliskiren time course data from curated studies (see Table 6 for details) were used to fit key model parameters, as summarized in Table 8. The fitted parameters include rates related to tissue distribution, partition coefficients, and key pharmacokinetic processes such as urinary excretion, absorption, fecal excretion, and bile export of aliskiren. All curated plasma, serum, and urine aliskiren data were included in the parameter fitting process. Table 8 provides a comprehensive overview of the fitted parameters employed in the model to enhance the accuracy of simulations.

Table 8: **Parameters fitted in the PBPK Model.** Summary of fitted parameters, including descriptions, optimal values (rounded to the fourth digit), bounds, and units. Prefixes GU, LI, and KI denote intestinal, liver, and kidney model parameters, respectively.

Parameter	Description	Optimal value	Lower bound	Upper bound	Unit
$ftissue_{ali}$	Rate of tissue distribution	0.01	0.01	10	$\frac{l}{min}$
Kp_{ali}	Tissue/plasma partition coefficient	1111.14	10	5E3	—
KI_ALIEX_k	Rate of aliskiren urinary excretion	0.1912	0.1	10	$\frac{1}{min}$
GU_ALIIM_k	Rate of aliskiren import into enterocytes	0.6088	1E-4	1	$\frac{1}{min}$
GU_ALIPG_k	Rate of aliskiren PG export	0.0078	1E-4	1	$\frac{1}{min}$
GU_ALIABS_k	Rate of aliskiren absorption	0.0079	1E-4	1	$\frac{1}{min}$
GU_ALIEXC_k	Rate of aliskiren fecal excretion	0.7498	1E-4	1	$\frac{1}{min}$
LI_ALIEX_k	Rate for aliskiren export into bile	0.0023	1E-4	1	$\frac{1}{min}$

3.4 Model performance

The performance of the developed PBPK model for aliskiren was evaluated by comparing predicted time courses with curated time course data from clinical studies under various dosing protocols. The following sections describe the model’s performance for each tissue and present simulations of plasma, serum, and urine aliskiren concentrations for single oral doses and multiple oral doses, where urine data is available.

In the plots, solid lines represent the simulated data, while experimental data points are connected using dashed lines to ensure a clear comparison between model predictions and observed clinical data. Experimental errors, when available, are displayed as standard deviation (SD). The figure legends provide details about the administered dose of aliskiren, co-administered drugs, the sample size (denoted as n), and the standard deviation (SD), as far as the curated data reported it.

Figures 13 and 14 illustrate the dose dependency of aliskiren concentrations across different tissues and compartments for oral (PO) and intravenous (IV) administration, respectively. These figures demonstrate how varying doses of aliskiren (75 mg, 150 mg, 300 mg, and 600 mg) affect its distribution, metabolism, and excretion.

Figure 13 presents the results for oral administration (PO), showing the following parameters in order: aliskiren concentration in plasma, total plasma concentration (including metabolites), metabolite concentration in the intestine, aliskiren concentration in urine, total concentration in urine (aliskiren and metabolites), metabolite concentration in the liver, aliskiren concentration in feces, and total concentration in feces (aliskiren and metabolites). These plots highlight the time-dependent behavior of aliskiren and its metabolites under oral dosing conditions.

Figure 14 focuses on intravenous administration (IV), showcasing the same parameters as in Figure 13. However, due to the direct entry of aliskiren into the bloodstream, the plots show higher peak concentrations in plasma and faster distribution. The plots also demonstrate the time-dependent kinetics of aliskiren and its metabolites, including their presence in the intestine, urine, liver, and feces.

These comprehensive simulations provide a clear comparison of aliskiren’s pharmacokinetics for oral and intravenous administration under varying dose levels.

DoseDependency (PO)

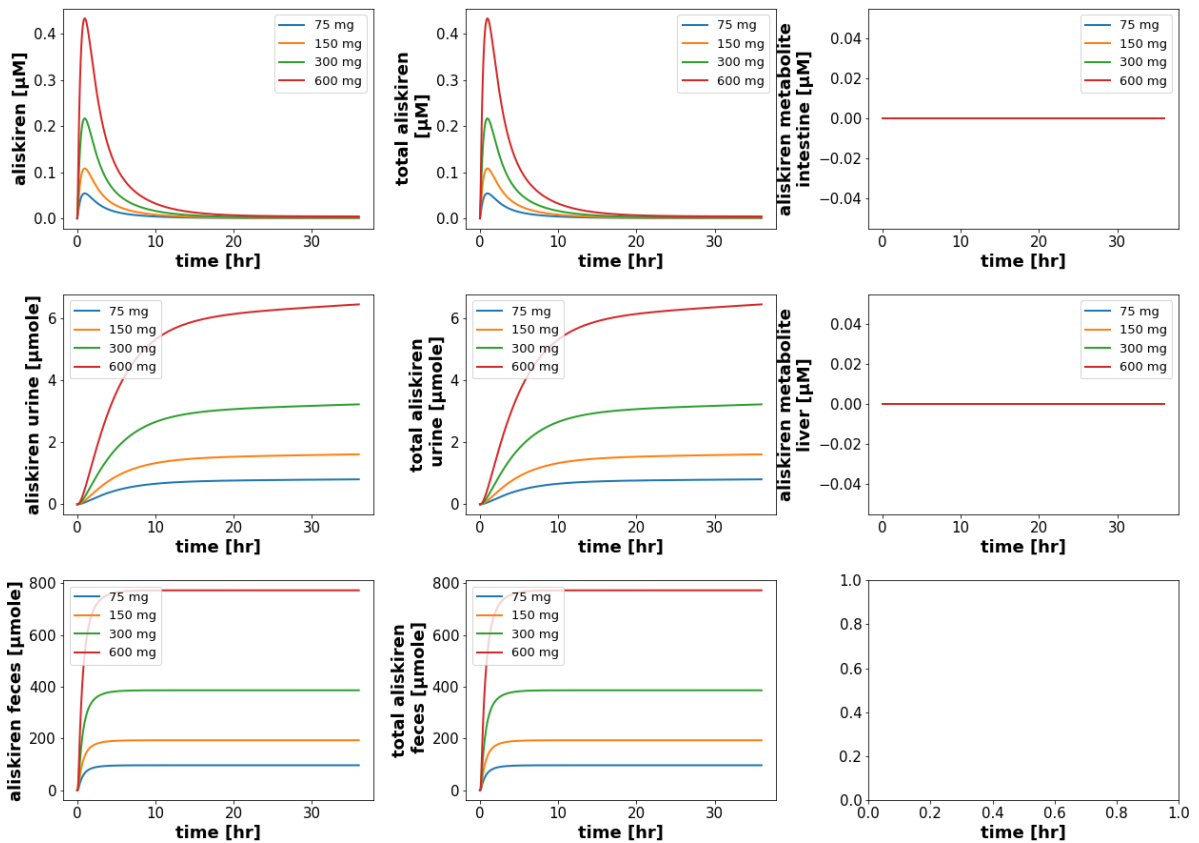


Figure 13: **Dose Dependency Experiment for oral application (po).** Simulated time-course profiles of aliskiren and total aliskiren (aliskiren and metabolites) concentrations in various compartments under varying oral dose levels (75 mg, 150 mg, 300 mg, and 600 mg). The panels illustrate: (top-left) aliskiren concentration in plasma, (top-center) total aliskiren concentration in plasma, (top-right) total aliskiren concentration in the intestine, (middle-left) aliskiren in urine, (middle-center) total aliskiren in urine, (middle-right) total aliskiren in the liver, (bottom-left) aliskiren in feces, and (bottom-center) total aliskiren in feces.

DoseDependency (IV)

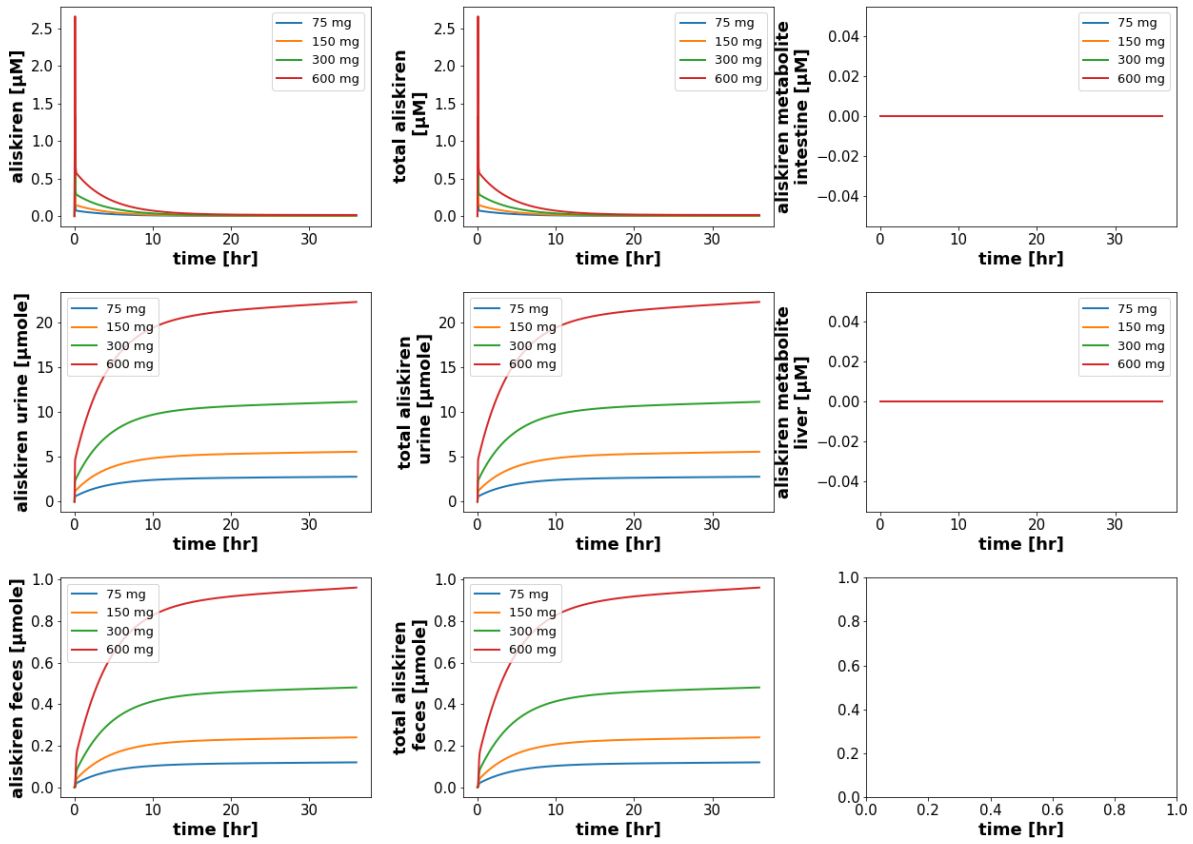


Figure 14: **Dose Dependency Experiment for intravenous application (iv).** Simulated time-course profiles of aliskiren and total aliskiren (aliskiren and metabolites) concentrations in various compartments under varying intravenous dose levels (75 mg, 150 mg, 300 mg, and 600 mg). The panels depict: (top-left) aliskiren concentration in plasma, (top-center) total aliskiren concentration in plasma, (top-right) total aliskiren concentration in the intestine, (middle-left) aliskiren in urine, (middle-center) total aliskiren in urine, (middle-right) total aliskiren in the liver, (bottom-left) aliskiren in feces, and (bottom-center) total aliskiren in feces.

3.4.1 Single dose

Figure 15 illustrates concentration time course for different dosages. Fisher et al. studied dosages from 75 mg to 600 mg. The order of the simulation and the experimental data are aligning but not the AUC and cmax values. illustrates the concentration-time profiles for aliskiren at different single oral doses, ranging from 75 mg to 600 mg, based on the study by *Fisher et al* [22]. The figure compares the simulated results with experimental data. While the order of the dose-response relationship in the simulations aligns with the experimental data (higher doses correspond to higher plasma concentrations), discrepancies remain in the predicted *AUC* (area under the curve) and c_{max} (maximum concentration) values.

The simulation underestimates the c_{max} for the higher doses (300 mg and 600 mg), indicating that the absorption or bioavailability parameters in the model may require refinement. Despite this limitation, the model successfully captures the general pharmacokinetic trends, indicating that it can be a useful tool for dose-dependent analyses, although further calibration is needed.

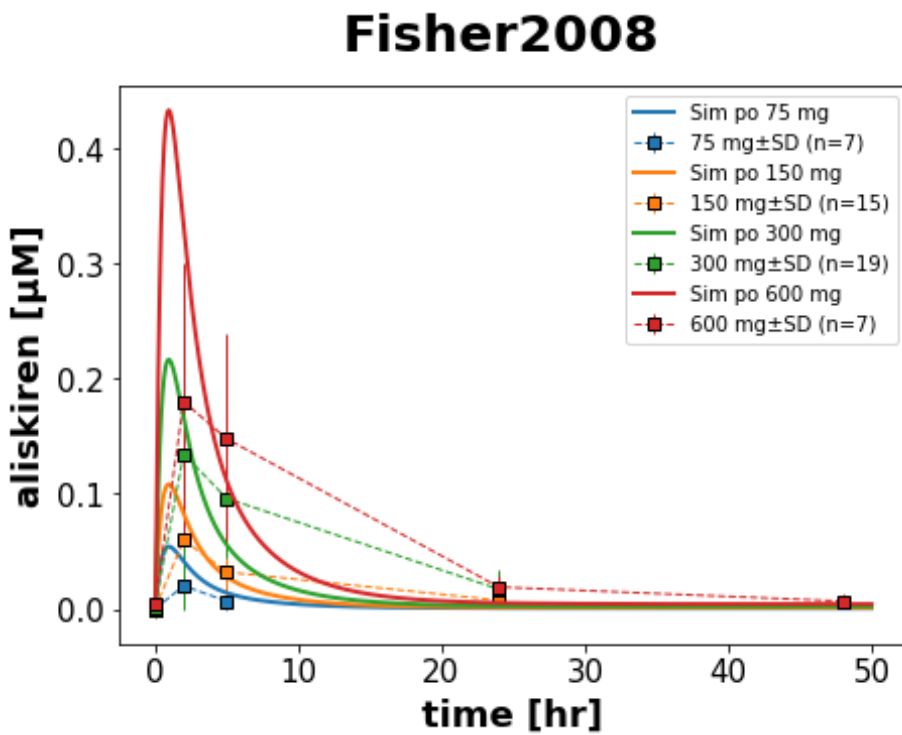


Figure 15: **Simulation of Fisher2008** [22]. This figure shows the simulated and experimental plasma concentration profiles of aliskiren for escalating doses in healthy normotensive subjects on a low-sodium diet. The study design ensured consistent conditions to evaluate aliskiren's pharmacokinetics, with all subjects receiving the 300-mg dose, while other doses were distributed among the group.

Figure 16 displays the concentration-time profiles for aliskiren following single oral doses of 75 mg, 150 mg, 300 mg, and 600 mg, as studied by *Hu et al.* [27]. The figure compares the simulated results with the experimental data. The general dose-response relationship is captured in the simulations, with higher doses leading to higher plasma concentrations. However, discrepancies are evident, particularly at the higher doses (300 mg and 600 mg), where the simulated *AUC* (area under the curve) and c_{max} (maximum concentration) values are underestimated compared to the experimental data.

These differences suggest that the model may not fully account for the absorption kinetics or bioavailability of aliskiren at higher doses. Despite these limitations, the model provides a good representation of the overall pharmacokinetic trends, demonstrating its utility for single-dose pharmacokinetic analyses with room for refinement.

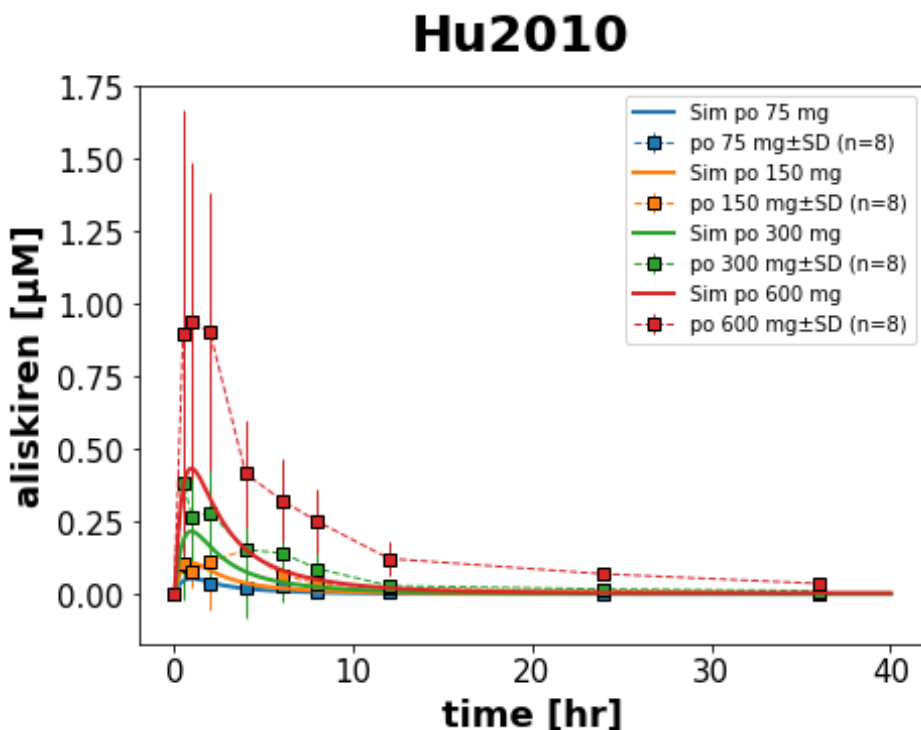


Figure 16: **Simulation of Hu2010 (single dose)** [27]. The figure depicts the simulated and experimental plasma concentration-time profiles for aliskiren following single doses of 75 mg, 150 mg, 300 mg, and 600 mg in healthy Chinese subjects

Figure 17 depicts the total excretion of aliskiren in urine and feces over time, based on the study by *Waldmeier et al.* [78]. The simulations are compared to experimental data, with urine excretion represented by blue lines and feces excretion by orange lines. The results indicate that most of the aliskiren is excreted through feces, with very limited excretion in urine, consistent with the experimental observations.

While the simulated fecal excretion aligns closely with the experimental data in terms of the total amount excreted, the model fails to capture the observed delay in fecal excretion, where experimental data show a lag before elimination begins. This missing delay suggests that the model may not fully incorporate the transit or metabolism processes affecting fecal excretion. Additionally, urinary excretion is slightly underestimated, highlighting room for refinement in predicting elimination pathways.

These results emphasize the predominance of fecal elimination for aliskiren while identifying areas where the model can be improved to better replicate the timing and dynamics of excretion processes.

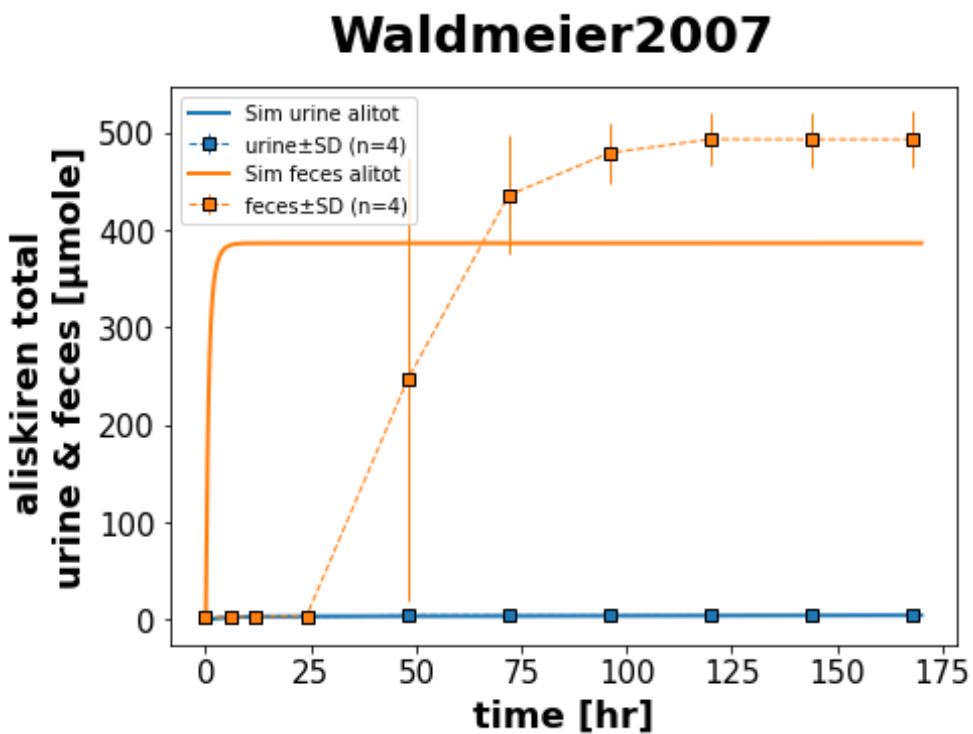


Figure 17: **Simulation of Waldmeier2007 (urine and feces data)** [78]. The figure shows the simulation of cumulative excretion of radioactivity (aliskiren labeled with ^{14}C) in human urine and feces following a single 300-mg oral dose. The figure illustrates the time-dependent distribution of aliskiren excreted through urine (blue line) and feces (orange line), with experimental data represented by markers and error bars (mean \pm SD, $n = 4$).

3.4.2 Multiple dose

Figure 18 illustrates the simulated and experimental concentration-time profiles for aliskiren following multiple daily doses of 300 mg over 11 days, based on the study by *Hu et al.* [27]. The model captures the overall trend of periodic peaks and troughs associated with repeated dosing, as well as the establishment of steady-state concentrations after several days.

While the general agreement between the simulation and experimental data is evident, minor discrepancies exist in the c_{max} , particularly during the later dosing intervals, where the simulated concentrations slightly overestimate the observed values. This indicates that the model may require adjustments to better reflect the dynamics of drug accumulation and elimination under steady-state conditions. Nonetheless, the model provides valuable insights into the pharmacokinetics of aliskiren during multiple dosing regimens.

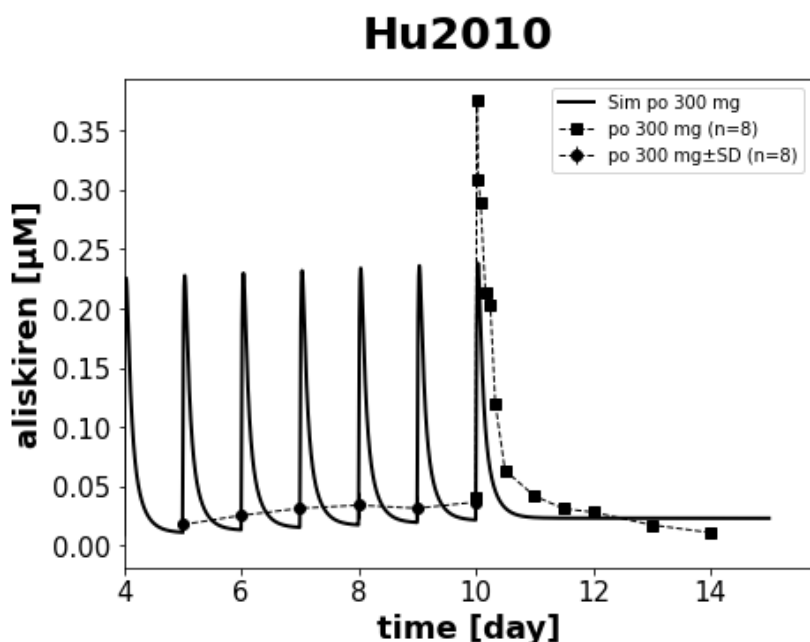


Figure 18: **Simulation of Hu2010 (multiple dosing)** [27]. The figure depicts simulated and experimental plasma concentration-time profiles for aliskiren during repeated once-daily dosing of 300 mg for 11 days in eight healthy Chinese subjects.

Figure 19 presents simulated and experimental pharmacokinetic data for aliskiren administered at daily doses of 40 mg, 80 mg, 160 mg, and 640 mg over 7 days, as studied by *Nussberger et al.* [40]. The panels show aliskiren plasma concentrations and cumulative urinary excretion over time for each dose. The simulations capture the dose-dependent increase in plasma concentrations and urinary excretion, reflecting the expected pharmacokinetic trends.

However, the model slightly underestimates urinary excretion at higher doses (160 mg and 640 mg), which may indicate that renal clearance or saturation effects are not fully accounted for. Additionally, while the plasma concentrations align well with experimental data for lower doses, small deviations in the AUC and c_{max} are observed at higher doses, suggesting the need for refinement in absorption or elimination parameters.

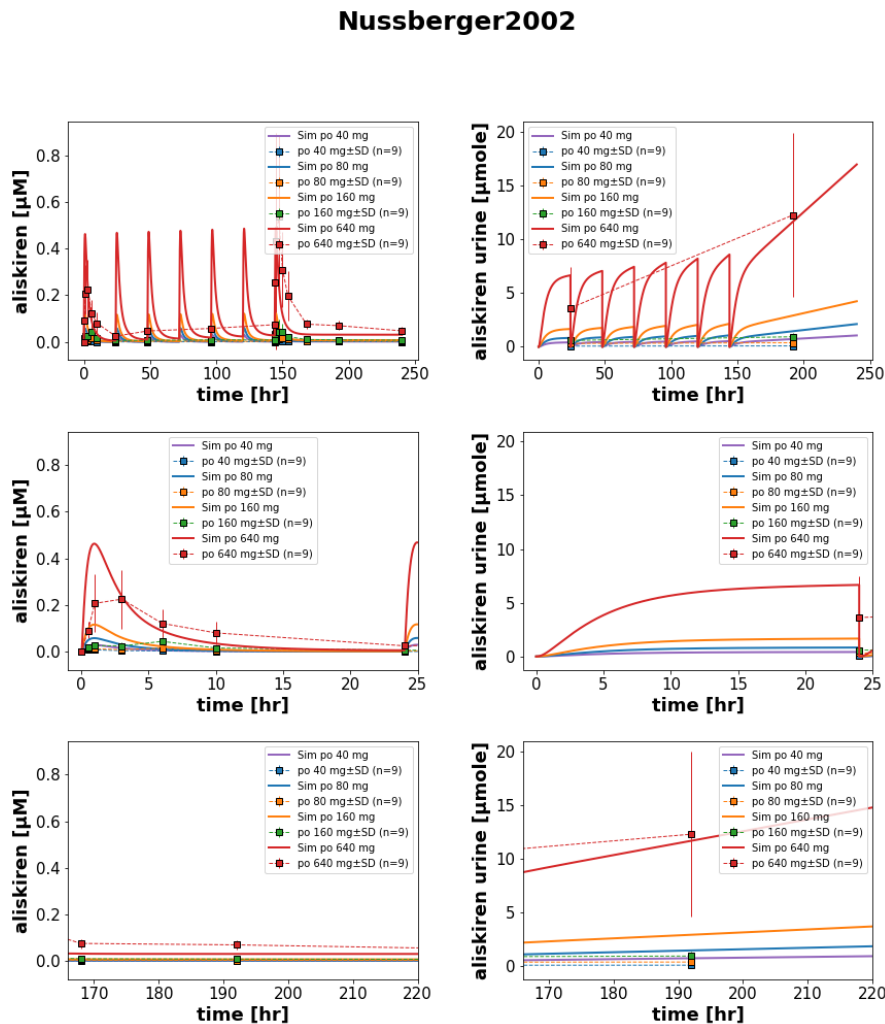


Figure 19: Simulation of Nussberger2002 [40]. The figure presents simulated and experimental plasma concentrations (left panels) and cumulative urinary excretion (right panels) of aliskiren for multiple dosing schemes over 7 days with doses of 40 mg, 80 mg, 160 mg, and 640 mg. Each dose cohort included 9 participants. The panels are displaying different time intervals. Experimental data (mean \pm SD) are shown as markers, and simulations as solid lines.

3.5 Model application

The developed PBPK model of aliskiren was used to study differences in pharmacokinetics between healthy individuals and patients with either hepatic or renal impairment, as well as the effects of drug-drug interactions. Parameters relevant to these questions were systematically scanned, and the resulting changes in aliskiren pharmacokinetics were evaluated.

These scans address the key research questions of this thesis: I. How does hepatorenal impairment influence the pharmacokinetics of aliskiren, and II. What effects do co-administered medications have on the pharmacokinetics of aliskiren. All scans were conducted for a single oral dose of 150 mg of aliskiren, unless otherwise stated.

Due to the incomplete model, scans for some parameters, such as renal function, severity of cirrhosis, or enzyme activity, remain suboptimal, and the pharmacodynamic aspects (which are important to answer III.) have yet to be addressed.

3.5.1 Hepatic functional impairment

Figure 20 represents how aliskiren concentrations vary across different tissues and compartments under varying levels of cirrhosis. The structure of this figure is consistent with the Dose Dependency Experiments (see Figures 13 and 14), which explore the effects on aliskiren’s distribution, metabolism, and excretion.

Figure 20 presents results for various stages of cirrhosis, focusing on the following parameters: aliskiren plasma concentration, total plasma concentration (including metabolites), metabolite concentration in the intestine, aliskiren concentration in urine, total urinary concentration (aliskiren and metabolites), metabolite concentration in the liver, aliskiren concentration in feces, and total fecal concentration (aliskiren and metabolites). The different stages of cirrhosis can be simulated by varying the parameter for renal impairment, $f_{cirrhosis}$.

These plots show how aliskiren and its metabolites change over time under different levels of cirrhosis. The colors in the plots match those in Figure 4 and align with simulations for hepatic functional impairment (like the study from *Vaidyanathan et al.* [74]).

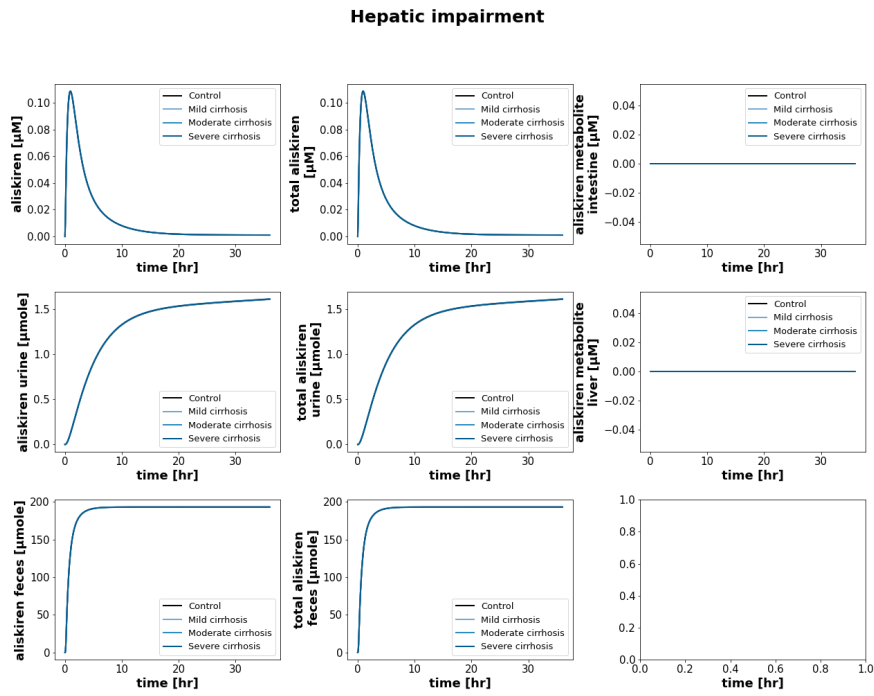


Figure 20: Pharmacokinetics of aliskiren under varying degrees of cirrhosis (normal, mild, moderate, and severe cirrhosis). Simulated time-course profiles of aliskiren and total aliskiren (aliskiren and metabolites) concentrations in various compartments for a single 300 mg dose. Panels illustrate: (top-left) aliskiren concentration in plasma, (top-center) total aliskiren concentration in plasma, (top-right) total aliskiren concentration in the intestine, (middle-left) aliskiren in urine, (middle-center) total aliskiren in urine, (middle-right) total aliskiren in the liver, (bottom-left) aliskiren in feces, and (bottom-center) total aliskiren in feces. Overlapping curves indicate no change in concentrations under different degrees of hepatic impairment, suggesting an incomplete model or limited impact of cirrhosis on the parameterized compartments.

Figure 21 illustrates the application of the hepatic impairment model to simulate aliskiren pharmacokinetics in healthy subjects and individuals with varying degrees of hepatic impairment (mild, moderate, and severe). The simulations represent a single 300 mg dose of aliskiren, with each subplot corresponding to a different level of hepatic impairment [74].

The results show that hepatic impairment does not significantly alter aliskiren plasma concentrations across the different impairment stages, as the curves for mild, moderate, and severe impairments largely overlap with those of the healthy subjects. This overlap suggests that hepatic metabolism may play a limited role in aliskiren clearance or that the model lacks sufficient sensitivity to detect differences due to hepatic impairment.

While the model captures overall trends in aliskiren pharmacokinetics, its inability to differentiate between the impairment stages highlights the need for further refinement. Stratified clinical data will be integrated to validate the model’s predictions across mild, moderate, and severe impairment groups. Additionally, population variability will be introduced through virtual simulations, accounting for a range of physiological conditions. Nonlinear clearance equations and time-dependent modeling will further enhance the ability to capture dynamic pharmacokinetic changes associated with disease progression. These refinements aim to improve the model’s ca-

pacity to reflect the distinct pharmacokinetics of aliskiren across varying stages of hepatorenal impairment.

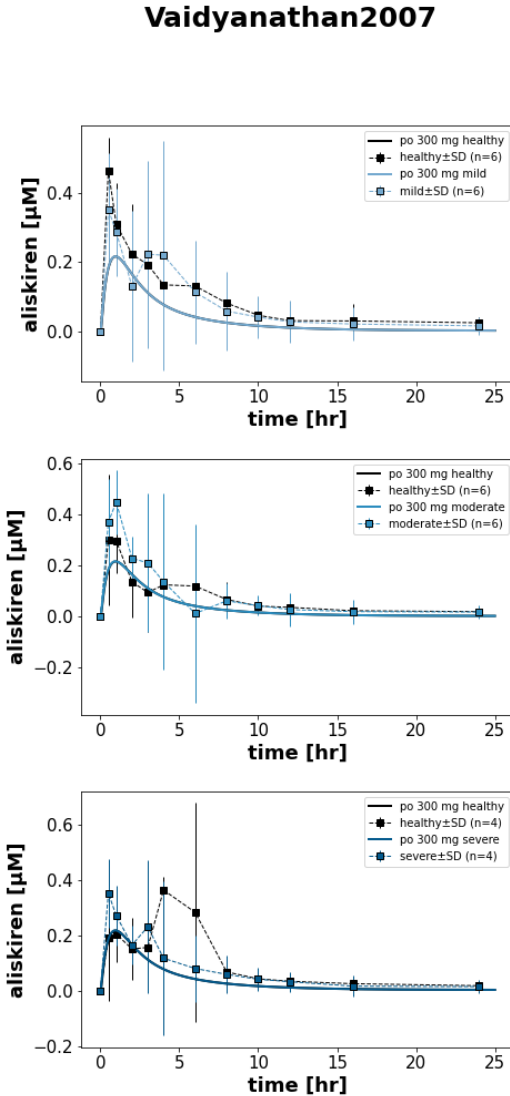


Figure 21: Simulation of Vaidyanathan2007 [74]. Plasma concentration-time profiles for aliskiren in patients with mild ($n = 6$), moderate ($n = 6$), and severe ($n = 4$) hepatic impairment compared with matched healthy subjects. Plasma concentrations are presented following the administration of a single 300-mg oral dose. Each panel compares plasma concentrations in healthy individuals ($n = 6$ for mild and moderate, $n = 4$ for severe) with those in patients experiencing varying degrees of hepatic impairment. Data are shown as mean \pm SD, with simulated values represented by solid lines and experimental data by markers. The figure illustrates the impact of hepatic impairment on aliskiren pharmacokinetics, with changes becoming more pronounced as impairment severity increases.

3.5.2 Renal functional impairment

Figure 22 portrays how aliskiren concentrations vary across different tissues and compartments under varying levels of renal impairment. The structure of this figure is consistent with the Dose Dependency Experiments (see Figures 13 and 14), which explore the effects on aliskiren's distribution, metabolism, and excretion.

Figure 22 presents results for various stages of renal impairment, focusing on the following parameters: aliskiren plasma concentration, total plasma concentration (including metabolites), metabolite concentration in the intestine, aliskiren concentration in urine, total urinary concentration (aliskiren and metabolites), metabolite concentration in the liver, aliskiren concentration in feces, and total fecal concentration (aliskiren and metabolites). The different stages of renal impairment can be simulated by varying the parameter for renal impairment, $K_{frenalfunction}$. These plots show how aliskiren and its metabolites change over time under different levels of renal impairment. The colors in the plots match those in Figure 5 and align with simulations for renal functional impairment (like the study from *Vaidyanathan et al.* [68]).

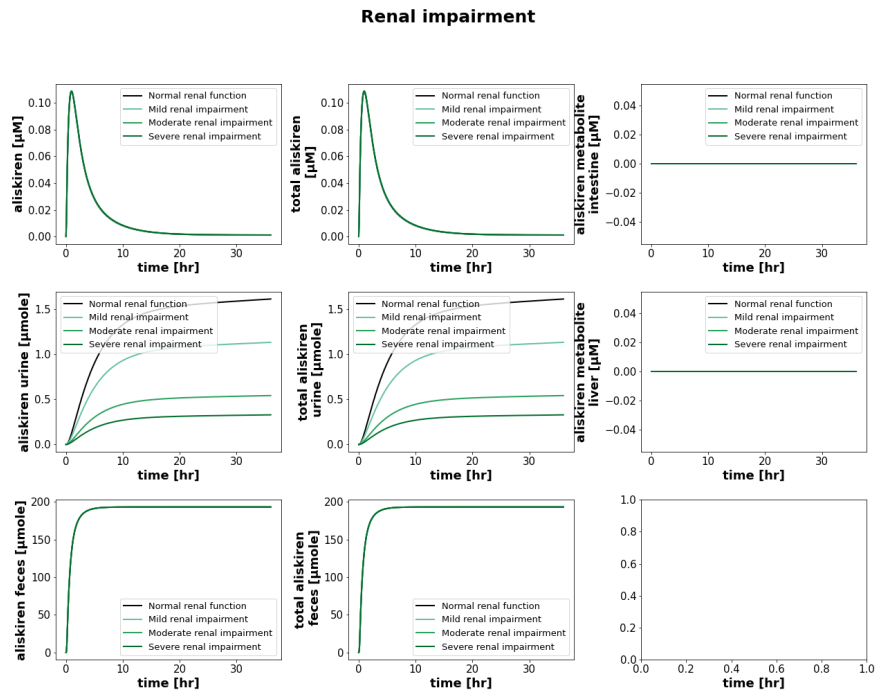
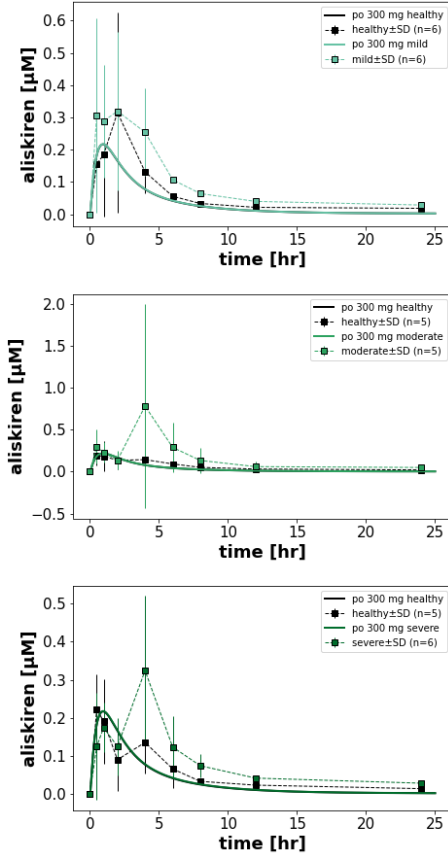


Figure 22: Pharmacokinetics of aliskiren under varying degrees of renal function (normal, mild, moderate, and severe impairment). Simulated time-course profiles of aliskiren and total aliskiren (aliskiren and metabolites) concentrations in various compartments for a single 300 mg dose. Panels demonstrate: (top-left) aliskiren concentration in plasma, (top-center) total aliskiren concentration in plasma, (top-right) total aliskiren concentration in the intestine, (middle-left) aliskiren in urine, (middle-center) total aliskiren in urine, (middle-right) total aliskiren in the liver, (bottom-left) aliskiren in feces, and (bottom-center) total aliskiren in feces. Overlapping curves indicate no change in concentrations under different degrees of renal impairment, suggesting an incomplete model or limited impact of renal impairment on the parameterized compartments.

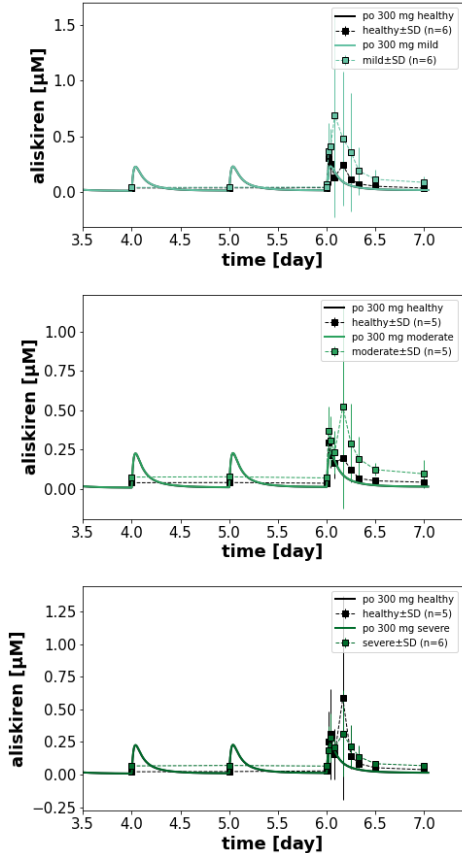
Figure 23 presents the application of the renal impairment model, with each subplot representing different renal impairment levels alongside pooled healthy subjects. Subfigure 23a depicts the results for a single 300 mg dose, while Subfigure 23b shows the outcomes for multiple 300 mg doses administered over 7 days [68]. Each renal impairment level is visualized using its corresponding color from Figure 5 for clarity.

The model successfully simulates the pharmacokinetics of aliskiren across different levels of renal impairment, with healthy, mild, moderate, and severe impairments included. However, the simulations for the different impairment stages overlap significantly, making it difficult to distinguish their individual effects. This overlap limits the model's ability to highlight the specific pharmacokinetic differences between the impairment stages.

Despite these limitations, the model provides useful insights into the overall trends of aliskiren pharmacokinetics in renal impairment. Further refinement is needed to resolve the overlapping simulations and improve the differentiation between impairment stages to better align with experimental data. As in the part for the hepatic impairment, stratified clinical data will be integrated to validate the model's predictions across mild, moderate, and severe impairment groups. Additionally, population variability will be introduced through virtual simulations, accounting for a range of physiological conditions. Nonlinear clearance equations and time-dependent modeling will further enhance the ability to capture dynamic pharmacokinetic changes associated with disease progression.

Vaidyanathan2007b (single dose)

(a) Simulation of Vaidyanathan2007b (single dose)

Vaidyanathan2007b (multiple dose)

(b) Simulation of Vaidyanathan2007b (multiple dose)

Figure 23: **Simulation of Vaidyanathan2007b [68].** The left panels (a) show plasma concentration-time profiles following a single 300-mg oral dose of aliskiren in healthy subjects and in patients with mild ($n = 6$), moderate ($n = 5$), and severe ($n = 5$) renal impairment. The right panels (b) display plasma concentrations during multiple once-daily doses of 300 mg for 7 days, highlighting steady-state pharmacokinetics between days 5 and 7. Data are presented as mean \pm SD, with experimental values shown as markers and simulated values as solid lines. The comparison demonstrates the effect of renal impairment on aliskiren pharmacokinetics, with increased plasma concentrations and delayed elimination observed in patients with higher levels of impairment, particularly under multiple dosing conditions.

3.5.3 Drug-drug interactions (enzyme activities)

Drug-drug interaction studies were conducted to better understand the pharmacokinetics of aliskiren. Co-administered drugs can cause an increase or decrease in the AUC or c_{max} , which reflects changes in absorption, distribution, metabolism, or excretion. These changes provide insights into how the co-administered drugs affect the enzymes involved in aliskiren's pharmacokinetics, which are critical for its ADME (Absorption, Distribution, Metabolism, and Excretion) profile.

Using the formulas for drug-drug interactions and the resulting effects described in Section 2.7, combined with the data from the curated studies (Table 6), the impact of co-administered drugs on aliskiren's pharmacokinetics was analyzed. The results include statistical evaluations using t-tests (shown in the Tables 9 and 10) and visualizations of the effects on both AUC and c_{max} . These findings are presented in the following sections, with detailed results provided in the Tables 9 and 10. The symbols in parentheses were used to represent the varying effects of the drugs (see Table 5 for more details).

Figures 24 and 25 show that the drugs in the studies affect aliskiren's pharmacokinetic parameters differently. Some drugs lower the values (left side of the plots), others increase them (right side), and some have no effect.

Table 9: Drug-Drug Interaction with aliskiren: AUC values

Study	Drug	Effect	Ratio	σ_{Ratio}	t-statistic	p-value	df	α
Ayalasomayajula2008a [5]	allopurinol	\emptyset	7.89E-01	7.89E-01	7.89E-01	7.89E-01	38	
Vaidyanathan2006 [66]	amlodipine	\uparrow	9.11E-02	9.11E-02	9.11E-02	9.11E-02	35	
Tapaninen2011a [63]	apple juice	$\downarrow\downarrow$	2.06E-02	2.06E-02	2.06E-02	2.06E-02	22	*
Vaidyanathan2008a [69]	atorvastatin	\uparrow	2.38E-11	2.38E-11	2.38E-11	2.38E-11	38	***
Ayalasomayajula2008a [5]	celecoxib	\emptyset	3.87E-01	3.87E-01	3.87E-01	3.87E-01	42	
Ayalasomayajula2008a [5]	cimetidine	\emptyset	2.05E-01	2.05E-01	2.05E-01	2.05E-01	42	
Rebello2011a [50]	cyclosporine	$\uparrow\uparrow$	4.33E-06	4.33E-06	4.33E-06	4.33E-06	23	***
Rebello2011a [50]	cyclosporine	$\uparrow\uparrow$	2.20E-08	2.20E-08	2.20E-08	2.20E-08	18	***
Vaidyanathan2008a [69]	digoxin	\emptyset	8.45E-01	8.45E-01	8.45E-01	8.45E-01	38	
Vaidyanathan2008c [72]	fenofibrate	\emptyset	6.54E-01	6.54E-01	6.54E-01	6.54E-01	32	
Vaidyanathan2008b [67]	furosemide	\emptyset	7.37E-01	7.37E-01	7.37E-01	7.37E-01	40	
Rebello2012 [52]	grapefruit juice	\downarrow	1.81E-02	1.81E-02	1.81E-02	1.81E-02	50	*
Tapaninen2010 [60]	grapefruit juice	$\downarrow\downarrow$	5.96E-03	5.96E-03	5.96E-03	5.96E-03	20	**
Vaidyanathan2006 [66]	hctz	\emptyset	7.54E-01	7.54E-01	7.54E-01	7.54E-01	42	
Vaidyanathan2007b [68]	irbesartan	\uparrow	1.35E-01	1.35E-01	1.35E-01	1.35E-01	10	
Vaidyanathan2007b [68]	irbesartan	$\uparrow\uparrow$	1.99E-01	1.99E-01	1.99E-01	1.99E-01	8	
Vaidyanathan2007b [68]	irbesartan	\uparrow	6.39E-02	6.39E-02	6.39E-02	6.39E-02	9	
Vaidyanathan2007b [68]	irbesartan	$\uparrow\uparrow$	1.30E-01	1.30E-01	1.30E-01	1.30E-01	10	
Vaidyanathan2007b [68]	irbesartan	$\uparrow\uparrow$	1.39E-01	1.39E-01	1.39E-01	1.39E-01	8	
Vaidyanathan2007b [68]	irbesartan	\emptyset	8.72E-01	8.72E-01	8.72E-01	8.72E-01	9	
Vaidyanathan2008b [67]	ismn	\emptyset	9.29E-01	9.29E-01	9.29E-01	9.29E-01	34	
Tapaninen2011 [61]	itraconazole	$\uparrow\uparrow\uparrow$	3.57E-07	3.57E-07	3.57E-07	3.57E-07	20	***
Vaidyanathan2008a [69]	ketoconazole	\uparrow	1.17E-07	1.17E-07	1.17E-07	1.17E-07	39	***
Vaidyanathan2008c [72]	metformin	\downarrow	5.00E-02	5.00E-02	5.00E-02	5.00E-02	36	*
Tapaninen2011a [63]	orange juice	$\downarrow\downarrow$	2.27E-02	2.27E-02	2.27E-02	2.27E-02	22	*
Vaidyanathan2008c [72]	pioglitazone	\emptyset	8.53E-01	8.53E-01	8.53E-01	8.53E-01	56	
Vaidyanathan2006 [66]	ramipril	\emptyset	3.34E-01	3.34E-01	3.34E-01	3.34E-01	32	
Tapaninen2010b [64]	rifampicin	$\downarrow\downarrow$	2.98E-02	2.98E-02	2.98E-02	2.98E-02	22	*
Vaidyanathan2006 [66]	valsartan	\downarrow	1.14E-02	1.14E-02	1.14E-02	1.14E-02	35	*
Rebello2011 [51]	verapamil	\uparrow	1.17E-03	1.17E-03	1.17E-03	1.17E-03	34	**

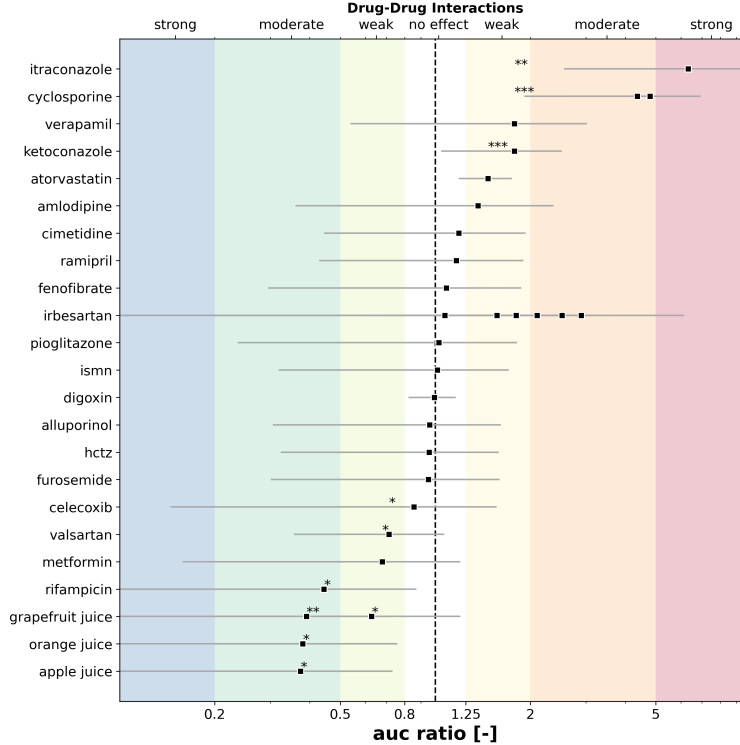


Figure 24: Drug-Drug Interaction with aliskiren: plot for the AUC values

Table 10: Drug-Drug Interaction with aliskiren: c_{max} values

Study	Drug	Effect	Ratio	σ_{Ratio}	t-statistic	p-value	df	α
Ayalasomayajula2008a [5]	allopurinol	\emptyset	5.59E-01	5.59E-01	5.59E-01	5.59E-01	38	
Vaidyanathan2006 [66]	amlodipine	\uparrow	1.92E-01	1.92E-01	1.92E-01	1.92E-01	35	
Tapaninen2011a [63]	apple juice	$\downarrow\downarrow$	5.20E-03	5.20E-03	5.20E-03	5.20E-03	22	**
Vaidyanathan2008a [69]	atorvastatin	\uparrow	7.63E-02	7.63E-02	7.63E-02	7.63E-02	38	
Ayalasomayajula2008a [5]	celecoxib	\emptyset	9.10E-01	9.10E-01	9.10E-01	9.10E-01	42	
Ayalasomayajula2008a [5]	cimetidine	\emptyset	3.98E-01	3.98E-01	3.98E-01	3.98E-01	42	
Rebello2011a [50]	cyclosporine	$\uparrow\uparrow$	7.76E-04	7.76E-04	7.76E-04	7.76E-04	25	***
Rebello2011a [50]	cyclosporine	$\downarrow\downarrow$	5.27E-05	5.27E-05	5.27E-05	5.27E-05	20	***
Vaidyanathan2008a [69]	digoxin	\emptyset	8.13E-01	8.13E-01	8.13E-01	8.13E-01	38	
Vaidyanathan2008c [72]	fenofibrate	\emptyset	4.91E-01	4.91E-01	4.91E-01	4.91E-01	32	
Vaidyanathan2008b [67]	furosemide	\emptyset	5.22E-01	5.22E-01	5.22E-01	5.22E-01	40	
Rebello2012 [52]	grapefruit juice	$\downarrow\downarrow$	9.26E-03	9.26E-03	9.26E-03	9.26E-03	54	**
Tapaninen2010 [60]	grapefruit juice	$\downarrow\downarrow\downarrow$	5.79E-05	5.79E-05	5.79E-05	5.79E-05	20	***
Vaidyanathan2006 [66]	hctz	\downarrow	4.47E-02	4.47E-02	4.47E-02	4.47E-02	42	*
Vaidyanathan2007b [68]	irbesartan	\emptyset	9.67E-01	9.67E-01	9.67E-01	9.67E-01	10	
Vaidyanathan2007b [68]	irbesartan	$\uparrow\uparrow$	2.39E-01	2.39E-01	2.39E-01	2.39E-01	8	
Vaidyanathan2007b [68]	irbesartan	\uparrow	2.42E-01	2.42E-01	2.42E-01	2.42E-01	9	
Vaidyanathan2007b [68]	irbesartan	$\uparrow\uparrow$	8.65E-02	8.65E-02	8.65E-02	8.65E-02	10	
Vaidyanathan2007b [68]	irbesartan	\uparrow	2.65E-01	2.65E-01	2.65E-01	2.65E-01	8	
Vaidyanathan2007b [68]	irbesartan	\downarrow	4.13E-01	4.13E-01	4.13E-01	4.13E-01	9	
Vaidyanathan2008b [67]	ismn	\emptyset	7.61E-01	7.61E-01	7.61E-01	7.61E-01	34	
Tapaninen2011 [61]	itraconazole	$\uparrow\uparrow\uparrow$	2.99E-05	2.99E-05	2.99E-05	2.99E-05	20	***
Vaidyanathan2008a [69]	ketoconazole	\uparrow	8.72E-03	8.72E-03	8.72E-03	8.72E-03	39	**
Vaidyanathan2008c [72]	metformin	\downarrow	4.16E-02	4.16E-02	4.16E-02	4.16E-02	36	*
Tapaninen2011a [63]	orange juice	$\downarrow\downarrow$	8.03E-03	8.03E-03	8.03E-03	8.03E-03	22	**
Vaidyanathan2008c [72]	pioglitazone	\emptyset	7.50E-01	7.50E-01	7.50E-01	7.50E-01	56	
Vaidyanathan2006 [66]	ramipril	\uparrow	1.67E-01	1.67E-01	1.67E-01	1.67E-01	32	
Tapaninen2010b [64]	rifampicin	\downarrow	1.85E-01	1.85E-01	1.85E-01	1.85E-01	22	
Vaidyanathan2006 [66]	valsartan	\downarrow	4.06E-02	4.06E-02	4.06E-02	4.06E-02	35	*
Rebello2011 [51]	verapamil	\uparrow	1.84E-03	1.84E-03	1.84E-03	1.84E-03	34	**

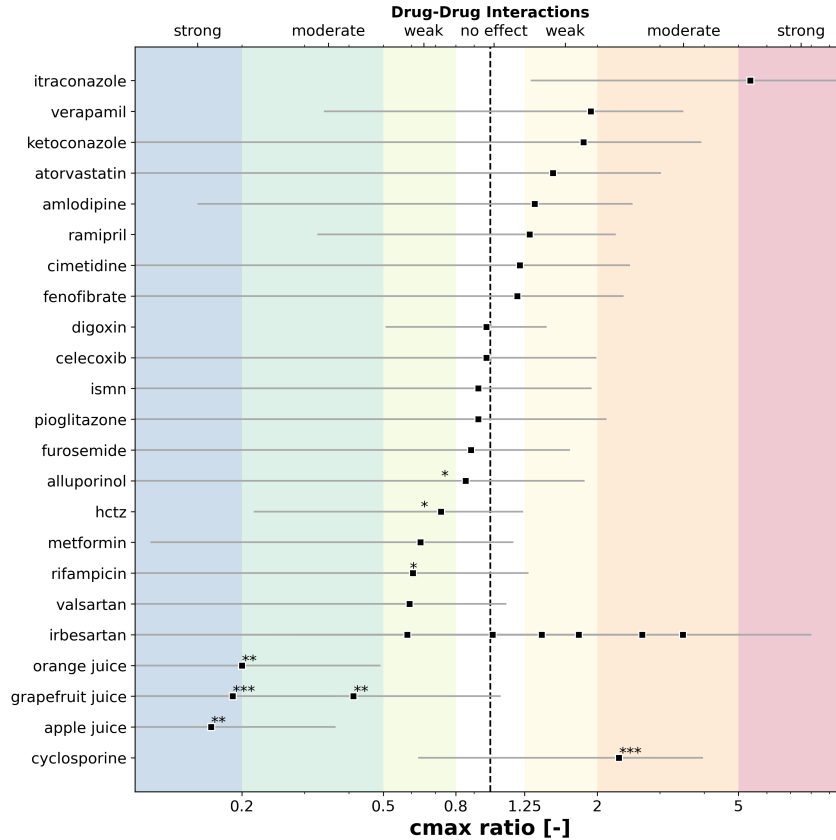


Figure 25: Drug-Drug Interaction with aliskiren: plot for the C_{max} values

Figure 26 demonstrates the results for varying CYP3A4 activities, focusing on the following pharmacokinetic parameters: aliskiren plasma concentration, total plasma concentration (including metabolites), metabolite concentration in the intestine, aliskiren concentration in urine, total urinary concentration (aliskiren and metabolites), metabolite concentration in the liver, aliskiren concentration in feces, and total fecal concentration (aliskiren and metabolites). Surprisingly, the simulations reveal no significant changes in absorption or metabolite levels with varying CYP3A4 activities. This result is unexpected, as CYP3A4 is a key enzyme involved in the metabolism of aliskiren. A variation in CYP3A4 activity should ideally result in changes in metabolite concentrations, reflecting the enzyme's role in metabolizing the drug. The lack of observable changes suggests potential limitations in the current model, possibly due to incomplete parameterization or insufficient representation of enzyme-related metabolism. This discrepancy highlights the need for further refinement of the model to accurately simulate the effects of CYP3A4 activity on aliskiren pharmacokinetics.

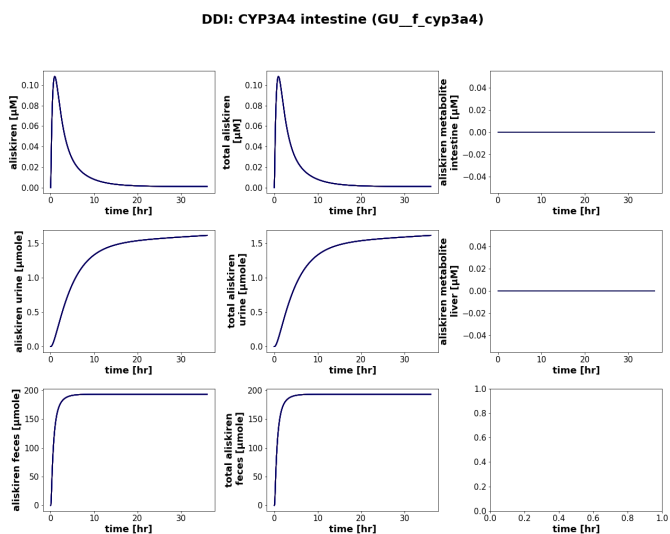


Figure 26: Scan of CYP3A4 in the intestine. Simulated time-course profiles of aliskiren and total aliskiren (aliskiren and metabolites) concentrations in various compartments for a single 300 mg dose. Panels illustrate: (top-left) aliskiren concentration in plasma, (top-center) total aliskiren concentration in plasma, (top-right) total aliskiren concentration in the intestine, (middle-left) aliskiren in urine, (middle-center) total aliskiren in urine, (middle-right) total aliskiren in the liver, (bottom-left) aliskiren in feces, and (bottom-center) total aliskiren in feces. The red lines represent reduced CYP3A4 activity, while the blue lines indicate increased CYP3A4 activity. The overlapping curves suggest that the current model is incomplete for exploring the impact of CYP3A4 metabolism on aliskiren and its metabolites, particularly for differentiating the effects of varying CYP3A4 activity. Refinements to the model are necessary to better capture the role of CYP3A4 in the metabolism and disposition of aliskiren, ensuring a more accurate representation of its pharmacokinetic behavior.

Figure 27 exhibits the results for varying OATP (organic anion-transporting polypeptide) activities, focusing on the following pharmacokinetic parameters: aliskiren plasma concentration, total plasma concentration (including metabolites), metabolite concentration in the intestine, aliskiren concentration in urine, total urinary concentration (aliskiren and metabolites), metabolite concentration in the liver, aliskiren concentration in feces, and total fecal concentration (aliskiren and metabolites). The red lines represent reduced OATP activity, while the blue lines indicate increased OATP activity. The results demonstrate that increased OATP activity leads to a higher *AUC* (area under the curve), indicating enhanced absorption of aliskiren. Additionally, decreased OATP activity results in a higher amount of aliskiren being excreted in feces. These findings align with the role of OATP in facilitating the transport of aliskiren into enterocytes, which is visualized in Figures 7 and 8. However, the simulations do not show any significant changes in metabolite concentrations, which is unexpected given the importance of OATP in absorption and subsequent metabolism. This limitation suggests that the current model does not fully account for the downstream effects of altered OATP activity on metabolite formation and distribution.

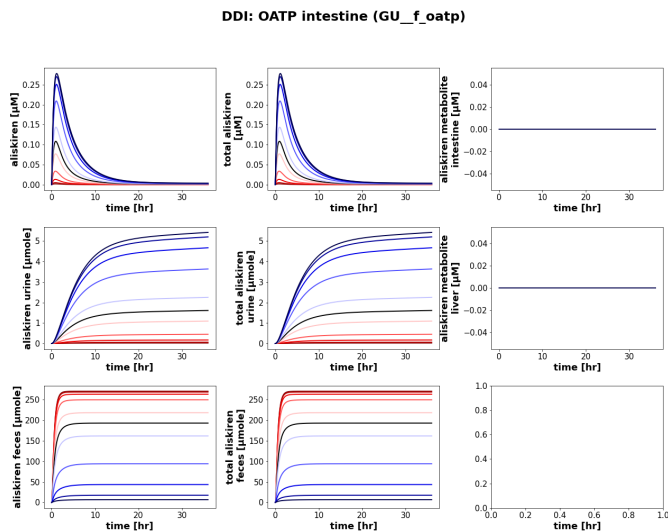


Figure 27: Scan of OATP in the intestine. Simulated time-course profiles of aliskiren and total aliskiren (aliskiren and metabolites) concentrations in various compartments for a single 300 mg dose. Panels illustrate: (top-left) aliskiren concentration in plasma, (top-center) total aliskiren concentration in plasma, (top-right) total aliskiren concentration in the intestine, (middle-left) aliskiren in urine, (middle-center) total aliskiren in urine, (middle-right) total aliskiren in the liver, (bottom-left) aliskiren in feces, and (bottom-center) total aliskiren in feces. The red lines represent reduced OATP activity, while the blue lines indicate increased OATP activity. If overlapping curves are observed, particularly for metabolites (e.g., aliskiren metabolite concentration in the intestine or liver), it suggests that the current model does not fully capture the role of OATP-mediated transport in metabolite dynamics. This overlap indicates that OATP activity changes are not significantly impacting metabolite levels in the compartments, potentially pointing to a lack of parameter sensitivity or missing pathways for metabolite formation and clearance.

Figure 28 portrays the results for varying P-gp (P-glycoprotein) activities, focusing on the following pharmacokinetic parameters: aliskiren plasma concentration, total plasma concentration (including metabolites), metabolite concentration in the intestine, aliskiren concentration in urine, total urinary concentration (aliskiren and metabolites), metabolite concentration in the liver, aliskiren concentration in feces, and total fecal concentration (aliskiren and metabolites). The red lines represent reduced P-gp activity, while the blue lines indicate increased P-gp activity. The results show that decreased P-gp activity leads to a higher *AUC* (area under the curve), indicating enhanced absorption of aliskiren. Conversely, increased P-gp activity results in more aliskiren being excreted in feces, reflecting P-gp's role in transporting aliskiren from enterocytes back into the intestinal lumen. These findings align with the established role of P-gp in modulating drug absorption and are consistent with data visualized in Figures 7 and 8. However, the simulations do not reveal significant changes in metabolite concentrations, which is unexpected given the critical role of P-gp in drug absorption and subsequent metabolism. This discrepancy suggests that the current model does not fully account for the downstream effects of altered P-gp activity on metabolite formation and distribution.

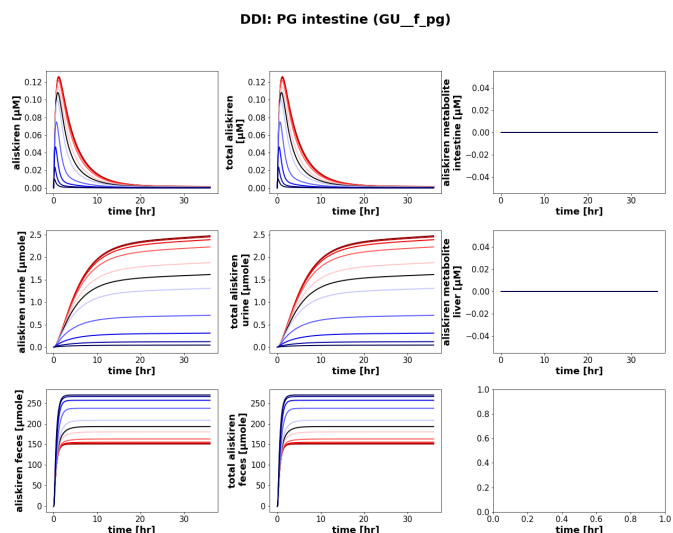


Figure 28: Scan of P-gp in the intestine. Simulated time-course profiles of aliskiren and total aliskiren (aliskiren and metabolites) concentrations in various compartments for a single 300 mg dose. Panels illustrate: (top-left) aliskiren concentration in plasma, (top-center) total aliskiren concentration in plasma, (top-right) total aliskiren concentration in the intestine, (middle-left) aliskiren in urine, (middle-center) total aliskiren in urine, (middle-right) total aliskiren in the liver, (bottom-left) aliskiren in feces, and (bottom-center) total aliskiren in feces. The red lines represent reduced OATP activity, while the blue lines indicate increased OATP activity. If overlapping curves are observed, particularly for metabolites (e.g., aliskiren metabolite concentration in the intestine or liver), it suggests that the current model does not fully capture the role of P-gp-mediated transport in metabolite dynamics. Refinements to the model are required to better represent the interaction between P-gp activity and aliskiren pharmacokinetics, ensuring a more accurate depiction of how P-gp influences metabolite levels and transport dynamics.

Figure 29 is similar to Figure 26, with the primary difference being the compartment analyzed. It presents the results for varying CYP3A4 activities in the liver and focuses on the following pharmacokinetic parameters: aliskiren plasma concentration, total plasma concentration (including metabolites), metabolite concentration in the intestine, aliskiren concentration in urine, total urinary concentration (aliskiren and metabolites), metabolite concentration in the liver, aliskiren concentration in feces, and total fecal concentration (aliskiren and metabolites). The simulations again show no significant changes in absorption or metabolite levels with varying CYP3A4 activities. This result is unexpected, as CYP3A4 is a key enzyme involved in the metabolism of aliskiren. Variations in CYP3A4 activity would typically result in observable changes in metabolite concentrations, reflecting the enzyme's role in drug metabolism. The lack of changes in metabolite concentrations suggests limitations in the current model. Specifically, the unfinished model does not fully account for metabolite dynamics, which limits its ability to represent CYP3A4-mediated metabolism accurately. Addressing this gap in future iterations of the model will be critical for capturing the full pharmacokinetic and pharmacodynamic profiles of aliskiren.

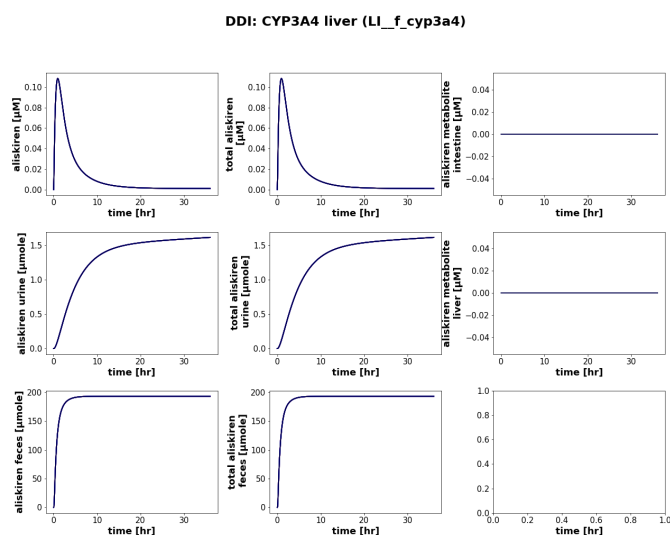


Figure 29: Scan of CYP3A4 in the liver. Simulated time-course profiles of aliskiren and total aliskiren (aliskiren and metabolites) concentrations in various compartments for a single 300 mg dose. Panels illustrate: (top-left) aliskiren concentration in plasma, (top-center) total aliskiren concentration in plasma, (top-right) total aliskiren concentration in the intestine, (middle-left) aliskiren in urine, (middle-center) total aliskiren in urine, (middle-right) total aliskiren in the liver, (bottom-left) aliskiren in feces, and (bottom-center) total aliskiren in feces. The red lines represent reduced CYP3A4 activity, while the blue lines indicate increased CYP3A4 activity. The overlapping curves suggest that the current model is incomplete for exploring the impact of CYP3A4 metabolism on aliskiren and its metabolites, particularly for differentiating the effects of varying CYP3A4 activity. Refinements to the model are necessary to better capture the role of CYP3A4 in the metabolism and disposition of aliskiren, ensuring a more accurate representation of its pharmacokinetic behavior.

Rebello et al. studied the effect of aliskiren administered alone and in combination with grapefruit juice in 28 participants [52]. Figure 30 compares the simulations with experimental data from this study. The results show that the simulation for aliskiren alone predicts higher concentrations compared to aliskiren in combination with grapefruit juice, which aligns with the experimental trends. However, discrepancies remain between the simulations and experimental data in both *AUC* and c_{max} , indicating that the model does not fully capture the observed pharmacokinetics.

The reduction in aliskiren levels with grapefruit juice is consistent with its known impact on enzyme activity, likely affecting absorption or metabolism. While the model provides valuable insights into drug-drug interactions, further refinement is necessary to better align the simulations with experimental data and improve its predictive accuracy.

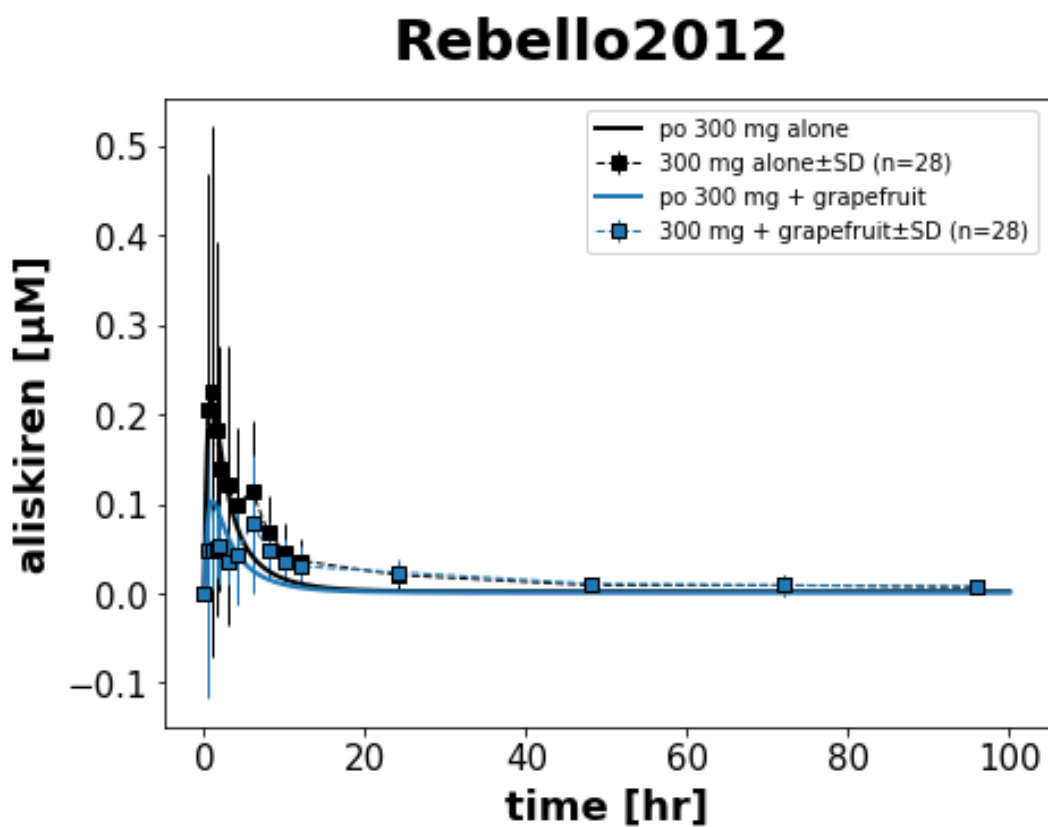


Figure 30: **Simulation of Rebello2012 [52]**. The figure shows plasma concentration-time profiles of aliskiren following a single 300-mg oral dose administered alone or co-administered with grapefruit juice. Experimental data are presented as mean \pm SD ($n = 28$) and are compared to simulated profiles. The black lines and markers represent aliskiren administered alone, while the blue lines and markers indicate aliskiren co-administered with grapefruit juice.

Tapaninen et al. investigated the effect of co-administering orange juice and apple juice on the pharmacokinetics of aliskiren in 12 participants [63]. Figure 31 compares the simulations with experimental data from this study. The results indicate that the presence of orange juice or apple juice reduces aliskiren concentrations compared to administration alone, which aligns with the experimental trends. However, discrepancies remain in the model's ability to accurately replicate the *AUC* and c_{max} values observed in the experimental data. The reduction in aliskiren levels with orange juice and apple juice likely results from their known effects on drug absorption, possibly through interactions with transporters or enzymes. While the model captures the general trend of reduced concentrations with juice co-administration, further refinement is required to enhance the alignment of the simulations with experimental data and improve the predictive accuracy of such drug-food interactions.

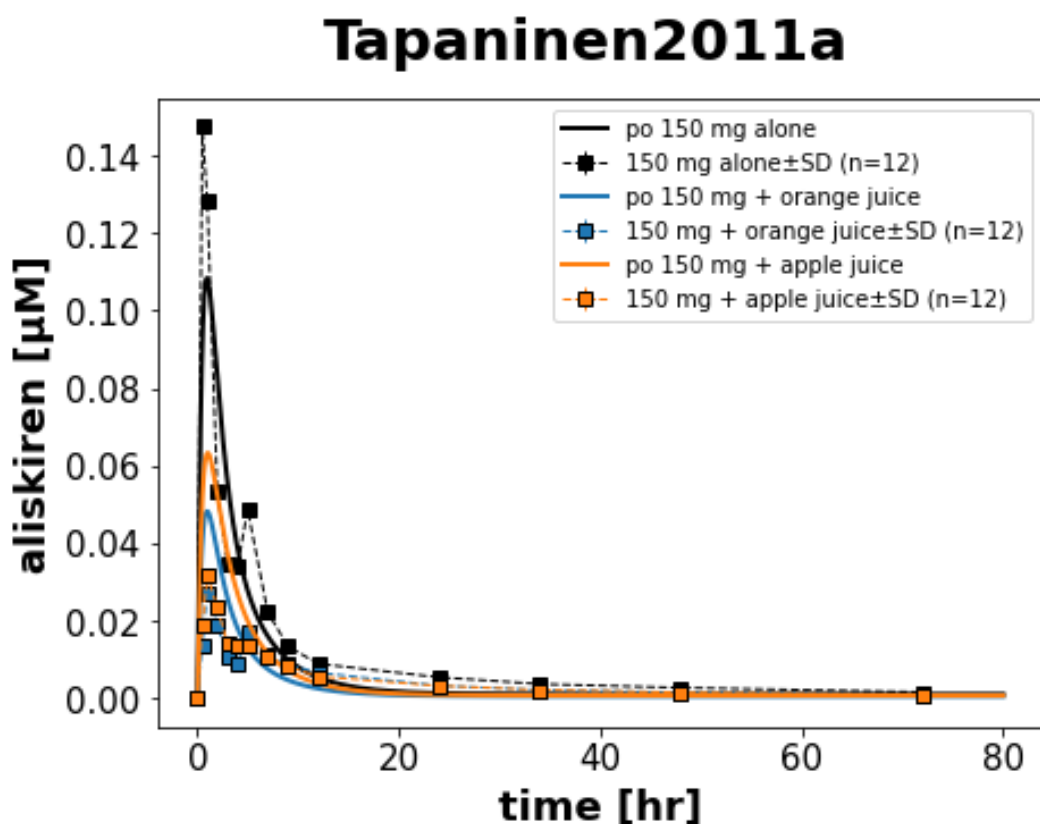


Figure 31: **Simulation of Tapaninen2011a** [63]. The figure portrays plasma concentration-time profiles of aliskiren following a single 150-mg oral dose administered alone, co-administered with orange juice, or co-administered with apple juice. Experimental data are shown as mean \pm SD ($n = 12$) and are compared to simulated profiles. The black lines and markers represent aliskiren administered alone, while blue and orange lines and markers represent co-administration with orange juice and apple juice, respectively.

3.6 Summary

The PBPK/PD model of aliskiren was developed to study the effects of hepatorenal impairment, drug-drug interactions, and the influence of aliskiren on the Renin-Angiotensin-Aldosterone System (RAAS). The results provided insights into how these factors affect aliskiren's distribution, metabolism, and excretion, as well as its pharmacodynamic effects using a whole-body and RAAS model.

The model was able to simulate pharmacokinetics for single and multiple doses of aliskiren and showed general trends in its behavior under different conditions. However, it remains incomplete due to missing pharmacokinetic outputs and the lack of a fully integrated pharmacodynamic component. This means the predictions are not yet fully accurate or aligned with expected outcomes.

While the simulations showed useful results, the model could not fully capture differences caused by varying levels of hepatorenal impairment or changes in enzyme activity. This highlights the need for further refinement and additional data to improve its accuracy.

In summary, the model provides a strong starting point for understanding aliskiren's pharmacokinetics, but further development is needed to accurately predict its behavior under complex physiological conditions. The model is able to simulate the pharmacokinetics for different dosages for single and multiple dose but it is not able to simulate the differences in the hepatorenal impairments or the enzyme activities.

4 Discussion

4.1 Data

The data curated for the aliskiren model represent a standard database; however, several challenges were encountered due to inconsistencies in the dataset. One key issue was the high interindividual variability observed in pharmacokinetic studies, which made it difficult to align the time courses across different studies.

For example, studies by *Burckhardt et al.* and *Waldmeier et al.* demonstrated significant differences in aliskiren pharmacokinetics among individuals. In the study by *Burckhardt et al.*, three individuals exhibited distinct times to reach maximal concentration and varying *AUCs*, primarily due to differences in drug absorption (see Figure 36) [10]. Similarly, *Waldmeier et al.* reported comparable issues with four individuals showing variability in absorption and pharmacokinetics (see Figure 50) [78]. This variability highlights a challenge in achieving a consistent pharmacokinetic profile for aliskiren.

Most of the curated studies (see Table 6) reported different pharmacokinetic outcomes and, when available, showed large standard deviations. This variability limits the ability to derive an average, reliable pharmacokinetic profile for aliskiren. Another example of high interindividual variability can be seen in the comparison of studies by *Fisher et al.* and *Hu et al.* (see Figures 15 and 16) [22, 27]. For a 600 mg dose of aliskiren, *Fisher et al.* reported a maximal plasma concentration (c_{max}) of approximately 0.2 μM , while *Hu et al.* reported a concentration closer to 1 μM for the same dose. These differences further emphasize the inconsistency in the data. Additionally, the data for aliskiren's metabolites and excretion were insufficient, making it difficult to fully characterize the distribution and elimination of the drug throughout the body. While sufficient data were available to explore drug-drug interactions, these studies often lacked information about the varying time courses influenced by enzyme activity, which are critical for understanding the pharmacokinetic and pharmacodynamic behavior of aliskiren.

In summary, the challenges with the curated data, including high variability, insufficient metabolite and excretion data, and inconsistencies across studies, limit the ability to create a fully reliable and predictive aliskiren model. Future studies with standardized protocols and a focus on consistent reporting of pharmacokinetic parameters are essential to improve the robustness of the model.

4.2 Model performance

The PBPK/PD model provides a robust foundation for simulating aliskiren's pharmacokinetics across different tissues and dosing regimens, but key areas require further refinement to improve its accuracy and predictive capability.

One notable limitation is the incomplete representation of fecal excretion delays, as observed in experimental studies. For instance, *Waldmeier et al.* [78] (see Figure 17) reported significant delays in fecal excretion, a phenomenon the model currently fails to replicate. Addressing this issue would allow for better predictions of aliskiren's elimination profile.

Additionally, discrepancies were observed in the absorption kinetics of aliskiren. Simulated plasma concentrations consistently peak earlier and lower than experimental data. For example,

the model predicts a c_{max} of approximately $0.4 \mu\text{M}$ at 2 hours, compared to the experimentally observed c_{max} of $0.6 \mu\text{M}$ at 4 hours in the study by *Vaidyanathan et al.* [73]. Similar absorption-related discrepancies are evident in studies by *Hu et al.*, *Tapaninen et al.*, and *Zhao et al.* [27, 60, 86], suggesting the need for further optimization of absorption phase parameters.

A critical limitation is the absence of a pharmacodynamic (PD) component in the current model. Without a PD framework, the model cannot evaluate aliskiren's downstream effects on the Renin-Angiotensin-Aldosterone System (RAAS), which limits its application in studying therapeutic efficacy, drug-drug interactions, and conditions such as renal and hepatic impairment. Integrating pharmacodynamics would provide a more comprehensive understanding of aliskiren's physiological and therapeutic impacts.

Discrepancies in drug-drug interaction (DDI) scenarios further highlight areas for refinement. For instance, the model underpredicted the increase in AUC for cyclosporine and ketoconazole (CYP3A4 inhibitors) (see Figures 38 and 47), likely due to oversimplified representations of enzyme inhibition mechanisms. Similarly, for enzyme inducers like rifampicin (see Figure 41), the predicted effect on both intestinal and hepatic metabolism did not fully align with experimental data, indicating the need to enhance the modeling of first-pass metabolism. The current model assumes a uniform and static process for first-pass metabolism, which does not adequately capture the interaction between intestinal and liver metabolism under varying physiological and DDI conditions.

Furthermore, the model assumes uniform enzyme expression across populations, which overlooks interindividual variability in factors such as CYP3A4 activity, transporter expression, and gastrointestinal motility. This assumption likely contributes to deviations in AUC and c_{max} predictions for certain scenarios. Incorporating population variability through virtual population simulations could improve the model's ability to capture interindividual differences, particularly in diverse patient groups.

Despite these limitations, the model effectively captures general pharmacokinetic trends under both single and multiple dosing schemes. Future refinements should focus on incorporating delayed fecal excretion, optimizing absorption kinetics, refining enzyme and transporter activity estimates, and integrating pharmacodynamics. Additionally, enhanced modeling of first-pass metabolism and interindividual variability would allow for more accurate predictions, particularly in scenarios involving enzyme modulators and complex DDIs. By addressing these areas, the PBPK/PD model could become a more powerful tool for understanding aliskiren's behavior across a wide range of physiological conditions.

4.3 Impairments

The model accounts for hepatic and renal impairments by introducing parameters to simulate these conditions. Specifically, the parameter $f_{cirrhosis}$ represents the severity of cirrhosis, and $KI_frenalfunction$ is used to simulate varying degrees of renal impairment. Figures 20 and 22 provide insights into how aliskiren is distributed throughout the body under different stages of impairment.

While the model is a useful starting point, it currently has limitations. It cannot fully simulate the impact of specific impairment stages, as the parameter effects appear to overlap across

different stages of impairment. For example, in the simulations based on *Vaidyanathan et al.* [74, 68] (see Figures 21 and 23), the curves for healthy individuals and those with impairments are nearly identical. This lack of differentiation does not align with experimental data, which clearly show distinct pharmacokinetic profiles for various stages of impairment.

A noticeable limitation is the absence of significant effects from different stages of cirrhosis. This is unexpected, given the liver’s critical role in drug metabolism and enterohepatic circulation (EHC). The model’s inability to capture these effects highlights the need for further refinement to better simulate the interplay between hepatic and renal impairments.

4.4 Drug-drug interactions

Several studies listed in Table 6 have explored drug-drug interactions between aliskiren and other compounds. Experimental data from studies such as *Rebello et al.* [50] reveal significant differences in the *AUCs* and c_{max} values of aliskiren when administered alone versus in combination with other drugs. These differences arise from the varying effects of co-administered drugs on enzymes involved in the absorption, distribution, metabolism, and excretion (ADME) of aliskiren.

The model includes the ability to scan different enzyme activities, such as GU_f_{cyp3a4} (CYP3A4 activity in the intestine), LI_f_{cyp3a4} (CYP3A4 activity in the liver), GU_f_{pg} (P-glycoprotein activity in the intestine), and GU_oatp (OATP activity in the intestine). These parameters are crucial for understanding how enzyme activity influences the pharmacokinetics of aliskiren. However, some key aspects remain unresolved.

For instance, the CYP3A4 activity scans (see Figures 26 and 29) should display variations in metabolite concentrations in the liver and intestine as CYP3A4 activity changes. However, the model does not currently include any visible metabolites, which limits its accuracy. Similar to the impairments section, simulations also appear to overlap or stack inappropriately, as observed in studies by *Ayalasomayajula et al.*, *Rebello et al.*, *Tapaninen et al.*, and *Vaidyanathan et al.* [5, 50, 60, 71]. This overlap suggests an incomplete representation of drug-drug interactions and their impact on aliskiren pharmacokinetics. In summary, while the model provides a framework for examining the influence of enzyme activity on drug-drug interactions, it lacks the ability to capture metabolite variations and properly distinguish between effects of different interactions. Further refinements are needed to integrate metabolite data and resolve overlapping simulations to achieve a more complete understanding of aliskiren’s pharmacokinetics in the presence of other drugs.

5 Outlook

Model refinement

The model is not complete, as important aspects like metabolism and excretion are not fully included. To better understand how aliskiren is distributed in the body, the model needs to be finished, with metabolites added and missing data for excretion incorporated to improve the simulations. The main issue is the lack of data on metabolites and excretion in the studies used. Looking for more studies beyond *Waldmeier et al.* could help provide useful data on excretion and metabolites [78].

While the PBPK model successfully captured key trends in aliskiren's pharmacokinetics under various dosing and interaction scenarios, several areas for improvement have been identified. Future iterations of the model should incorporate population variability to better account for interindividual differences in enzyme activity, transporter expression, and gastrointestinal motility, as demonstrated in the Figures 36 and 50. Implementing population-based simulations or virtual populations could enhance the predictive power of the model, particularly for diverse patient groups.

Another key area for improvement lies in the modeling of first-pass metabolism. Enhancing the representation of intestinal and hepatic metabolism as distinct but interconnected processes would enable a more detailed understanding of aliskiren's bioavailability, especially under the influence of enzyme modulators.

Drug-drug interactions and parameter fit

Some studies like *Rebello et al.* or *Tapaninen et al.* looked at aliskiren and how it interacts with other drugs when taken together (see Table 6 for more details) [51, 60]. The model focused on parameters like GU_f_{cyp3a4} (CYP3A4 activity in the intestine), LI_f_{cyp3a4} (CYP3A4 activity in the liver), GU_f_{pg} (P-glycoprotein activity in the intestine), and GU_oatp (OATP activity in the intestine). These parameters were analyzed, and their optimal values were identified via parameter fitting, but they were not fully included in the model. This is why there were only small differences between aliskiren taken alone and aliskiren taken with other drugs.

Completing the model is important so that updated values for enzyme activity can be added. This would make the model more accurate and better at predicting how drugs interact with aliskiren. This is important not only for enzyme activities but also for all parameters that were fitted or used in scans, as they also must be re-fitted to create a more accurate and reliable model once the model is finished.

Parameter scan

Understanding aliskiren's pharmacokinetics can be improved by running parameter scans after completing the model. Scans for factors like renal function ($KI_f_{renal\ function}$), the severity of cirrhosis ($f_{cirrhosis}$), or enzyme activity levels for the P-glycoprotein, OATP or CYP3A4 can help explore how these parameters affect the drug. This would provide clearer insights and support better treatment planning.

Pharmacodynamics

In addition to the pharmacokinetic data of aliskiren, some studies, such as those by *Balcarek et al.* and *Fisher et al.*, have also published pharmacodynamic data [7, 22]. This data was curated but not implemented in the model because the RAAS (Renin-Angiotensin-Aldosterone System) part of the model is incomplete.

Once the RAAS is fully added to the model, the pharmacodynamic data from these studies can be included and simulated. These simulations would help improve the understanding of how aliskiren inhibits the RAAS and lowers blood pressure.

Exploring the effects of aging, cardiovascular disease, and other Impairments

A valuable future direction could involve studying conditions like type 2 diabetes, aging, and cardiovascular disease (CVD) to better understand how they affect drugs like aliskiren. *Zhao et al.* studied healthy people and patients with type 2 diabetes and found that diabetes does not significantly change how aliskiren works in the body. This means aliskiren remains effective in patients with diabetes [86].

Aging is another important factor. As people get older, changes like reduced kidney and liver function, altered body composition, and differences in how drugs bind to proteins can affect how drugs are processed. While aliskiren is mostly excreted unchanged and does not depend heavily on the kidneys or liver, it's important to study its effects in older adults. Older people often have other health conditions and take multiple medications, which could impact how the drug works. *Vaidyanathan et al.* found that aliskiren exposure is slightly higher in elderly patients (65 years) compared to younger adults (18–45 years) after a single dose [73].

Cardiovascular disease (CVD) is another area to study. CVD often causes changes in blood flow and heart function, which can affect how drugs work. Since high blood pressure is a major part of CVD and one of the main conditions treated with aliskiren, understanding how CVD impacts the drug's effectiveness is important.

Future research should focus on creating models that include diabetes, aging, and CVD to better understand how these factors affect aliskiren. This would help make sure the drug is safe and effective for a wide range of patients.

6 Acknowledgment

I would like to thank my supervisor, Dr. Matthias König, who was a great help to me during the project and was able to give me a lot in this area. Thanks to his patience and knowledge in the field, I was able to acquire knowledge and gain practical experience almost without any problems, which I really appreciate.

A special acknowledgement goes to my family and friends who have supported and motivated me during this time, allowing me to maintain my focus as much as possible.

This work was supported by the Federal Ministry of Education and Research (BMBF, Germany) within ATLAS by grant number 031L0304B and by the German Research Foundation (DFG) within the Research Unit Program FOR 5151 "QuaLiPerF (Quantifying Liver Perfusion-Function Relationship in Complex Resection - A Systems Medicine Approach)" by grant number 436883643 and by grant number 465194077 (Priority Programme SPP 2311, Subproject Sim-LivA). This work was supported by the BMBF-funded de.NBI Cloud within the German Network for Bioinformatics Infrastructure (de.NBI) (031A537B, 031A533A, 031A538A, 031A533B, 031A535A, 031A537C, 031A534A, 031A532B).

The following images were created with **BioRender**:

- Figure 1, Figure 3, Figure 4, Figure 5, Figure 7

The following images were created with **Cytoscape**:

- Figure 8, Figure 9, Figure 10, Figure 11, Figure 12

Supplements

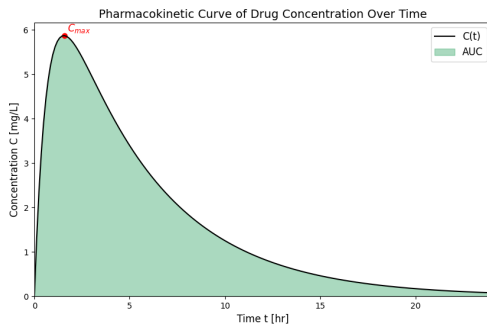


Figure 32: Visualization of the area under the curve AUC and the maximal plasma concentration c_{max}

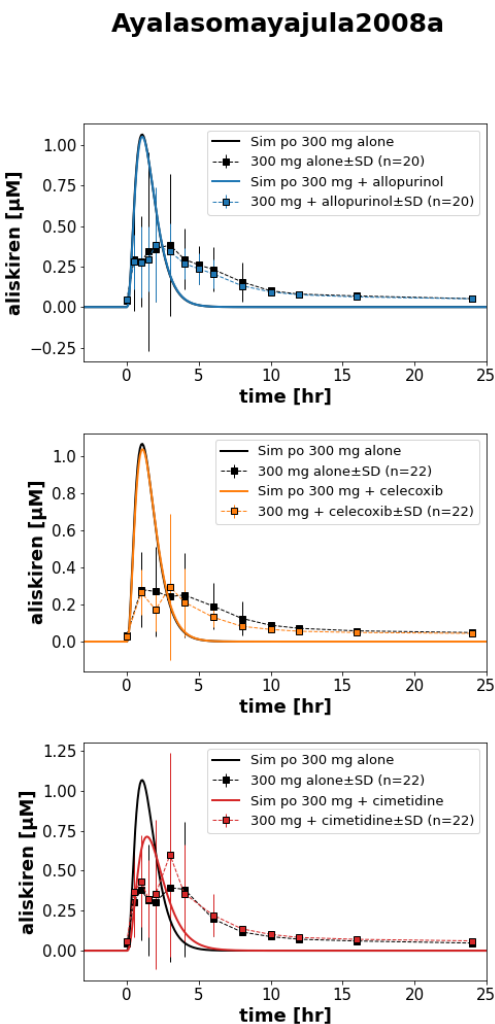


Figure 33: Simulation of Ayalasomayajula2008a [5]. Plasma concentration-time profiles for aliskiren following once-daily administration of a 300-mg dose alone or co-administered with allopurinol ($n = 20$), celecoxib ($n = 22$), or cimetidine ($n = 22$) in healthy subjects. The figure shows plasma concentrations of aliskiren at steady state. Experimental data are presented as mean \pm SD, with simulated profiles shown as solid lines.

Balcarek2014

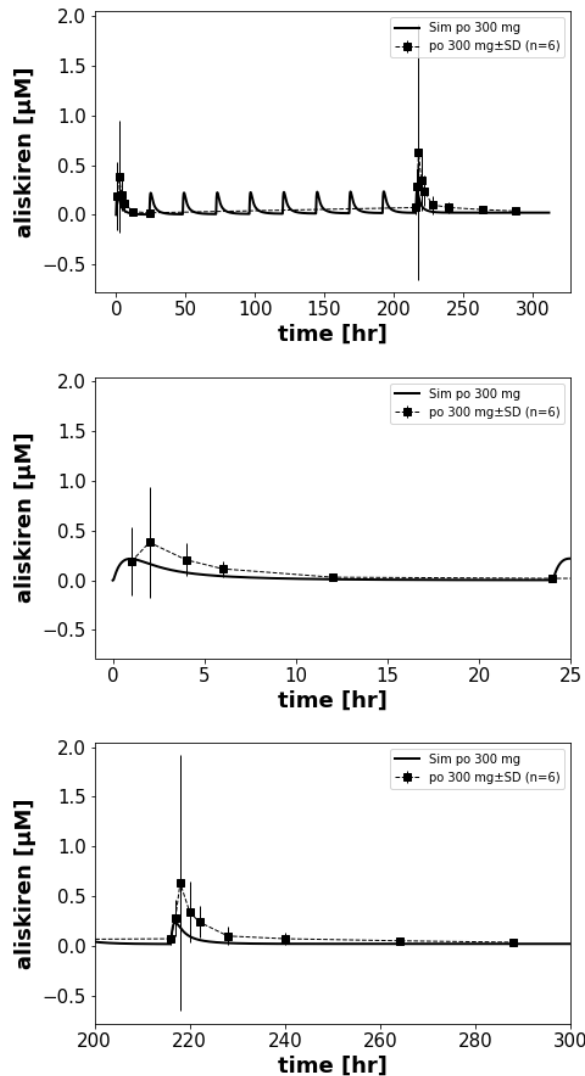


Figure 34: **Simulation of Balcarek2014 [7].** Plasma concentration-time profiles for aliskiren following a once-daily 300-mg oral dose for 10 consecutive days in healthy subjects ($n = 6$). The top panel illustrates the full 10-day dosing period and the decline post-final dose, while the middle and bottom panels provide zoomed-in views of the initial 25 hours and the steady-state phase (days 9–10), respectively. Experimental data are presented as mean \pm SD (markers), and simulated values are shown as solid lines.

Burckhardt2014

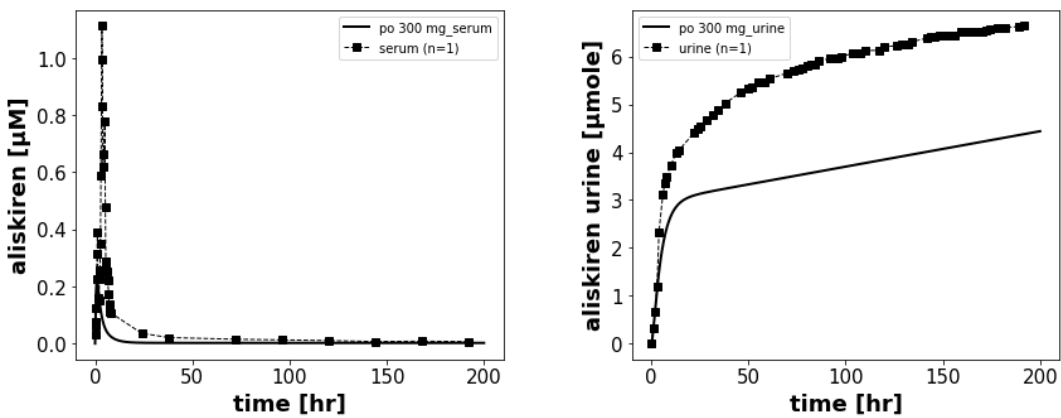


Figure 35: **Simulation of Burckhardt2014** [11]. Plasma and cumulative urinary concentration-time profiles for aliskiren following a single 300-mg oral dose in one subject. The left panel illustrates plasma concentrations, while the right panel shows cumulative urinary excretion. Experimental data ($n = 1$) are displayed as markers, and simulated profiles are represented by solid lines.

Burckhardt2014a

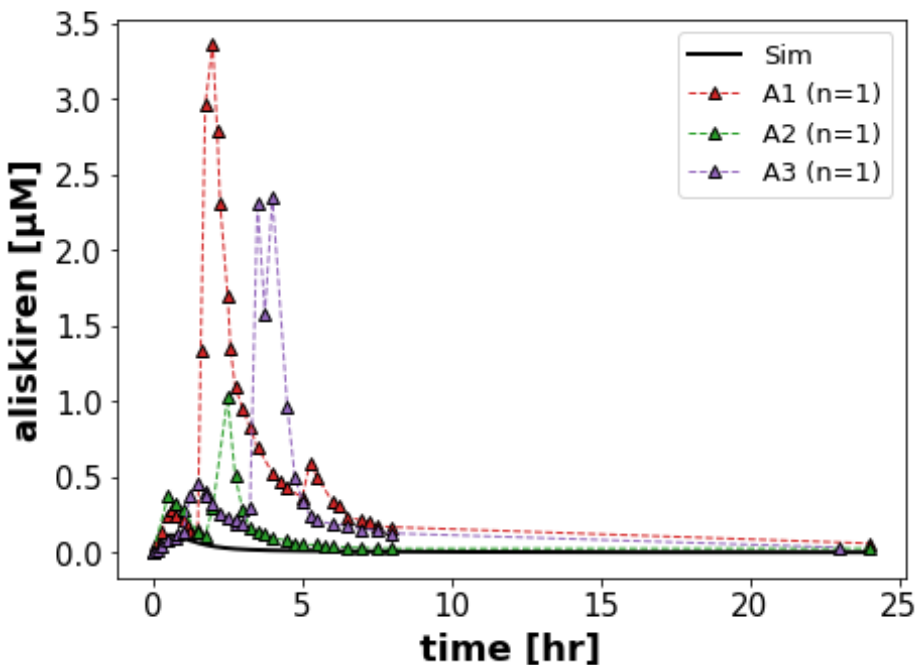


Figure 36: **Simulation of Burckhardt2014a** [10]. Plasma concentration-time profiles for aliskiren following a single 300-mg oral dose in three individual subjects (A1, A2, and A3). Experimental data for each subject are shown as markers, and the simulation of the aliskiren concentration in the plasma is represented by solid lines. The figure highlights interindividual variability in plasma concentrations, particularly during the absorption and distribution phases, with the simulation closely matching individual pharmacokinetic trends.

Rebello2011

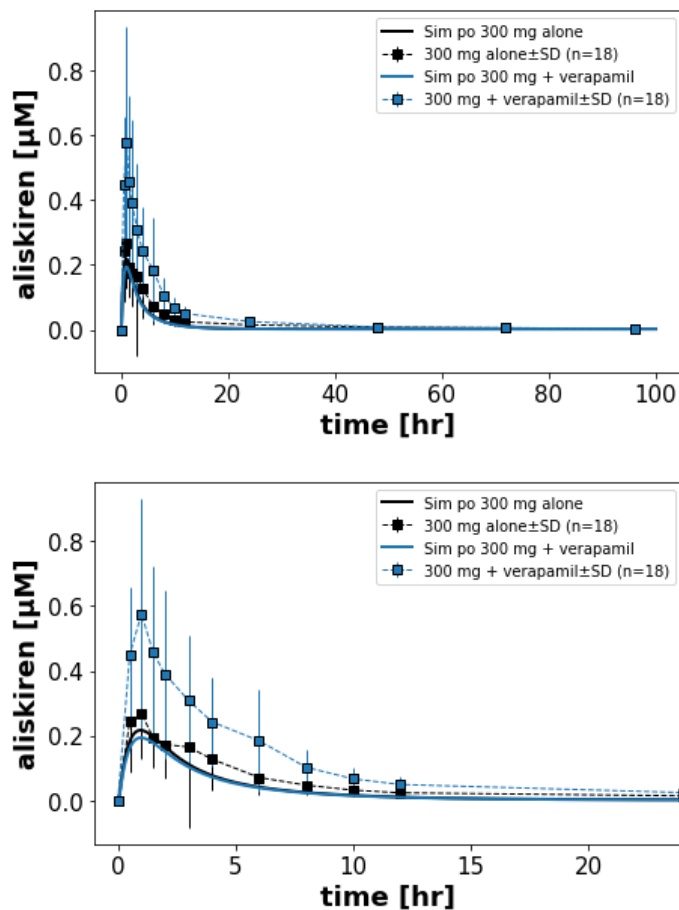


Figure 37: **Simulation of Rebello2011 [51].** Plasma concentration-time profiles for aliskiren following a single 300-mg oral dose administered alone or co-administered with verapamil in healthy subjects ($n = 18$). The top panel shows the full 100-hour observation period, while the bottom panel provides a closer view of the first 24 hours. Experimental data are presented as mean \pm SD (markers), with simulated profiles depicted as solid lines.

Rebello2011a

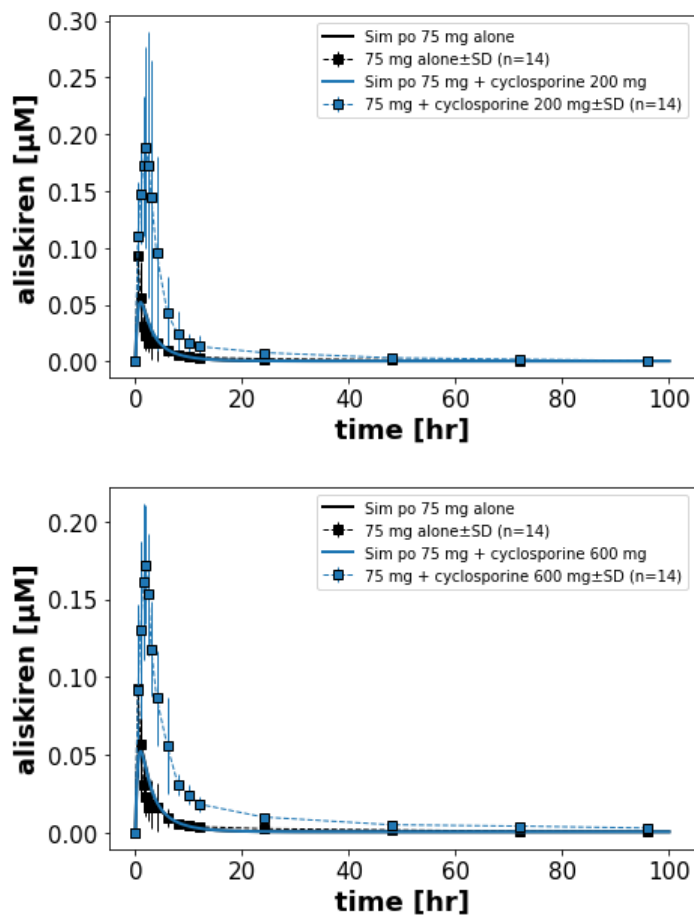


Figure 38: **Simulation of Rebello2011a [50].** Plasma concentration-time profiles for aliskiren following a single 75-mg oral dose administered alone or co-administered with cyclosporine at doses of 200 mg (top panel) or 600 mg (bottom panel) in healthy subjects ($n = 14$). Experimental data are presented as mean \pm SD (markers), while simulated profiles are shown as solid lines.

Tapaninen2010

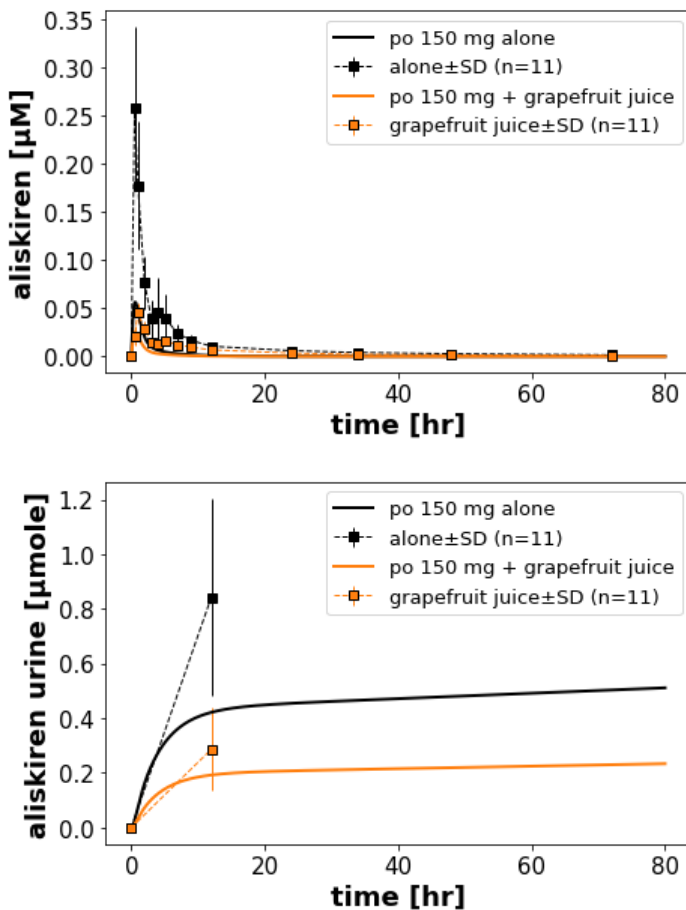


Figure 39: **Simulation of Tapaninen2010** [60]. Plasma and urinary concentration-time profiles for aliskiren following a single 150-mg oral dose administered alone or co-administered with grapefruit juice in healthy subjects ($n = 11$). The top panel shows plasma concentration profiles, while the bottom panel illustrates cumulative urinary excretion. Experimental data are presented as mean \pm SD (markers), and simulated profiles are depicted as solid lines.

Tapaninen2010a

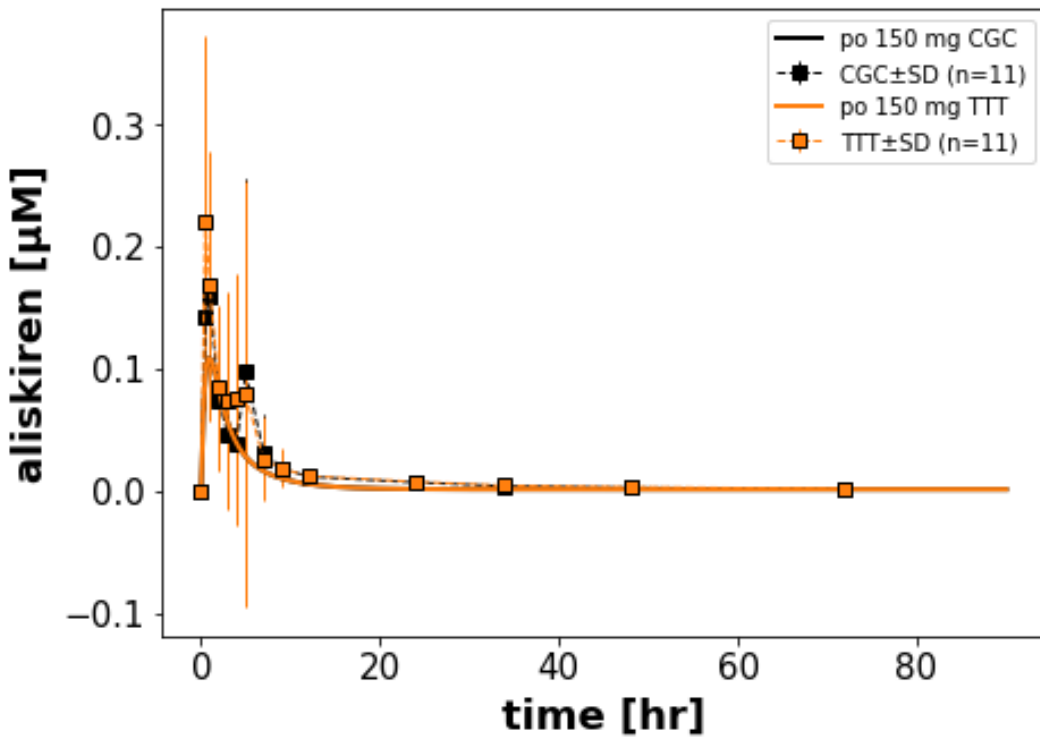


Figure 40: **Simulation of Tapaninen2010a [62].** Plasma concentration-time profiles of aliskiren following a single 150-mg oral dose in subjects homozygous for the ABCB1 c.1236C-c.2677G-c.3435C (CGC, n = 11; black lines and markers) or ABCB1 c.1236T-c.2677T-c.3435T (TTT, n = 11; orange lines and markers) haplotypes. Data are presented as weight-adjusted mean \pm SEM. ABCB1 (P-glycoprotein) is a key membrane transporter involved in drug absorption and excretion. The minimal differences observed between CGC and TTT haplotypes suggest that these genetic variants have a limited effect on aliskiren's pharmacokinetics.

Tapaninen2010b

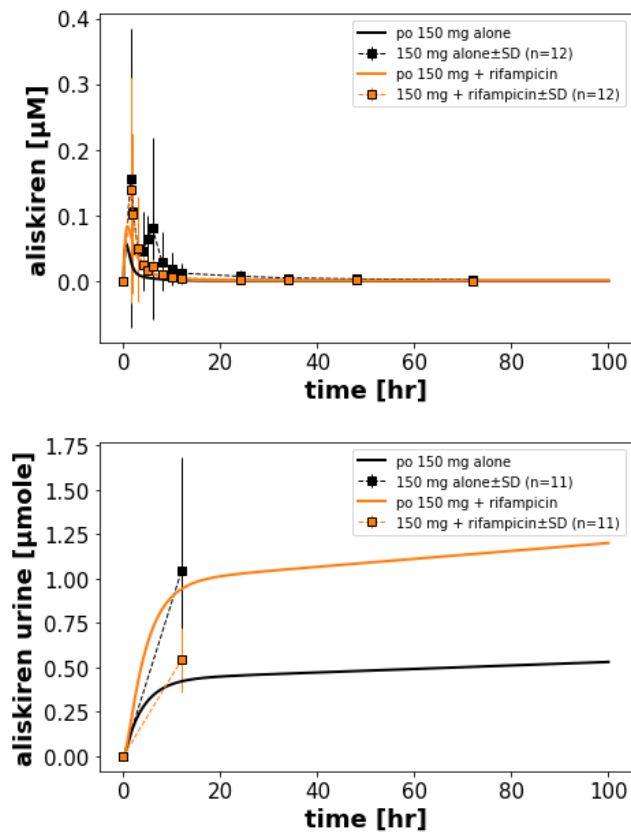


Figure 41: **Simulation of Tapaninen2010b [64].** Plasma and urinary concentration-time profiles for aliskiren following a single 150-mg oral dose administered alone or co-administered with rifampicin in healthy subjects ($n = 12$ for plasma, $n = 11$ for urine). The top panel shows plasma concentrations, while the bottom panel illustrates cumulative urinary excretion. Simulated profiles are shown as solid lines, and experimental data are presented as markers (mean \pm SD).

Tapaninen2011

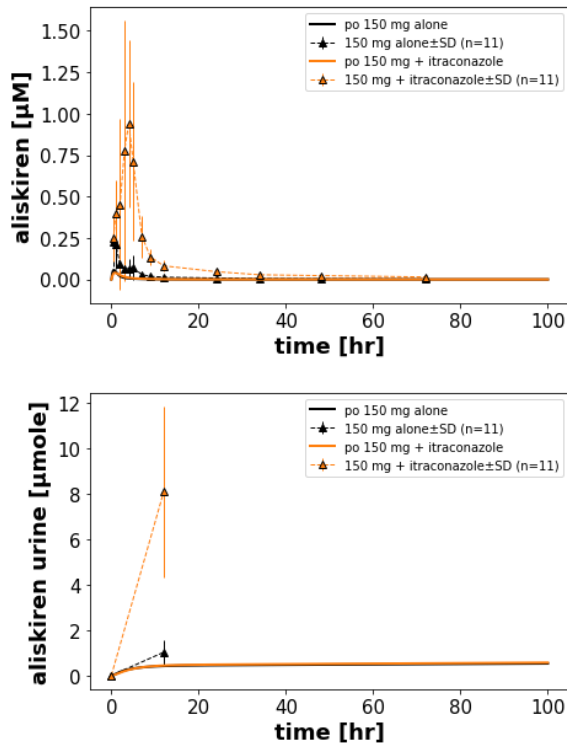


Figure 42: **Simulation of Tapaninen2011 [61].** Plasma and urinary concentration-time profiles for aliskiren following a single 150-mg oral dose administered alone or co-administered with itraconazole in healthy subjects ($n = 11$). The top panel displays plasma concentrations, and the bottom panel shows cumulative urinary excretion. Simulated profiles are shown as solid lines, and experimental data are presented as markers (mean \pm SD).

Vaidyanathan2006

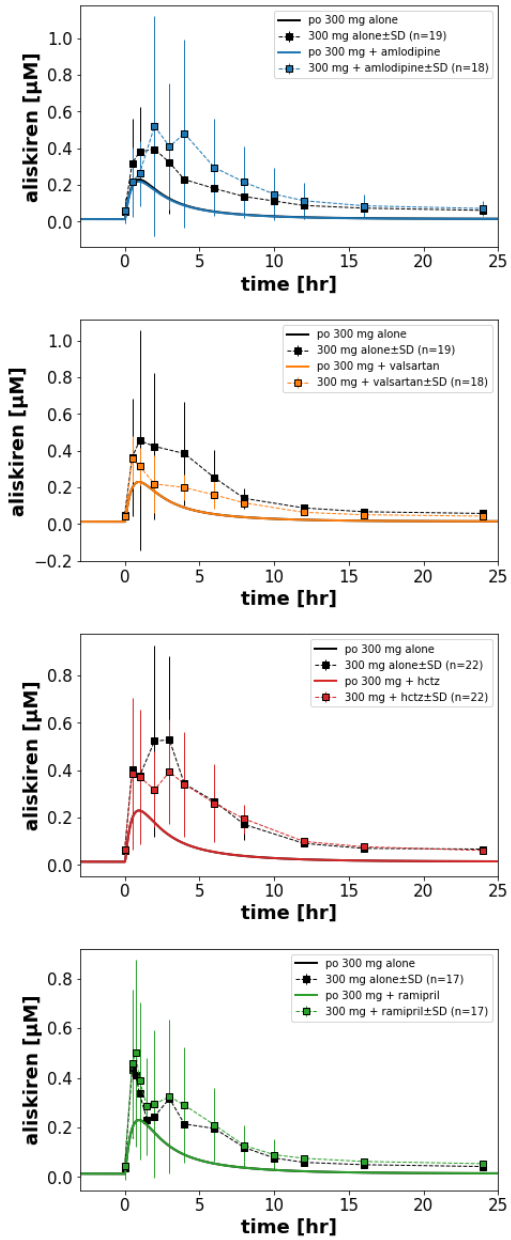


Figure 43: **Simulation of Vaidyanathan2006 [66].** The figure presents plasma concentration-time profiles for aliskiren in healthy subjects undergoing multiple-dose schemes. Aliskiren was administered alone for 14 days, followed by an additional 14 days in combination with amlodipine. In another scheme, aliskiren was given alone for 7 days, followed by 4 additional days in combination with valsartan. Similarly, aliskiren was administered alone for 7 days before being combined with hydrochlorothiazide (HCTZ) for 4 additional days, and in a separate scheme, aliskiren was given alone for 7 days, followed by 6 days in combination with ramipril. Simulated profiles are shown as solid lines, while experimental data are presented as markers (mean \pm SD)

Vaidyanathan2006a

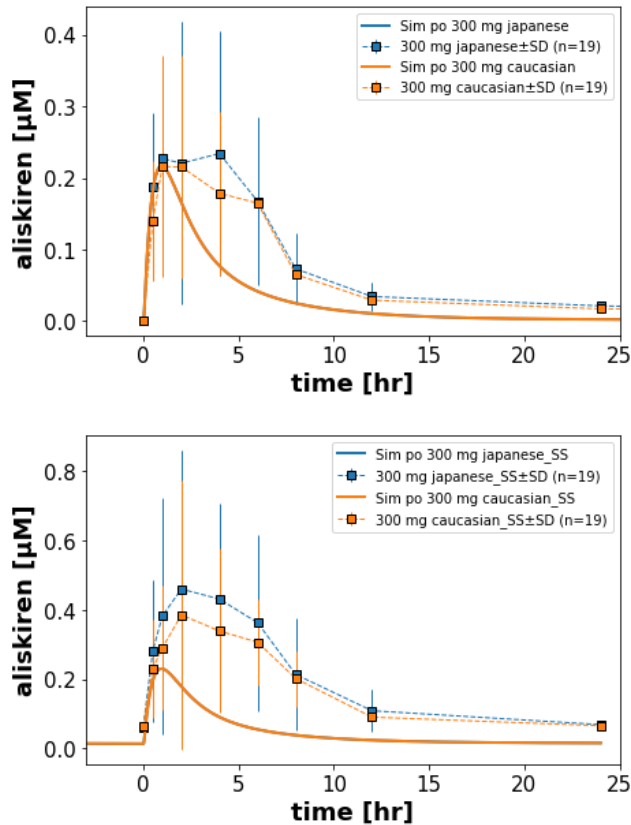


Figure 44: **Simulation of Vaidyanathan2006a** [71]. Plasma concentration-time profiles for aliskiren in Japanese and Caucasian subjects following a single 300-mg oral dose (top panel) and after multiple once-daily doses for 7 days (bottom panel). Simulated profiles are shown as solid lines, while experimental data are presented as markers (mean \pm SD, n = 19 for each group).

Vaidyanathan2007a

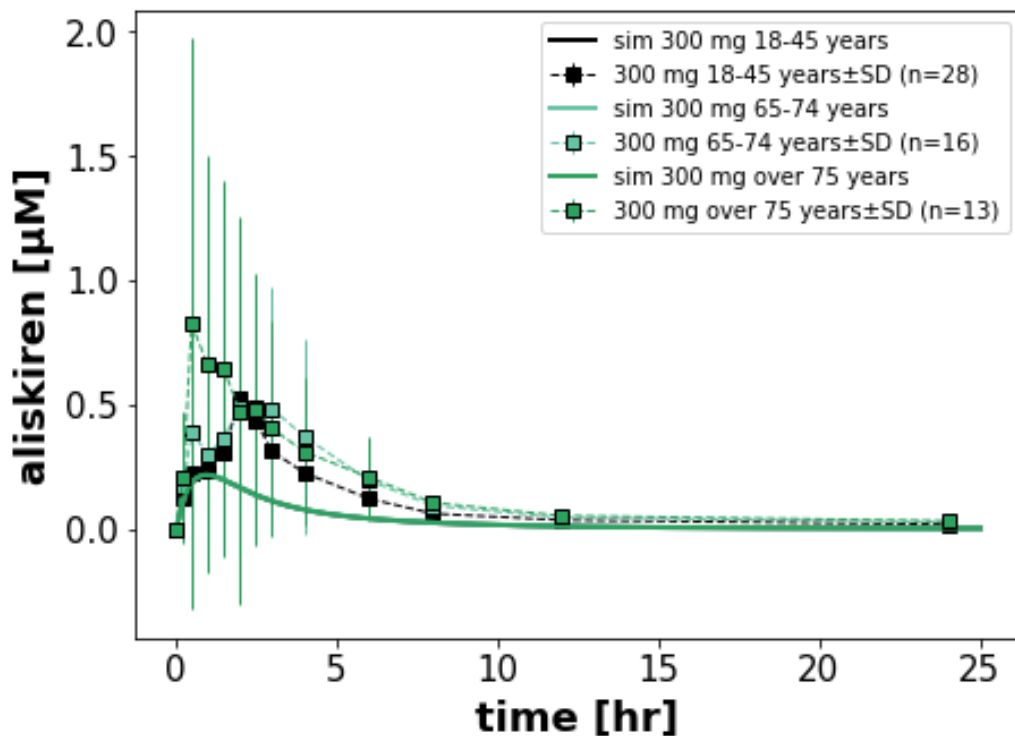


Figure 45: **Simulation of Vaidyanathan2007a** [73]. Plasma concentration-time profiles for aliskiren following a single 300-mg oral dose across different age groups: 18–45 years ($n = 28$), 65–74 years ($n = 16$), and over 75 years ($n = 13$). Simulated profiles are shown as solid lines, while experimental data are presented as markers (mean \pm SD).

Vaidyanathan2007b (multiple dose, DDI)

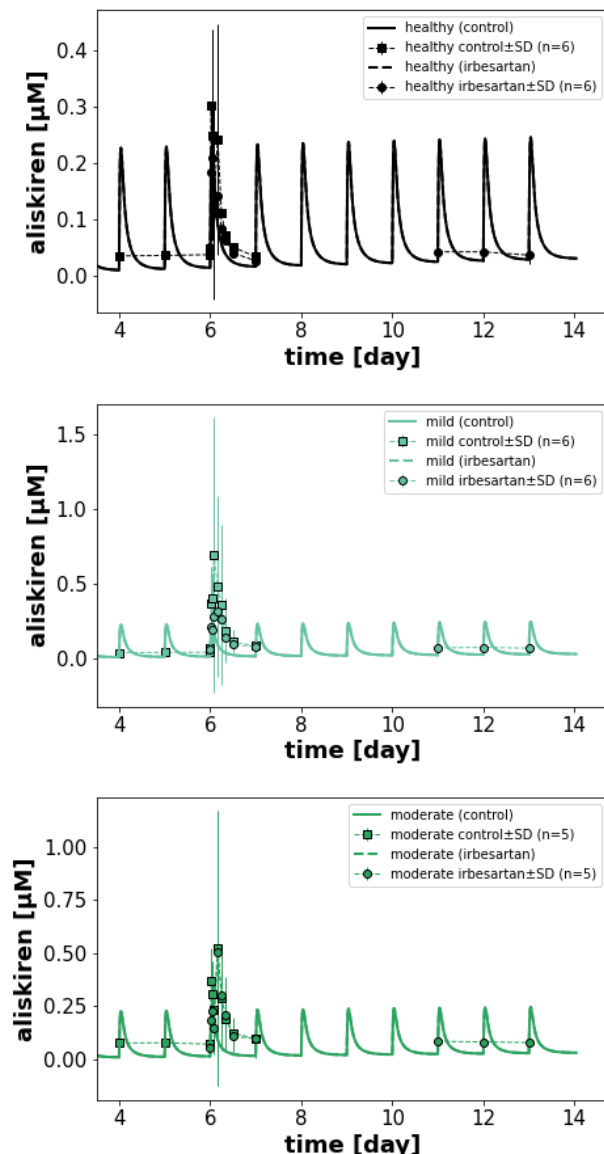


Figure 46: **Simulation of Vaidyanathan2007b (multiple dosing with Drug-Drug Interaction (DDI))** [68]. Plasma concentration-time profiles for aliskiren during multiple dosing with and without co-administration of irbesartan in healthy subjects and subjects with mild or moderate renal impairment. Aliskiren was administered once daily for 7 days, followed by an additional 7 days of combination therapy with irbesartan. The top panel shows profiles for healthy subjects ($n = 6$), the middle panel represents subjects with mild renal impairment ($n = 6$), and the bottom panel shows profiles for subjects with moderate renal impairment ($n = 5$). Simulated profiles are depicted as solid lines, and experimental data are shown as markers (mean \pm SD).

Vaidyanathan2008a

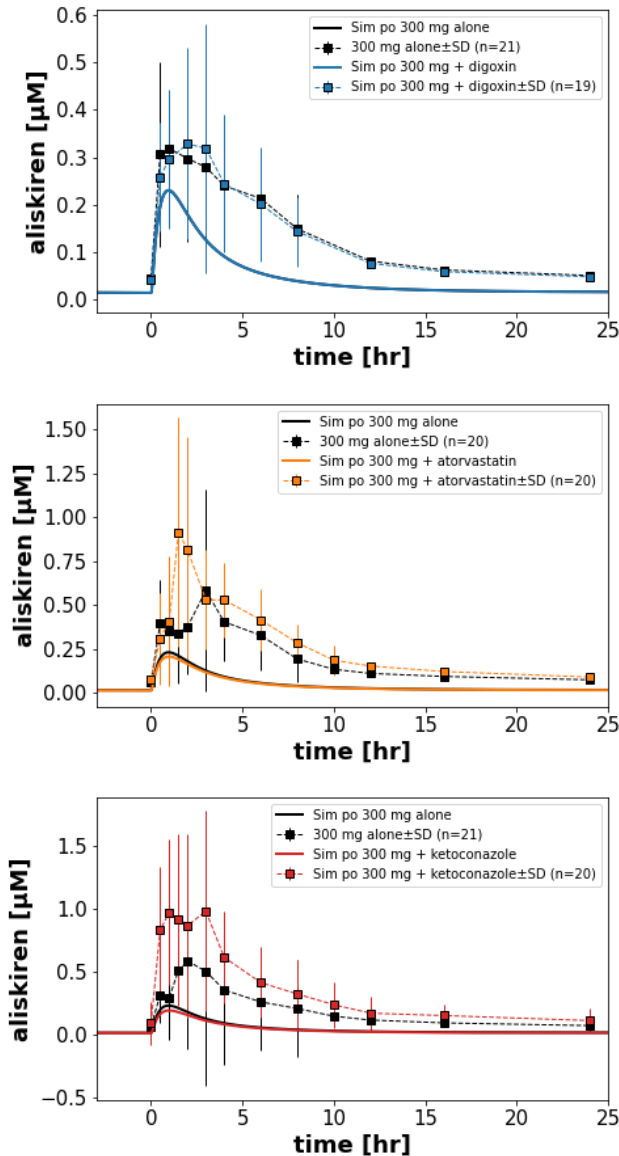


Figure 47: **Simulation of Vaidyanathan2008a [69].** This figure shows plasma concentration-time profiles for aliskiren during multiple-dose regimens in healthy subjects. Aliskiren was administered alone for 7 days, followed by additional combination therapy with either digoxin, atorvastatin, or ketoconazole. For the top panel, aliskiren was combined with digoxin for an additional 7 days (n = 19 for the combination, n = 21 for aliskiren alone). In the middle panel, aliskiren was combined with atorvastatin for an additional 6 days (n = 20), and in the bottom panel, aliskiren was combined with ketoconazole for an additional 6 days (n = 20). Simulated profiles are represented as solid lines, while experimental data are shown as markers (mean \pm SD).

Vaidyanathan2008b

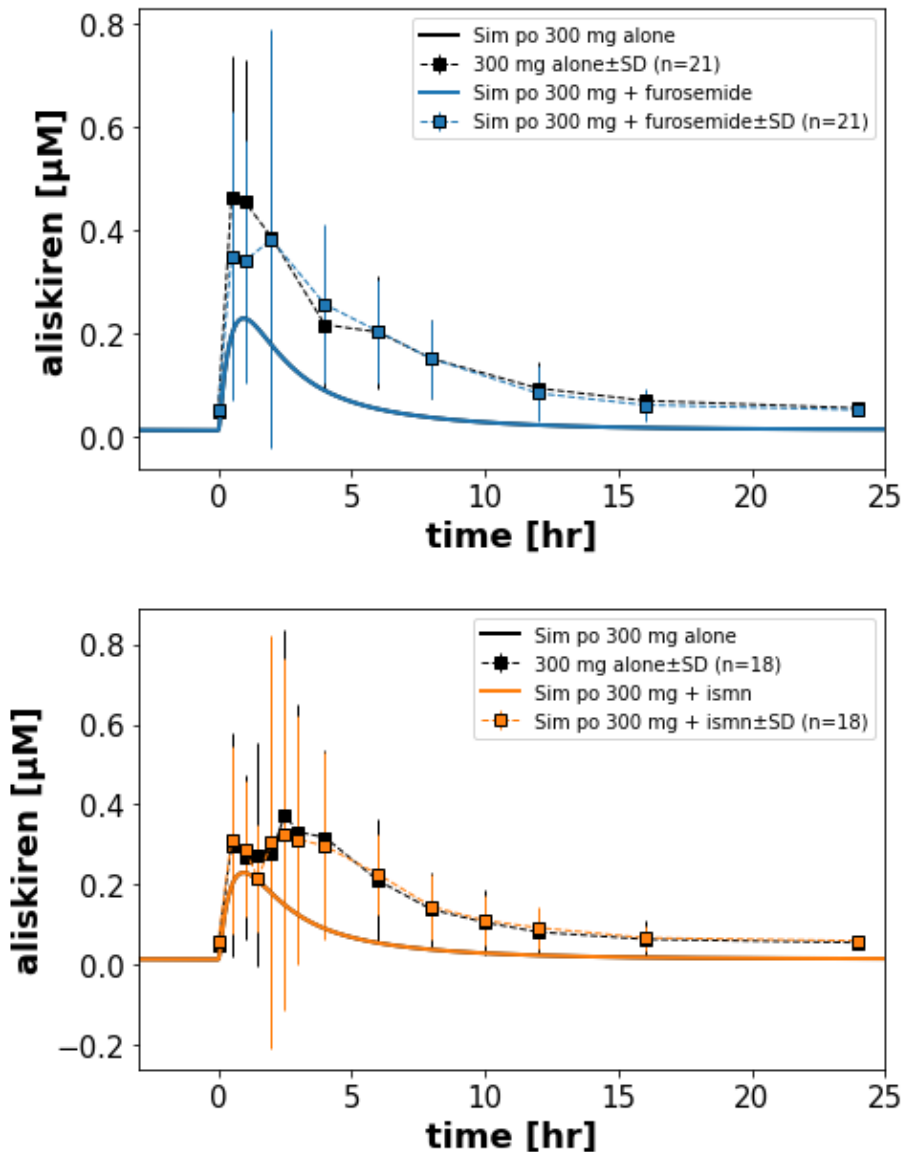


Figure 48: **Simulation of Vaidyanathan2008b [67].** Simulation of Vaidyanathan2008b [67]. Plasma concentration-time profiles for aliskiren during multiple-dose regimens in healthy subjects. Aliskiren was administered alone for 7 days, followed by an additional 3 days in combination with either furosemide (top panel) or isosorbide mononitrate (ISMN, bottom panel). In the top panel, the combination with furosemide ($n = 21$) is compared to aliskiren alone ($n = 21$). In the bottom panel, the combination with ISMN ($n = 18$) is compared to aliskiren alone ($n = 18$). Simulated profiles are shown as solid lines, while experimental data are represented as markers (mean \pm SD).

Vaidyanathan2008c

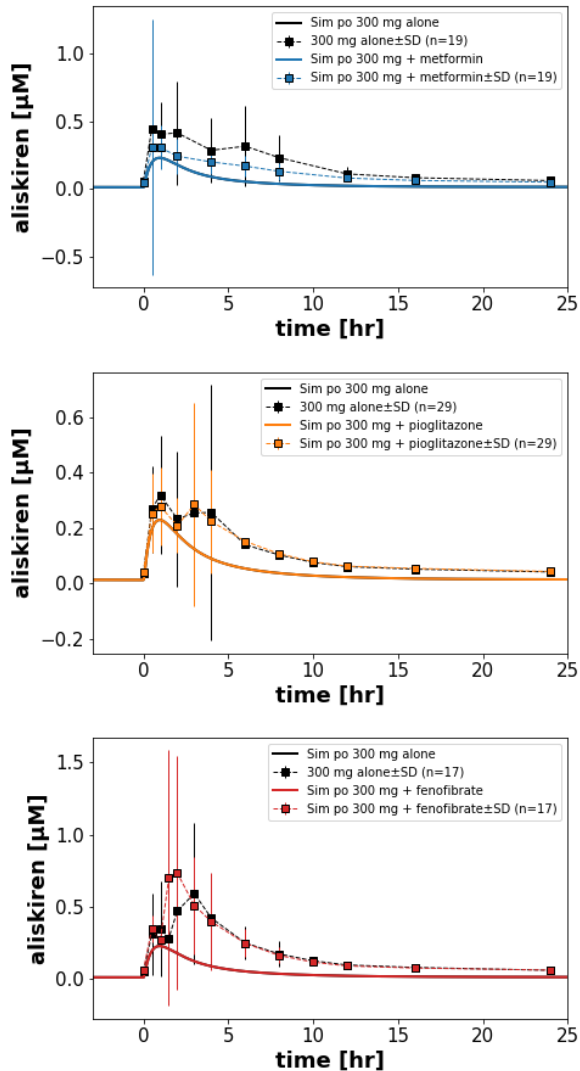


Figure 49: **Simulation of Vaidyanathan2008c [72].** Simulation of Vaidyanathan2008c [72]. This figure presents plasma concentration-time profiles for aliskiren during multiple-dose regimens in healthy subjects. Aliskiren was administered alone for 7 days, followed by additional combination therapy with metformin, pioglitazone, or fenofibrate. In the top panel, aliskiren was combined with metformin for an additional 4 days ($n = 19$). The middle panel shows aliskiren combined with pioglitazone for an additional 7 days ($n = 29$), while the bottom panel illustrates aliskiren combined with fenofibrate for an additional 5 days ($n = 17$). Simulated profiles are depicted as solid lines, while experimental data are represented as markers (mean \pm SD).

Waldmeier2007

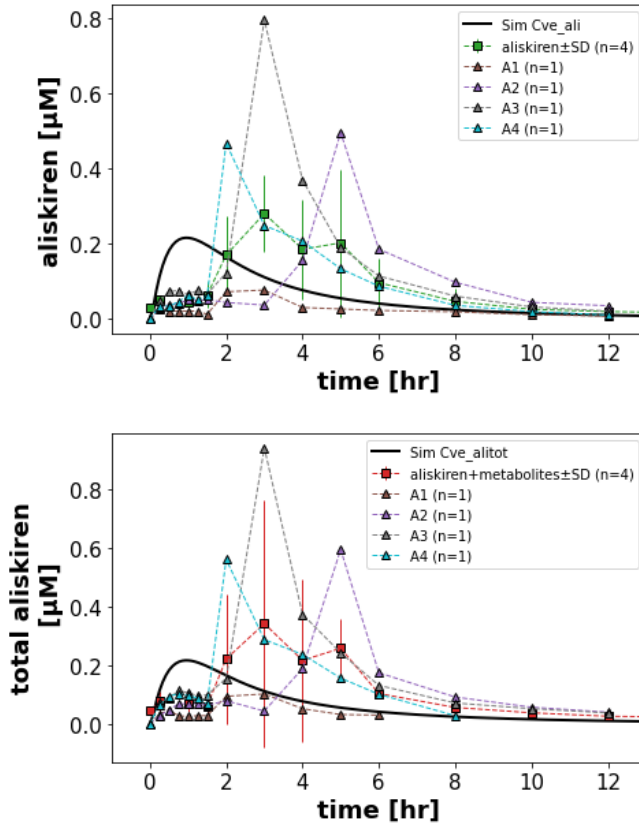


Figure 50: **Simulation of Waldmeier2007 (plasma data)** [78]. The top panel displays plasma concentration-time profiles for aliskiren alone in four individual subjects (A1–A4) and as mean \pm SD ($n = 4$), with simulated profiles shown as solid lines. The bottom panel illustrates total plasma concentrations of aliskiren and its metabolites (alitot) over time, represented as mean \pm SD ($n = 4$) and individual profiles (A1–A4). Simulated profiles for aliskiren and alitot are shown as solid lines. The figure highlights the contribution of metabolites to total plasma concentrations and the variability between individual subjects.

Zhao2006

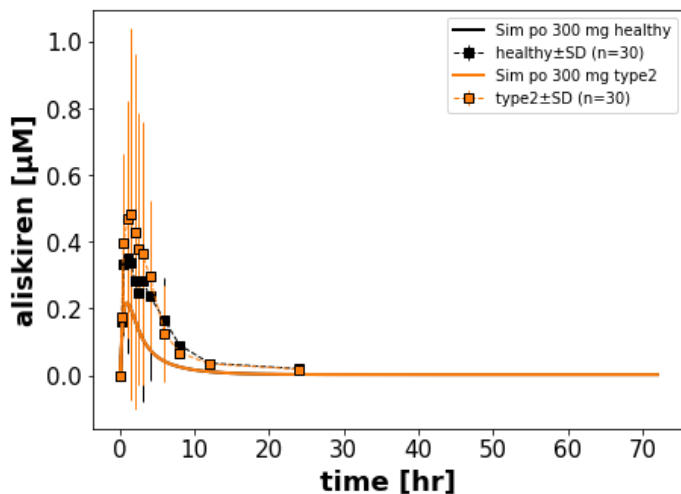


Figure 51: **Simulation of Zhao2006 [86].** Plasma concentration-time profiles for aliskiren following a single 300-mg oral dose in healthy subjects ($n = 30$) and subjects with type 2 diabetes mellitus ($n = 30$). Simulated profiles are shown as solid lines, while experimental data are presented as markers (mean \pm SD).

References

- [1] European Medicines Agency (EMA). *European Medicines Agency*. URL: <https://www.ema.europa.eu/en/homepage> (visited on 12/25/2024).
- [2] U.S. Food and Drug Administration (FDA). *U.S. Food and Drug Administration*. URL: <https://www.fda.gov/> (visited on 12/25/2024).
- [3] Karl Andersen, Myron H. Weinberger, Brent Egan, Christian M. Constance, Mohammed A. Ali, James Jin, and Deborah L. Keefe. „Comparative Efficacy and Safety of Aliskiren, an Oral Direct Renin Inhibitor, and Ramipril in Hypertension: A 6-Month, Randomized, Double-Blind Trial“. In: *Journal of Hypertension* 26.3 (Mar. 2008), pp. 589–599. DOI: 10.1097/HJH.0b013e3282f3ad9a. pmid: 18300872.
- [4] American Heart Association. *Understanding Blood Pressure Readings*. URL: <https://www.heart.org/en/health-topics/high-blood-pressure/understanding-blood-pressure-readings> (visited on 12/10/2024).
- [5] Surya Ayala-Somayajula, Stéphanie Tchaloyan, Ching-Ming Yeh, Marie-Noelle Bizot, Hans Armin Dieterich, Dan Howard, and William P. Dole. „A Study of the Pharmacokinetic Interactions of the Direct Renin Inhibitor Aliskiren with Allopurinol, Celecoxib and Cimetidine in Healthy Subjects.“ In: *Current medical research and opinion* 24.3 (Mar. 2008), pp. 717–726. DOI: 10.1185/030079908X260934. pmid: 18234150.
- [6] Michel Azizi, Randy Webb, Juerg Nussberger, and Norman K. Hollenberg. „Renin Inhibition with Aliskiren: Where Are We Now, and Where Are We Going?“ In: *Journal of hypertension* 24.2 (Feb. 2006), pp. 243–256. DOI: 10.1097/01.hjh.0000202812.72341.99. pmid: 16508564.
- [7] Joanna Balcarek, Bruno Sevá Pessôa, Catherine Bryson, Michel Azizi, Joël Ménard, Ingrid M. Garrelds, Gerard McGeehan, Richard A. Reeves, Sue G. Griffith, A. H. Jan Danser, and Richard Gregg. „Multiple Ascending Dose Study with the New Renin Inhibitor VTP-27999: Nephrocentric Consequences of Too Much Renin Inhibition.“ In: *Hypertension (Dallas, Tex. : 1979)* 63.5 (May 2014), pp. 942–950. DOI: 10.1161/HYPERTENSIONAHA.113.02893. pmid: 24470465.
- [8] Vivencio Barrios and Carlos Escobar. „Aliskiren in the Management of Hypertension.“ In: *American journal of cardiovascular drugs : drugs, devices, and other interventions* 10.6 (2010), pp. 349–358. DOI: 10.2165/11584980-00000000-00000. pmid: 21090828.
- [9] Natale Daniele Brunetti, Luisa De Gennaro, Pier Luigi Pellegrino, Andrea Cuculo, Luigi Ziccardi, Antonio Gaglione, and Matteo Di Biase. „Direct Renin Inhibition: Update on Clinical Investigations with Aliskiren.“ In: *European journal of cardiovascular prevention and rehabilitation : official journal of the European Society of Cardiology, Working Groups on Epidemiology & Prevention and Cardiac Rehabilitation and Exercise Physiology* 18.3 (June 2011), pp. 424–437. DOI: 10.1177/1741826710389387. pmid: 21450645.

- [10] Bjoern B. Burckhardt, Jutta Tins, and Stephanie Laer. „Liquid Chromatography-Tandem Mass Spectrometry Method for Determination of Aliskiren in Saliva and Its Application to a Clinical Trial with Healthy Volunteers.“ In: *Journal of pharmaceutical and biomedical analysis* 96 (Aug. 5, 2014), pp. 118–126. DOI: 10.1016/j.jpba.2014.03.021. pmid: 24739274.
- [11] Bjoern B. Burckhardt, Jutta Tins, and Stephanie Laer. „Simultaneous Quantitative and Qualitative Analysis of Aliskiren, Enalapril and Its Active Metabolite Enalaprilat in Undiluted Human Urine Utilizing LC-ESI-MS/MS.“ In: *Biomedical chromatography : BMC* 28.12 (Dec. 2014), pp. 1679–1691. DOI: 10.1002/bmc.3201. pmid: 24788577.
- [12] David A. Calhoun, Yves Lacourcière, Yann Tong Chiang, and Robert D. Glazer. „Triple Antihypertensive Therapy with Amlodipine, Valsartan, and Hydrochlorothiazide: A Randomized Clinical Trial“. In: *Hypertension (Dallas, Tex.: 1979)* 54.1 (July 2009), pp. 32–39. DOI: 10.1161/HYPERTENSIONAHA.109.131300. pmid: 19470877.
- [13] Ingolf Cascorbi. „Role of Pharmacogenetics of ATP-binding Cassette Transporters in the Pharmacokinetics of Drugs“. In: *Pharmacology & Therapeutics* 112.2 (Nov. 2006), pp. 457–473. DOI: 10.1016/j.pharmthera.2006.04.009. pmid: 16766035.
- [14] Huifang Cheng and Raymond C. Harris. „Potential Side Effects of Renin Inhibitors—Mechanisms Based on Comparison with Other Renin-Angiotensin Blockers.“ In: *Expert opinion on drug safety* 5.5 (Sept. 2006), pp. 631–641. DOI: 10.1517/14740338.5.5.631. pmid: 16907653.
- [15] Steven G. Chrysant. „Aliskiren-Hydrochlorothiazide Combination for the Treatment of Hypertension.“ In: *Expert review of cardiovascular therapy* 6.3 (Mar. 2008), pp. 305–314. DOI: 10.1586/14779072.6.3.305. pmid: 18327992.
- [16] Rainer Dietz, Ralf Dechend, Chuek-Man Yu, Manesh Bheda, Jessica Ford, Margaret F. Prescott, and Deborah L. Keefe. „Effects of the Direct Renin Inhibitor Aliskiren and Atenolol Alone or in Combination in Patients with Hypertension“. In: *Journal of the renin-angiotensin-aldosterone system: JRAAS* 9.3 (Sept. 2008), pp. 163–175. DOI: 10.1177/1470320308096411. pmid: 18957387.
- [17] Waymon Drummond, Mark A. Munger, Mohammed Rafique Essop, Mojdeh Maboudian, Mahmudul Khan, and Deborah L. Keefe. „Antihypertensive Efficacy of the Oral Direct Renin Inhibitor Aliskiren as Add-on Therapy in Patients Not Responding to Amlodipine Monotherapy“. In: *Journal of Clinical Hypertension (Greenwich, Conn.)* 9.10 (Oct. 2007), pp. 742–750. DOI: 10.1111/j.1524-6175.2007.06614.x. pmid: 17917501.
- [18] Sean T. Duggan, Claudine M. Chwieduk, and Monique P. Curran. „Aliskiren: A Review of Its Use as Monotherapy and as Combination Therapy in the Management of Hypertension.“ In: *Drugs* 70.15 (Oct. 22, 2010), pp. 2011–2049. DOI: 10.2165/11204360-000000000-00000. pmid: 20883056.
- [19] FDA. *Drug Development and Drug Interactions — Table of Substrates, Inhibitors and Inducers*. URL: <https://www.fda.gov/drugs/drug-interactions-labeling/drug-development-and-drug-interactions-table-substrates-inhibitors-and-inducers#table1-3> (visited on 12/19/2024).

- [20] FDA. *FDA Approved Products: Tekturna (Aliskiren) Oral Tablets and Pellets*. 2020. URL: https://www.accessdata.fda.gov/drugsatfda_docs/label/2020/021985s039lbl.pdf (visited on 01/02/2025).
- [21] FDA. *For Healthcare Professionals — FDA's Examples of Drugs That Interact with CYP Enzymes and Transporter Systems*. URL: <https://www.fda.gov/drugs/drug-interactions-labeling/healthcare-professionals-fdas-examples-drugs-interact-cyp-enzymes-and-transporter-systems> (visited on 12/19/2024).
- [22] Naomi D. L. Fisher, A. H. Jan Danser, J. Nussberger, William P. Dole, and Norman K. Hollenberg. „Renal and Hormonal Responses to Direct Renin Inhibition with Aliskiren in Healthy Humans“. In: *Circulation* 117.25 (June 24, 2008), pp. 3199–3205. DOI: 10.1161/CIRCULATIONAHA.108.767202. pmid: 18559696.
- [23] James E. Frampton and Monique P. Curran. „Aliskiren: A Review of Its Use in the Management of Hypertension.“ In: *Drugs* 67.12 (2007), pp. 1767–1792. DOI: 10.2165/00003495-200767120-00008. pmid: 17683174.
- [24] F. Fyhrquist and O. Sajjonmaa. „Renin-Angiotensin System Revisited“. In: *Journal of Internal Medicine* 264.3 (Sept. 2008), pp. 224–236. DOI: 10.1111/j.1365-2796.2008.01981.x. pmid: 18793332.
- [25] Alan H. Gradman and Yoel Vivas. „New Drugs for Hypertension: What Do They Offer?“ In: *Current hypertension reports* 8.5 (Oct. 2006), pp. 425–432. DOI: 10.1007/s11906-006-0090-z. pmid: 16965731.
- [26] J Grzegorzewski, J Brandhorst, K Green, D Eleftheriadou, Y Duport, F Bartsch, A Köller, DYJ Ke, S De Angelis, and Matthias König. *PK-DB: Pharmacokinetics Database for Individualized and Stratified Computational Modeling*. DOI: 10.1093/nar/gkaa990. pmid: 33151297. URL: <https://pk-db.com/> (visited on 12/10/2024).
- [27] Pei Hu, Michael Bartlett, Rajesh S. Karan, Ji Jiang, Shuyang Zhang, Jianyan Zhang, Dan Howard, Ching-Ming Yeh, Suliman Al-Fayoumi, Venkateswar Jarugula, and William P. Dole. „Pharmacokinetics, Safety and Tolerability of Single and Multiple Oral Doses of Aliskiren in Healthy Chinese Subjects: A Randomized, Single-Blind, Parallel-Group, Placebo-Controlled Study.“ In: *Clinical drug investigation* 30.4 (2010), pp. 221–228. DOI: 10.2165/11533050-000000000-00000. pmid: 20192280.
- [28] S-M Huang, R Temple, D C Throckmorton, and L J Lesko. „Drug Interaction Studies: Study Design, Data Analysis, and Implications for Dosing and Labeling“. In: *Clinical Pharmacology & Therapeutics* 81.2 (Feb. 2007), pp. 298–304. DOI: 10.1038/sj.cpt.6100054. URL: <http://doi.wiley.com/10.1038/sj.cpt.6100054> (visited on 12/19/2024).
- [29] Michael Hucka, Frank T. Bergmann, Claudine Chaouiya, Andreas Dräger, Stefan Hoops, Sarah M. Keating, Matthias König, Nicolas Le Novère, Chris J. Myers, Brett G. Olivier, Sven Sahle, James C. Schaff, Rahuman Sheriff, Lucian P. Smith, Dagmar Waltemath, Darren J. Wilkinson, and Fengkai Zhang. „The Systems Biology Markup Language (SBML): Language Specification for Level 3 Version 2 Core Release 2“. In: *Journal of Integrative Bioinformatics* 16.2 (June 20, 2019). DOI: 10.1515/jib-2019-0021. URL: <https://doi.org/10.1515/jib-2019-0021>

//www.degruyter.com/document/doi/10.1515/jib-2019-0021/html (visited on 04/19/2024).

- [30] Sadayoshi Ito, Noriko Nakura, Stephanie Le Breton, and Deborah Keefe. „Efficacy and Safety of Aliskiren in Japanese Hypertensive Patients with Renal Dysfunction.“ In: *Hypertension research : official journal of the Japanese Society of Hypertension* 33.1 (Jan. 2010), pp. 62–66. DOI: 10.1038/hr.2009.175. pmid: 19927154.
- [31] Venkateswar Jarugula, Ching-Ming Yeh, Dan Howard, Christopher Bush, Deborah L. Keefe, and William P. Dole. „Influence of Body Weight and Gender on the Pharmacokinetics, Pharmacodynamics, and Antihypertensive Efficacy of Aliskiren.“ In: *Journal of clinical pharmacology* 50.12 (Dec. 2010), pp. 1358–1366. DOI: 10.1177/0091270009359525. pmid: 20150520.
- [32] Sarah M. Keating, Dagmar Waltemath, Matthias König, Fengkai Zhang, Andreas Dräger, Claudine Chaouiya, Frank T. Bergmann, Andrew Finney, Colin S. Gillespie, Tomáš Helikar, Stefan Hoops, Rahuman S. Malik-Sheriff, Stuart L. Moodie, Ion I. Moraru, Chris J. Myers, Aurélien Naldi, Brett G. Olivier, Sven Sahle, James C. Schaff, Lucian P. Smith, Maciej J. Swat, Denis Thieffry, Leandro Watanabe, Darren J. Wilkinson, Michael L. Blinov, Kimberly Begley, James R. Faeder, Harold F. Gómez, Thomas M. Hamm, Yuichiro Inagaki, Wolfram Liebermeister, Allyson L. Lister, Daniel Lucio, Eric Mjolsness, Carole J. Proctor, Karthik Raman, Nicolas Rodriguez, Clifford A. Shaffer, Bruce E. Shapiro, Joerg Stelling, Neil Swainston, Naoki Tanimura, John Wagner, Martin Meier-Schellersheim, Herbert M. Sauro, Bernhard Palsson, Hamid Bolouri, Hiroaki Kitano, Akira Funahashi, Henning Hermjakob, John C. Doyle, Michael Hucka, and SBML Level 3 Community members. „SBML Level 3: An Extensible Format for the Exchange and Reuse of Biological Models“. In: *Molecular Systems Biology* 16.8 (Aug. 2020), e9110. DOI: 10.15252/msb.20199110. pmid: 32845085.
- [33] Matthias König. *Sbmlsim: SBML Simulation Made Easy*. Version 0.2.2. [object Object], Sept. 27, 2021. DOI: 10.5281/ZENODO.5531088. URL: <https://zenodo.org/record/5531088> (visited on 04/19/2024).
- [34] Matthias König. *Sbmlutils: Python Utilities for SBML*. Version 0.9.0. Zenodo, Aug. 15, 2024. DOI: 10.5281/ZENODO.13325770. URL: <https://zenodo.org/doi/10.5281/zenodo.13325770> (visited on 09/13/2024).
- [35] Matthias König, Andreas Dräger, and Hermann-Georg Holzhütter. „CySBML: A Cytoscape Plugin for SBML“. In: *Bioinformatics* 28.18 (Sept. 15, 2012), pp. 2402–2403. DOI: 10.1093/bioinformatics/bts432. URL: <https://academic.oup.com/bioinformatics/article/28/18/2402/251682> (visited on 04/19/2024).
- [36] Yusuf Ali Kulanoglu and Matthias König. *Aliskiren Model*. URL: https://github.com/matthiaskoenig/aliskiren-model/blob/main/models/aliskiren_body_flat.md (visited on 12/11/2024).
- [37] Yusuf Ali Kulanoglu and Matthias König. *Physiologically Based Pharmacokinetic (PBPK) Model of Aliskiren*. Version 0.5.1. Zenodo, Sept. 13, 2024. DOI: 10.5281/ZENODO.13758734. URL: <https://zenodo.org/doi/10.5281/zenodo.13758734> (visited on 09/13/2024).

- [38] Carlene M. M. Lawes, Stephen Vander Hoorn, Anthony Rodgers, and International Society of Hypertension. „Global Burden of Blood-Pressure-Related Disease, 2001“. In: *Lancet (London, England)* 371.9623 (May 3, 2008), pp. 1513–1518. DOI: 10.1016/S0140-6736(08)60655-8. pmid: 18456100.
- [39] Beatrice Amelie Stemmer Mallol. *A Physiologically Based Pharmacokinetic (PBPK) Model of the Probe Drug Talinolol for the Characterization of Intestinal P-glycoprotein*. 2023. URL: <https://livermetabolism.com/paper/theses/Bachelor.Thesis.Beatrice.Stemmer.Mallol.pdf> (visited on 01/02/2025).
- [40] Juerg Nussberger, Grégoire Wuerzner, Chris Jensen, and Hans R. Brunner. „Angiotensin II Suppression in Humans by the Orally Active Renin Inhibitor Aliskiren (SPP100): Comparison with Enalapril“. In: *Hypertension (Dallas, Tex.: 1979)* 39.1 (Jan. 2002), E1–8. DOI: 10.1161/hy0102.102293. pmid: 11799102.
- [41] Byung-Hee Oh. „Aliskiren, the First in a New Class of Direct Renin Inhibitors for Hypertension: Present and Future Perspectives.“ In: *Expert opinion on pharmacotherapy* 8.16 (Nov. 2007), pp. 2839–2849. DOI: 10.1517/14656566.8.16.2839. pmid: 17956203.
- [42] DrugBank Online. *Aliskiren*. URL: <https://go.drugbank.com/drugs/DB09026> (visited on 12/13/2024).
- [43] Eduardo Pimenta and Suzanne Oparil. „Renin Inhibitors: Novel Agents for Renoprotection or a Better Angiotensin Receptor Blocker for Blood Pressure Lowering?“ In: *Cardiology clinics* 26.4 (Nov. 2008), pp. 527–535. DOI: 10.1016/j.ccl.2008.06.003. pmid: 18929229.
- [44] PKPDAI. *Publications*. URL: <https://www.pkpdai.com/publications> (visited on 12/10/2024).
- [45] James L. Pool. „Direct Renin Inhibition: Focus on Aliskiren.“ In: *Journal of managed care pharmacy : JMCP* 13 (8 Suppl B Oct. 2007), pp. 21–33. DOI: 10.18553/jmcp.2007.13.s8-b.21. pmid: 17970614.
- [46] PubMed. *PubMed*. URL: <https://pubmed.ncbi.nlm.nih.gov/> (visited on 12/10/2024).
- [47] Helena Leal Pujol. *A Physiologically Based Model of Pravastatin- The Role of Genotypes and Hepatic or Renal Impairment on the Pharmacokinetics of Pravastatin*. 2022. URL: <https://livermetabolism.com/paper/theses/Bachelor.Thesis.Helena.Leal.Pujol.pdf> (visited on 01/02/2025).
- [48] Eleni Rapsomaniki, Adam Timmis, Julie George, Mar Pujades-Rodriguez, Anoop D. Shah, Spiros Denaxas, Ian R. White, Mark J. Caulfield, John E. Deanfield, Liam Smeeth, Bryan Williams, Aroon Hingorani, and Harry Hemingway. „Blood Pressure and Incidence of Twelve Cardiovascular Diseases: Lifetime Risks, Healthy Life-Years Lost, and Age-Specific Associations in 1·25 Million People“. In: *Lancet (London, England)* 383.9932 (May 31, 2014), pp. 1899–1911. DOI: 10.1016/S0140-6736(14)60685-1. pmid: 24881994.

- [49] Azhar Rashikh, Shibli Jameel Ahmad, Krishna Kolappa Pillai, and Abul Kalam Najmi. „Aliskiren as a Novel Therapeutic Agent for Hypertension and Cardio-Renal Diseases.“ In: *The Journal of pharmacy and pharmacology* 64.4 (Apr. 2012), pp. 470–481. DOI: 10.1111/j.2042-7158.2011.01414.x. pmid: 22420653.
- [50] Sam Rebello, Séverine Compain, Aimin Feng, Sam Hariy, Hans-Armin Dieterich, and Venkateswar Jarugula. „Effect of Cyclosporine on the Pharmacokinetics of Aliskiren in Healthy Subjects.“ In: *Journal of clinical pharmacology* 51.11 (Nov. 2011), pp. 1549–1560. DOI: 10.1177/0091270010385934. pmid: 21406600.
- [51] Sam Rebello, Selene Leon, Sam Hariy, Marion Dahlke, and Venkateswar Jarugula. „Effect of Verapamil on the Pharmacokinetics of Aliskiren in Healthy Participants.“ In: *Journal of clinical pharmacology* 51.2 (Feb. 2011), pp. 218–228. DOI: 10.1177/0091270010365717. pmid: 20413453.
- [52] Sam Rebello, Sally Zhao, Sam Hariy, Marion Dahlke, Natalya Alexander, Arpine Vapurcuyan, Imad Hanna, and Venkateswar Jarugula. „Intestinal OATP1A2 Inhibition as a Potential Mechanism for the Effect of Grapefruit Juice on Aliskiren Pharmacokinetics in Healthy Subjects.“ In: *European journal of clinical pharmacology* 68.5 (May 2012), pp. 697–708. DOI: 10.1007/s00228-011-1167-4. pmid: 22124880.
- [53] Detlef Schuppan and Nezam H. Afdhal. „Liver Cirrhosis“. In: *Lancet (London, England)* 371.9615 (Mar. 8, 2008), pp. 838–851. DOI: 10.1016/S0140-6736(08)60383-9. pmid: 18328931.
- [54] Reza Sepehrdad, William H. Frishman, Charles T. Jr Stier, and Domenic A. Sica. „Direct Inhibition of Renin as a Cardiovascular Pharmacotherapy: Focus on Aliskiren.“ In: *Cardiology in review* 15.5 (2007 Sep-Oct), pp. 242–256. DOI: 10.1097/CRD.0b013e318093e43a. pmid: 17700383.
- [55] Hassan Shahbaz, Preeti Rout, and Mohit Gupta. *Creatinine Clearance*. June 2024. URL: <https://www.ncbi.nlm.nih.gov/books/NBK544228/> (visited on 01/01/2025).
- [56] Endre T. Somogyi, Jean-Marie Bouteiller, James A. Glazier, Matthias König, J. Kyle Medley, Maciej H. Swat, and Herbert M. Sauro. „libRoadRunner: A High Performance SBML Simulation and Analysis Library“. In: *Bioinformatics* 31.20 (Oct. 15, 2015), pp. 3315–3321. DOI: 10.1093/bioinformatics/btv363. URL: <https://academic.oup.com/bioinformatics/article/31/20/3315/195758> (visited on 04/19/2024).
- [57] Jan A. Staessen, Yan Li, and Tom Richart. „Oral Renin Inhibitors.“ In: *Lancet (London, England)* 368.9545 (Oct. 21, 2006), pp. 1449–1456. DOI: 10.1016/S0140-6736(06)69442-7. pmid: 17055947.
- [58] Kalathil K. Sureshkumar. „Renin Inhibition with Aliskiren in Hypertension: Focus on Aliskiren/Hydrochlorothiazide Combination Therapy.“ In: *Vascular health and risk management* 4.6 (2008), pp. 1205–1220. DOI: 10.2147/vhrm.s3364. pmid: 19337534.

- [59] Kalathil K. Sureshkumar, Sapna Vasudevan, Richard J. Marcus, Sabiha M. Hussain, and Rita L. McGill. „Aliskiren: Clinical Experience and Future Perspectives of Renin Inhibition.“ In: *Expert opinion on pharmacotherapy* 9.5 (Apr. 2008), pp. 825–837. DOI: 10.1517/14656566.9.5.825. pmid: 18345958.
- [60] T. Tapaninen, P. J. Neuvonen, and M. Niemi. „Grapefruit Juice Greatly Reduces the Plasma Concentrations of the OATP2B1 and CYP3A4 Substrate Aliskiren.“ In: *Clinical pharmacology and therapeutics* 88.3 (Sept. 2010), pp. 339–342. DOI: 10.1038/clpt.2010.101. pmid: 20664534.
- [61] Tuija Tapaninen, Janne T. Backman, Kaisa J. Kurkinen, Pertti J. Neuvonen, and Mikko Niemi. „Itraconazole, a P-glycoprotein and CYP3A4 Inhibitor, Markedly Raises the Plasma Concentrations and Enhances the Renin-Inhibiting Effect of Aliskiren.“ In: *Journal of clinical pharmacology* 51.3 (Mar. 2011), pp. 359–367. DOI: 10.1177/0091270010365885. pmid: 20400651.
- [62] Tuija Tapaninen, Pertti J. Neuvonen, and Mikko Niemi. „Effect of ABCB1 Haplotypes on the Pharmacokinetics and Renin-Inhibiting Effect of Aliskiren.“ In: *European journal of clinical pharmacology* 66.9 (Sept. 2010), pp. 865–870. DOI: 10.1007/s00228-010-0836-z. pmid: 20496145.
- [63] Tuija Tapaninen, Pertti J. Neuvonen, and Mikko Niemi. „Orange and Apple Juice Greatly Reduce the Plasma Concentrations of the OATP2B1 Substrate Aliskiren.“ In: *British journal of clinical pharmacology* 71.5 (May 2011), pp. 718–726. DOI: 10.1111/j.1365-2125.2010.03898.x. pmid: 21204914.
- [64] Tuija Tapaninen, Pertti J. Neuvonen, and Mikko Niemi. „Rifampicin Reduces the Plasma Concentrations and the Renin-Inhibiting Effect of Aliskiren.“ In: *European journal of clinical pharmacology* 66.5 (May 2010), pp. 497–502. DOI: 10.1007/s00228-010-0796-3. pmid: 20179914.
- [65] Mikiko Tsukimoto, Rikiya Ohashi, Nao Torimoto, Yoko Togo, Takashi Suzuki, Toshio Maeda, and Yoshiyuki Kagawa. „Effects of the Inhibition of Intestinal P-glycoprotein on Aliskiren Pharmacokinetics in Cynomolgus Monkeys.“ In: *Biopharmaceutics & drug disposition* 36.1 (Jan. 2015), pp. 15–33. DOI: 10.1002/bdd.1920. pmid: 25264342.
- [66] S. Vaidyanathan, J. Valencia, C. Kemp, C. Zhao, C.-M. Yeh, M.-N. Bizot, J. Denouel, H. A. Dieterich, and W. P. Dole. „Lack of Pharmacokinetic Interactions of Aliskiren, a Novel Direct Renin Inhibitor for the Treatment of Hypertension, with the Antihypertensives Amlodipine, Valsartan, Hydrochlorothiazide (HCTZ) and Ramipril in Healthy Volunteers.“ In: *International journal of clinical practice* 60.11 (Nov. 2006), pp. 1343–1356. DOI: 10.1111/j.1742-1241.2006.01164.x. pmid: 17073832.
- [67] Sujata Vaidyanathan, Michael Bartlett, Hans Armin Dieterich, Ching-Ming Yeh, Ana Antunes, Dan Howard, and William P. Dole. „Pharmacokinetic Interaction of the Direct Renin Inhibitor Aliskiren with Furosemide and Extended-Release Isosorbide-5-Mononitrate in Healthy Subjects.“ In: *Cardiovascular therapeutics* 26.4 (Win. 2008), pp. 238–246. DOI: 10.1111/j.1755-5922.2008.00058.x. pmid: 19035874.

- [68] Sujata Vaidyanathan, Hilde Bigler, ChingMing Yeh, Marie-Noelle Bizot, Hans Armin Dieterich, Dan Howard, and William P. Dole. „Pharmacokinetics of the Oral Direct Renin Inhibitor Aliskiren Alone and in Combination with Irbesartan in Renal Impairment.“ In: *Clinical pharmacokinetics* 46.8 (2007), pp. 661–675. DOI: 10.2165/00003088-200746080-00003. pmid: 17655373.
- [69] Sujata Vaidyanathan, Gian Camenisch, Helmut Schuetz, Christine Reynolds, Ching-Ming Yeh, Marie-Noelle Bizot, Hans Armin Dieterich, Dan Howard, and William P. Dole. „Pharmacokinetics of the Oral Direct Renin Inhibitor Aliskiren in Combination with Digoxin, Atorvastatin, and Ketoconazole in Healthy Subjects: The Role of P-glycoprotein in the Disposition of Aliskiren.“ In: *Journal of clinical pharmacology* 48.11 (Nov. 2008), pp. 1323–1338. DOI: 10.1177/0091270008323258. pmid: 18784280.
- [70] Sujata Vaidyanathan, Venkateswar Jarugula, Hans Armin Dieterich, Dan Howard, and William P. Dole. „Clinical Pharmacokinetics and Pharmacodynamics of Aliskiren.“ In: *Clinical pharmacokinetics* 47.8 (2008), pp. 515–531. DOI: 10.2165/00003088-200847080-00002. pmid: 18611061.
- [71] Sujata Vaidyanathan, Joanne Jermany, Chingming Yeh, Marie-Noelle Bizot, and Riccardo Camisasca. „Aliskiren, a Novel Orally Effective Renin Inhibitor, Exhibits Similar Pharmacokinetics and Pharmacodynamics in Japanese and Caucasian Subjects.“ In: *British journal of clinical pharmacology* 62.6 (Dec. 2006), pp. 690–698. DOI: 10.1111/j.1365-2125.2006.02696.x. pmid: 17118124.
- [72] Sujata Vaidyanathan, Mojdeh Maboudian, Vance Warren, Ching-Ming Yeh, Hans Armin Dieterich, Dan Howard, and William P. Dole. „A Study of the Pharmacokinetic Interactions of the Direct Renin Inhibitor Aliskiren with Metformin, Pioglitazone and Fenofibrate in Healthy Subjects.“ In: *Current medical research and opinion* 24.8 (Aug. 2008), pp. 2313–2326. DOI: 10.1185/03007990802259354. pmid: 18786303.
- [73] Sujata Vaidyanathan, Christine Reynolds, Ching-Ming Yeh, Marie-Noëlle Bizot, Hans Armin Dieterich, Dan Howard, and William P. Dole. „Pharmacokinetics, Safety, and Tolerability of the Novel Oral Direct Renin Inhibitor Aliskiren in Elderly Healthy Subjects.“ In: *Journal of clinical pharmacology* 47.4 (Apr. 2007), pp. 453–460. DOI: 10.1177/0091270006297921. pmid: 17389554.
- [74] Sujata Vaidyanathan, Vance Warren, Chingming Yeh, Marie-Noelle Bizot, Hans Armin Dieterich, and William P. Dole. „Pharmacokinetics, Safety, and Tolerability of the Oral Renin Inhibitor Aliskiren in Patients with Hepatic Impairment.“ In: *Journal of clinical pharmacology* 47.2 (Feb. 2007), pp. 192–200. DOI: 10.1177/0091270006294404. pmid: 17244770.
- [75] Paolo Verdecchia, Fabio Angeli, Giovanni Mazzotta, Giorgio Gentile, and Gianpaolo Rebaldi. „The Renin Angiotensin System in the Development of Cardiovascular Disease: Role of Aliskiren in Risk Reduction.“ In: *Vascular health and risk management* 4.5 (2008), pp. 971–981. DOI: 10.2147/vhrm.s3215. pmid: 19183745.

- [76] Paolo Verdecchia, Fabio Angeli, Giovanni Mazzotta, Paola Martire, Marta Garofoli, Giorgio Gentile, and Gianpaolo Rebaldi. „Aliskiren versus Ramipril in Hypertension.“ In: *Therapeutic advances in cardiovascular disease* 4.3 (June 2010), pp. 193–200. DOI: 10.1177/1753944710369682. pmid: 20418269.
- [77] Alberto Villamil, Steven G. Chrysant, David Calhoun, Bonnie Schober, Huang Hsu, Linda Matrisciano-Dimichino, and Jack Zhang. „Renin Inhibition with Aliskiren Provides Additive Antihypertensive Efficacy When Used in Combination with Hydrochlorothiazide“. In: *Journal of Hypertension* 25.1 (Jan. 2007), pp. 217–226. DOI: 10.1097/HJH.0b013e3280103a6b. pmid: 17143194.
- [78] Felix Waldmeier, Ulrike Glaenzel, Bernard Wirz, Lukas Oberer, Dietmar Schmid, Michael Seiberling, Jessica Valencia, Gilles-Jacques Riviere, Peter End, and Sujata Vaidyanathan. „Absorption, Distribution, Metabolism, and Elimination of the Direct Renin Inhibitor Aliskiren in Healthy Volunteers.“ In: *Drug metabolism and disposition: the biological fate of chemicals* 35.8 (Aug. 2007), pp. 1418–1428. DOI: 10.1124/dmd.106.013797. pmid: 17510248.
- [79] Ciaran Welsh, Jin Xu, Lucian Smith, Matthias König, Kiri Choi, and Herbert M Sauro. „libRoadRunner 2.0: A High Performance SBML Simulation and Analysis Library“. In: *Bioinformatics* 39.1 (Jan. 1, 2023). Ed. by Pier Luigi Martelli, btac770. DOI: 10.1093/bioinformatics/btac770. URL: <https://academic.oup.com/bioinformatics/article/doi/10.1093/bioinformatics/btac770/6883908> (visited on 04/19/2024).
- [80] Paul K. Whelton, Robert M. Carey, Giuseppe Mancia, Reinhold Kreutz, Joshua D. Bundy, and Bryan Williams. „Harmonization of the American College of Cardiology/American Heart Association and European Society of Cardiology/European Society of Hypertension Blood Pressure/Hypertension Guidelines“. In: *European Heart Journal* 43.35 (Sept. 14, 2022), pp. 3302–3311. DOI: 10.1093/eurheartj/ehac432. pmid: 36100239.
- [81] WHO. *Hypertension*. URL: <https://www.who.int/news-room/fact-sheets/detail/hypertension> (visited on 12/10/2024).
- [82] Wikipedia. *CYP3A4*. URL: <https://en.wikipedia.org/wiki/CYP3A4> (visited on 12/13/2024).
- [83] Wikipedia. *P-Glycoprotein*. URL: <https://en.wikipedia.org/wiki/P-glycoprotein> (visited on 12/13/2024).
- [84] Jeanette M. Wood, Jürgen Maibaum, Joseph Rahuel, Markus G. Grütter, Nissim-Claude Cohen, Vittorio Rasetti, Heinrich Rüger, Richard Göschke, Stefan Stutz, Walter Fuhrer, Walter Schilling, Pascal Rigollier, Yasuchika Yamaguchi, Frederic Cumin, Hans-Peter Baum, Christian R. Schnell, Peter Herold, Robert Mah, Chris Jensen, Eoin O'Brien, Alice Stanton, and Martin P. Bedigian. „Structure-Based Design of Aliskiren, a Novel Orally Effective Renin Inhibitor.“ In: *Biochemical and biophysical research communications* 308.4 (Sept. 5, 2003), pp. 698–705. DOI: 10.1016/s0006-291x(03)01451-7. pmid: 12927775.
- [85] Grégoire Wuerzner and Michel Azizi. „Renin Inhibition with Aliskiren.“ In: *Clinical and experimental pharmacology & physiology* 35.4 (Apr. 2008), pp. 426–430. DOI: 10.1111/j.1440-1681.2008.04890.x. pmid: 18307734.

- [86] Charlie Zhao, Sujata Vaidyanathan, Ching-Ming Yeh, Mojdeh Maboudian, and Hans Armin Dieterich. „Aliskiren Exhibits Similar Pharmacokinetics in Healthy Volunteers and Patients with Type 2 Diabetes Mellitus.“ In: *Clinical pharmacokinetics* 45.11 (2006), pp. 1125–1134. DOI: 10.2165/00003088-200645110-00006. pmid: 17048976.

Eigenständigkeitserklärung

Hiermit erkläre ich, dass ich die vorliegende Arbeit selbständig verfasst habe und sämtliche Quellen, einschließlich Internetquellen, die unverändert oder abgewandelt wiedergegeben werden, insbesondere Quellen für Texte, Grafiken, Tabellen und Bilder, als solche kenntlich gemacht habe. Ich versichere, dass ich die vorliegende Abschlussarbeit noch nicht für andere Prüfungen eingereicht habe. Mir ist bekannt, dass bei Verstößen gegen diese Grundsätze ein Verfahren wegen Täuschungsversuchs bzw. Täuschung gemäß der fachspezifischen Prüfungsordnung und/oder der Fächerübergreifenden Satzung zur Regelung von Zulassung, Studium und Prüfung der Humboldt-Universität zu Berlin (ZSP-HU) eingeleitet wird.

A handwritten signature in black ink, appearing to read "Kulanoglu". The signature is fluid and cursive, with a prominent 'K' at the beginning.

Berlin, den 05. Januar 2025, Yusuf Ali Kulanoglu